



**Set-up and comparison of the Droplet Digital PCR method  
with quantitative RT-PCR in assessing the levels of  
microRNA-124 from plasma and brain tissue of rats with  
traumatic brain injury**

**Shalini Das Gupta**

Thesis to obtain the Master of Science Degree in

**Biotechnology**

Supervisors: Dr. Noora Puhakka

Prof. Jorge Humberto Gomes Leitão

**Examination Committee:**

Chairperson: Prof. Isabel Maria Sá Correia Leite de Almeida

Supervisor: Prof. Jorge Humberto Gomes Leitão

Member of the Committee: Dr. Sílvia Andreia Bento da Silva Sousa Barbosa

**October 2015**



## **ACKNOWLEDGEMENTS**

The experimental work documented in this thesis was conducted at the A.I.Virtanen Institute for Molecular Sciences, Department of Neurobiology, University of Eastern Finland, to obtain the Master of Science Degree in Biotechnology under the Erasmus Mundus Master's Program in Systems Biology (euSYSBIO).

I would like to express my deepest gratitude to Prof. Isabel Sá Correia (Instituto Superior Técnico) and Prof. Erik Aurell (KTH Royal Institute of Technology), the co-ordinators of euSYSBIO, for organizing this wonderful course. I would also like to thank Karin Knutsson and Ana Barbosa for their continuous guidance regarding all practical matters. I would particularly like to thank Prof. Isabel Sá Correia for providing me the opportunity to prepare my thesis in the field of neurobiology, and for helping me with all practical issues involved in conducting my work at an external institute. I am immensely thankful to Prof. Asla Pitkänen (University of Eastern Finland), head of the Epilepsy research laboratory, for providing me the opportunity to conduct my thesis under her supervision, and for introducing me to the extremely intriguing world of neuroscience. I sincerely thank her for the valuable comments and suggestions throughout the entire work period. I would also like to sincerely thank my supervisor, Dr. Noora Puhakka, for her continuous guidance regarding the molecular biology experiments, and for her valuable suggestions and feedback regarding documentation of the results.

I thank all the present and former members of the Epilepsy research laboratory, Anu Lipsanen, Tamuna Bolkvadze, Xavier Ekolle Ndode-Ekane, Jenni Karttunen, Tiina Pirttimäki, Diana Mischczuk, Francesco Noe, Anssi Lipponen, Sofya Ziyatdinova, Niina Vuokila, Jenni Kyyriäinen, Amna Yasmin, Pedro Andrade, Zafar Sajjad Gondal, Johanna Hiltunen, Vicente Navarro Ferrandis, Ivette Bañuelos, Ying Wang and Cátia Palminha, for the wonderful "Epiclub" sessions, that significantly helped me in learning several interesting aspects of epilepsy research, and in actively participating in scientific discussions. I would specially like to thank Niina and Anssi for their valuable suggestions regarding improvements of the droplet digital PCR concept, and Pedro for his help in preparing the thesis abstract in Portuguese. My special thanks to Merja Lukkari for helping me in getting acquainted with the laboratory work, and to Jari Nissinen for his technical assistance. I would also like to thank Jussi Keinänen and Hanne Tanskanen for all the support regarding the practical issues.

I would also like to sincerely thank my supervisor Prof. Jorge Humberto Gomes Leitão (Instituto Superior Técnico), for providing me with his suggestions regarding preparation of the manuscript, and for his help in preparing the thesis abstract in Portuguese.

Finally, my warm regards to my family and friends, for the wonderful support and encouragement all through this work.

Lisbon, October 2015.

Shalini Dasgupta



## **ABSTRACT**

Traumatic brain injury (TBI) is the predominant cause of acquired epilepsy. The 30-y cumulative incidence of post-traumatic epilepsy (PTE) is 2.1% for mild, 4.2% for moderate, and 16.7% for severe injuries, which makes the pursuit of biomarkers that determine which injuries culminate in PTE paramount.

The hypothesis that plasma levels of brain-specific miR-124 may serve as a diagnostic marker in lateral FPI model of TBI, was tested in this work. Expression level of miR-124 was studied in plasma at both acute and chronic time points. The study of ipsilateral cortex was made only in the chronic time point. The ddPCR method was set up for miR-124 quantification from multiplexed and miR-124 specific cDNAs, and its sensitivity was compared with qRT-PCR. The relation between brain lesion size and corresponding miR-124 levels in plasma was also investigated.

The study underscored the potential of miR-124 as a biomarker for TBI at acute timepoint. In comparison to baseline, miR-124 elevations in 2 days post-TBI were 260% in qRT-PCR ( $p<0.01$ ), 223% ( $p<0.05$ ) in multiplexed ddPCR and 147% ( $p<0.05$ ) in miR-124 specific ddPCR datasets. In comparison to 2 days controls, miR-124 elevations were 180% in qRT-PCR ( $p<0.05$ ), 209% ( $p<0.05$ ) in multiplexed and 137% ( $p<0.05$ ) in miR-124 specific ddPCR datasets.

In perilesional cortex, miR-124 expression in TBI group was comparable to controls. Higher plasma miR-124 level was observed in animals with larger brain lesions.

**Keywords:** Biomarker, brain lesion, ddPCR, plasma, post-traumatic epilepsy, traumatic brain injury.



## **RESUMO**

O traumatismo crânio-encefálico (TCE) é a causa predominante de epilepsia secundária. Nos últimos 30 anos. A incidência cumulativa do pós-traumatismo crânio-encefálico na epilepsia secundária é de 2.1% nos traumatismos ligeiros, 4.2 % nos moderados e de 16.7% nas lesões graves. Este facto torna fulcral a busca de um biomarcador que identifique as lesões que culminarão numa epilepsia secundária.

No presente trabalho testámos a hipótese da utilização do miR-124, existente no plasma, como marcador clínico no modelo de TCE por percussão lateral por fluido. Esta expressão foi testada em duas fases, na fase aguda e na fase crónica. O córtex ipsilateral foi estudado apenas na fase crónica. Foram aplicadas duas técnicas, PCR digital (ddPCR) e qRT-PCR (multiplex e miR-124 specific cDNAs), tendo a sensibilidade de ambas as técnicas sido comparada. A relação entre a extensão da lesão e os níveis de miR-124 no plasma foi também investigada.

Este estudo evidenciou o miR-124 como potencial biomarcador nos TCEs na fase aguda. Quando se compararam os resultados das amostras provenientes do segundo dia pós-trauma com os de amostras controlo, verificámos um aumento de 260% em qRT-PCR ( $p<0,01$ ), 223% ( $p<0.05$ ) em multiplex ddPCR, e 147% ( $p<0.05$ ) com ddPCR específico para o miR-124. Ao compararmos estas mesmas amostras com as amostras controlo do mesmo dia, foi obtido um aumento de 180% no qRT-PCR ( $p<0.05$ ), 209% ( $p<0.05$ ) no ddPCR multiplex e 137% ( $p<0.05$ ) no ddPCR específico para miR-124.

Os resultados evidenciaram ainda níveis mais elevados de expressão de miR-124 no córtex perilesionado nas lesões mais extensas.

**Palavras-chave:** Biomarcador, lesão cerebral, ddPCR, plasma, epilepsia pós-traumática, traumatismo crânio-encefálico.





# TABLE OF CONTENTS

<b>1 INTRODUCTION</b> .....	<b>1</b>
<b>2 REVIEW OF THE LITERATURE</b> .....	<b>2</b>
2.1 Epilepsy .....	2
<b>2.1.1 Definition of epilepsy</b> .....	2
<b>2.1.2 Classifications of epilepsy and epileptic seizures</b> .....	2
2.2 Traumatic brain injury (TBI) – the predominant cause of acquired epilepsy.....	3
<b>2.2.1 Classifications of TBI</b> .....	3
<b>2.2.2 Primary and secondary brain damage post-TBI</b> .....	4
<b>2.2.3 Mechanisms of epileptogenesis associated with secondary injury</b> .....	4
<b>2.2.4 Animal models for TBI</b> .....	5
2.3 Post-traumatic epilepsy (PTE) as a consequence of TBI.....	7
2.4 Importance of biomarkers in characterization of TBI and epilepsy .....	8
<b>2.4.1 Characteristics of an ideal biomarker</b> .....	8
<b>2.4.2 MicroRNAs as biomarker candidates for diagnosis of TBI and epilepsy</b> .....	8
<b>2.4.3 Known miRNA biomarkers in TBI and epilepsy</b> .....	10
2.5 Challenges in profiling miRNAs from serum/plasma and other biofluids .....	11
2.6 Droplet Digital PCR in quantification of circulating miRNAs.....	12
<b>2.6.1 Advantages of ddPCR over qRT-PCR</b> .....	12
<b>2.6.2 Principle of ddPCR</b> .....	13
<b>2.6.3 TaqMan® and EvaGreen chemistries in PCR reactions</b> .....	13
2.7 Cresyl violet staining for analysis of brain cytoarchitecture in epilepsy .....	14
3.1 Objective.....	15
3.2 Hypotheses tested.....	15
3.3 Specific questions addressed.....	15
<b>4 MATERIALS AND METHODS</b> .....	<b>18</b>
4.1 Animals.....	18
4.2 Procedure for induction of lateral FPI.....	18
4.3 Sample preparation for microRNA analysis .....	18
<b>4.3.1 Extraction of plasma for miR-124 profiling</b> .....	18
<b>4.3.2 Extraction of brain tissue for miR-124 profiling</b> .....	19
4.4 Total RNA extraction from plasma and brain tissue .....	20
<b>4.4.1 RNA extraction protocol for plasma samples</b> .....	20
<b>4.4.2 RNA extraction protocol for brain tissue samples (ipsilateral cortex)</b> .....	21
4.5 cDNA synthesis with Exiqon miRCURY LNA™ Kit .....	21
4.6 qRT-PCR amplification with Exiqon kit for quality control .....	22
4.7 MicroRNA specific cDNA synthesis with TaqMan® small RNA assay.....	23
4.8 MicroRNA specific qRT-PCR reaction with TaqMan® chemistry.....	23
4.9 Absolute quantification of target miRNA concentration with ddPCR.....	24

4.10 Cost analysis for one PCR reaction (2 technical replicates) in TaqMan® qRT-PCR and ddPCR .....	25
4.11 Cresyl violet staining for characterization of lesion size .....	26
4.12 Statistical analysis .....	26
<b>5 RESULTS .....</b>	<b>28</b>
5.1 Mortality .....	28
5.2 Optimisation of the ddPCR protocol .....	28
<b>5.2.1 Dilution series from synthetic miR-124 and tissue samples .....</b>	<b>28</b>
<b>5.2.2 Optimisation of the annealing temperature using thermal gradients .....</b>	<b>29</b>
5.3 Quantification of miRNAs based on real-time qRT-PCR amplification .....	30
<b>5.3.1 Quality control for plasma samples with exogenous RNA spike-ins .....</b>	<b>30</b>
<b>5.3.2 Amplification of miR-103 in plasma as a possible endogenous control .....</b>	<b>32</b>
<b>5.3.3 Expression analysis of miR-124 in plasma across different time-points .....</b>	<b>33</b>
<b>5.3.4 Pattern of miR-124 expression in relation with lesion size .....</b>	<b>35</b>
5.4 Quantification of miR-124 with ddPCR from multiplexed RT products using TaqMan® chemistry .....	38
<b>5.4.1 Expression analysis of miR-124 in plasma across all timepoints .....</b>	<b>38</b>
<b>5.4.2 Droplet PCR based estimation of miR-124 expression in relation with lesion size ....</b>	<b>40</b>
5.5 Quantification of miR-124 with ddPCR from miR-124 specific RT products using TaqMan® chemistry .....	40
<b>5.5.1 Expression analysis of miR-124 in plasma across all timepoints .....</b>	<b>41</b>
<b>5.5.2 Droplet PCR based estimation of miR-124 expression in relation with lesion size ....</b>	<b>43</b>
5.6 Correlation between qRT-PCR and ddPCR expression patterns .....	44
5.7 Expression analysis of miR-124 in brain tissue samples (ipsilateral cortex) .....	46
<b>6 DISCUSSION .....</b>	<b>47</b>
6.1 Methodological considerations .....	48
<b>6.1.1 RNA isolation from plasma .....</b>	<b>48</b>
<b>6.1.2 Trade-off between Exiqon and TaqMan® chemistries .....</b>	<b>48</b>
<b>6.1.3 Absence of suitable endogenous control for plasma miRNA quantification .....</b>	<b>49</b>
<b>6.1.4 Limitations in optimizing the ddPCR protocol .....</b>	<b>49</b>
6.2 Potential of plasma miR-124 to act as a TBI biomarker .....	49
6.3 Sensitivity of ddPCR in assessing plasma levels of miR-124 .....	50
6.4 Relation between plasma levels of miR-124 at acute timepoints post-injury with histological changes observable at chronic timepoints .....	51
<b>7 CONCLUSION AND FUTURE WORK .....</b>	<b>53</b>
<b>8 REFERENCES .....</b>	<b>55</b>

## ***LIST OF TABLES***

<b>Table 1:</b> Reverse transcription reaction setup with Exiqon Universal cDNA synthesis kit .....	22
<b>Table 2:</b> Reagents and consumables for TaqMan qRT-PCR (single sample with two replicates) .....	25
<b>Table 3:</b> Reagents and consumables for TaqMan ddPCR (single sample with two replicates) .....	26

## LIST OF FIGURES

<b>Figure 1:</b> Study design for miR-124 profiling from (A) cohort A: tail vein plasma samples, (B) cohort B: brain tissue (ipsilateral cortex) samples .....	16
<b>Figure 2:</b> Implemented methodology for (A) miR-124 profiling from plasma and Nissl Staining in cohort A, (B) miR-124 profiling from ipsilateral cortex in cohort B .....	17
<b>Figure 3:</b> Animal cohorts used for (A) miR-124 profiling from tail vein plasma at -7 days, 2 days, 1 week and 3 months post-injury, (B) ipsilateral cortex at 3 months post-injury (Abbreviations: FPI-fluid percussion injury) .....	19
<b>Figure 4:</b> Target concentration / 20 $\mu$ L ddPCR well for the 1:5 dilution series of (A) synthetic miR-124, (B) ipsilateral cortex (exponential ddPCR based amplifications of miR-124 plotted to the logarithmic scale). .....	29
<b>Figure 5:</b> Annealing temperature gradient for ddPCR based miR-124 expression in (A) Ipsilateral cortex, (B) Plasma (blue-positive droplets, black-negative droplets). .....	30
<b>Figure 6:</b> (A) UniSp4 amplification represented as the mean $C_t$ for the three qRT-PCR replicates, (B) UniSp4 melt curve analysis, (C) UniSp6 amplification represented as the mean $C_t$ for the three qRT-PCR replicates, (D) UniSp6 melt curve analysis. ....	31
<b>Figure 7:</b> Analysis of miR-103 expression in plasma samples using TaqMan qRT-PCR chemistry....	33
<b>Figure 8:</b> (A) Analysis of miR-124 expression in plasma samples using TaqMan qRT-PCR chemistry, (B) Individual animal variability in miR-124 expression across the four timepoints of study, (C) Average miR-124 expressions for control and TBI animals across the four timepoints, ROC analysis for (D) 2 days control vs. 2 days post-TBI and (E) Baseline TBI vs. 2 days post-TBI (qRT-PCR dataset).....	35
<b>Figure 9:</b> (A) Site of impact for the lateral FPI, (B) Whole brain image for control rat 14 with no lesion due to absence of injury, (C) Whole brain image for TBI rat 9 with mid-size cavity, (D) Whole brain image for TBI rat 4 with big cavity, (E) Cresyl violet staining for control rat 7 reveals absence of lesion at the ipsilateral cortex, (F) Middle sized cavity observed at the ipsilateral cortex for TBI rat 9, with cell loss at the area of impact, (G) Large cavity with a higher extent of cell loss observed at the lesion area for TBI rat 4.....	36
<b>Figure 10:</b> (A) Up-regulation in miR-124 expression observed in plasma of rats characterized with larger brain lesions at 2 days post-injury (qRT-PCR data), ROC analysis for (B) control vs. big lesion group (C) control vs. smaller lesion group, (D) big lesion vs. smaller lesion group (qRT-PCR data). ....	37
<b>Figure 11:</b> (A) Expression profile for miR-124 across all timepoints in plasma (multiplexed ddPCR), (B) Individual animal variability in miR-124 expression across the four timepoints of study, (C) Average miR-124 expressions for control and TBI animals across the four timepoints, ROC analysis for (D) 2 days control vs. 2 days post-TBI, (E) Baseline TBI vs. 2 days post-TBI.. ....	39
<b>Figure 12:</b> No up-regulation in miR-124 expression observed in relation to lesion size with the ddPCR multiplex data. ....	40
<b>Figure 13:</b> (A) Expression profile for miR-124 across all timepoints in plasma samples with ddPCR (miR-124 specific ddPCR), (B) Individual animal variability in miR-124 expression across the four timepoints of study, (C) Average miR-124 expressions for control and TBI animals across the four timepoints, ROC analysis for (D) 2 days control vs. 2 days post-TBI and (E) Baseline TBI vs. 2 days post-TBI. ....	43

**Figure 14:** (A) Up-regulation in miR-124 expression was observed in the ddPCR method only for rats with larger brain lesions compared to controls (miR-124 specific dataset), ROC analysis for (B) control vs. big lesion group (C) control vs. smaller lesion group, (D) big lesion vs. smaller lesion group using the ddPCR quantification method for miR-124 specific dataset. .... 44

**Figure 15:** Correlation between qRT-PCR and ddPCR amplifications at 2 days post-TBI for (A) multiplexed cDNA, (B) miR-124 specific cDNA. Correlation between qRT-PCR and ddPCR amplifications across all timepoints for (C) multiplexed cDNA, (D) miR-124 specific cDNA. .... 45

**Figure 16:** Comparison of miR-124 expression between controls and TBI samples from ipsilateral cortex at 3 months post-injury, (A) without normalisation to U6, (B) data normalised to U6 expression. .... 46

## **LIST OF ABBREVIATIONS**

AEDs: Antiepileptic drugs	GLAST: Glutamate aspartate transporter
ANOVA: Analysis of variance	HSP: Heat shock protein
APOE: Apolipoprotein E	i.p: Intraperitoneal
AUC: Area under the curve	ILAE: International league against epilepsy
BBB: Blood-brain barrier	LNA: Locked nucleic acid
CA1: Cornu Ammonis 1 region of the hippocampus	LOC: Loss of consciousness
CA3: Cornu Ammonis 3 region of the hippocampus	miRNA: MicroRNA
CCI: Controlled cortical impact	MRI: Magnetic resonance imaging
CDEs: Common data elements	mRNA: Messenger RNAs
cDNA: Complementary DNA	MTLE: Mesial temporal lobe epilepsy
CNS: Central nervous system	NIH: National institutes of health
CSF: Cerebro-spinal fluid	NMDA: N-methyl-D-aspartate
C <sub>t</sub> : Threshold cycle	NTCs: No template controls
ddPCR: Droplet digital PCR	OD: Optical density
DNA: Deoxyribonucleic acid	PET: Positron emission tomography
dsDNA: Double stranded DNA	pre-miRNA: Precursor miRNA
EDTA: Ethylenediaminetetraacetic acid	pri-miRNA: Primary miRNA
EEG: Electroencephalography	PTA: Post-traumatic amnesia
FPI: Fluid percussion injury	PTE: Post traumatic epilepsy
GABA: $\gamma$ -aminobutyric acid	PTS: Post-traumatic seizures
GCS: Glasgow coma scale	PTZ: Pentylenetetrazol
	qRT-PCR: Quantitative reverse-transcription polymerase chain reaction
	RISC: RNA-induced silencing complex
	RNA: Ribonucleic acid

RNase: Ribonuclease

ROC: Receiver operator characteristics

ROS: Reactive oxygen species

rRNA: Ribosomal RNA

RT: Reverse transcription

SE: Status epilepticus

siRNA: Small interfering RNAs

snRNA: Small nuclear RNA

TBI: Traumatic brain injury

TLE: Temporal lobe epilepsy

T<sub>m</sub>: Annealing temperature

TNF: Tumor necrosis factor

tRNA: Transfer RNA

UNG: Uracil N-glycosylase

# **1 INTRODUCTION**

Epilepsy is a family of brain disorders, characterized by recurrent and unpredictable interruptions of the normal brain function, leading to seizures, periods of unusual behaviour and momentary loss of consciousness [1, 2]. It affects both sexes and people from all age group and geographical distribution [3]. About 50 million people worldwide are affected, with a significant majority of patients being drug-refractory [4, 5]. Epilepsy is strongly associated with psychological imbalances and social stigmatization, and most patients experience a discriminatory behaviour in various aspects of daily life [6]. Symptomatic epilepsies are the most common forms of epilepsy syndrome encountered in adults, with traumatic brain injury (TBI) being the predominant cause of post-traumatic epilepsy (PTE) in both civilian and military population [7, 8]. The brain insults trigger epileptogenic cascades, involving abnormal neurodegeneration and neuronal circuitry reorganization that predisposes the brain towards ictogenesis [9]. Current treatment methods for epilepsy focus on prevention/suppression of epileptic seizures with antiepileptic drugs (AEDs). However, reviews suggest that a large section of the treated population suffer from adverse side-effects of the medication [10], and 20-30% of the patients become unresponsive to any AED treatment [4, 11]. Thus, rather than suppressing seizure occurrence, prevention of the development of epilepsy (antiepileptogenesis) is gaining attention now.

Molecular biomarkers may play a significant role in determining susceptibility towards epilepsy after brain insults, characterization of epileptogenic progression, and for predicting response to implemented therapeutic approaches [12]. Recent studies particularly stress on understanding changes in microRNA (miRNA) profiles in the epileptogenic brain, since they are powerful players regulating and fine tuning a multitude of gene expression patterns [5, 13-16]. The human brain exhibits an exceptionally high miRNA expression level, suggesting significant association between neurological disorders and miRNA dysfunction [5]. It is also predicted that miRNA alterations occur much earlier in response to a disease state than conventional protein biomarkers, making them crucial for detection in early stages of disease development [17]. In fact, up-regulation of brain enriched miRNAs has been observed in blood samples of rats subjected to the lateral fluid percussion injury (FPI) model of TBI, 2 days post-trauma [18].

Thus, the aim of this thesis was to assess the expression levels of a brain enriched miRNA, miR-124, from plasma and ipsilateral cortex of rats subjected to lateral FPI. MiRNAs in circulating cell-free biofluids are of particular interest, since they are presumed to play a role in paracrine cellular communication. The hypothesis that plasma levels of brain enriched miRNAs can serve as potential diagnostic markers for development of brain injury, was tested in this work. Quantification of miR-124 was performed using quantitative reverse-transcription PCR (qRT-PCR) and droplet Digital PCR (ddPCR), at both acute and chronic timepoints. Sensitivity of the two techniques in miR-124 profiling from plasma was compared. In addition, brain lesions developed as an impact of injury was studied with cresyl violet staining, and relation between lesion size developed at a chronic timepoint and corresponding miR-124 levels in plasma at an acute timepoint was investigated. Finally, miR-124 expression in the ipsilateral cortex at a chronic timepoint was studied using ddPCR.



## **2 REVIEW OF THE LITERATURE**

### **2.1 Epilepsy**

#### **2.1.1 Definition of epilepsy**

Epilepsy is one of the world's oldest recognised medical conditions. The first description of epileptic seizures appear in Mesopotamian texts at around 2000 B.C. Initially considered as a divine intervention, the first formal characterization of epilepsy as a disease, demythologizing its divine origin, was performed by Hippocrates [19]. Epilepsy is a brain disorder, characterized by an enduring predisposition to generate epileptic seizures, and by its neurobiological, cognitive, psychological and social consequences [20]. Epileptic seizures are brief periods of hyperactivity, involving abnormal excessive or synchronous neuronal discharges in the brain [1]. Manifestations of seizures can vary from involuntary jerking movements to subtle momentary loss of consciousness [21]. Epilepsy is the 4<sup>th</sup> most common neurological problem after migraine, stroke and Alzheimer's disease [22]. Around 50 million people worldwide and 6 million in Europe have been diagnosed with active epilepsy, with about 30% drug-refractory cases [4, 11].

According to the International league against epilepsy (ILAE), a patient is diagnosed with epilepsy based on any one of the following criteria: (1) At least two unprovoked (or reflex) seizures occurring >24 h apart; (2) one unprovoked (or reflex) seizure and a probability of further seizures similar to the general recurrence risk (at least 60%) after two unprovoked seizures, occurring over the next 10 years; (3) diagnosis of an epilepsy syndrome. Epilepsy is considered resolved for individuals who either had an age-dependent epilepsy syndrome but are now past the applicable age, or who have remained seizure-free for the last 10 years and have not received antiseizure medications for at least the last 5 years [20].

#### **2.1.2 Classifications of epilepsy and epileptic seizures**

Based on origin and etiology, epilepsy is classified as idiopathic, symptomatic, provoked and cryptogenic. Epilepsies with no underlying cause other than a genetic or hereditary predisposition are classified as idiopathic epilepsies, whereas symptomatic epilepsies are cases of acquired conditions. Epilepsy as a symptom of an underlying pathology, such as hypoxia, TBI, SE, stroke, infection, congenital brain malformation, tumour or metabolic disorder is termed as symptomatic epilepsy. Epilepsies due to unknown or hidden causes are termed as cryptogenic epilepsies. In most cases, cryptogenic epilepsies are considered to be symptomatic. Provoked epilepsy includes seizures generated in response to provoking factors like fever, menstrual cycle, alcohol withdrawal and others [23, 24].

Epileptic seizures can be broadly classified as convulsive or absence seizures. Majority of the seizures are convulsive in nature, and can be further classified as partial (focal) or generalised, based on their onset of location. Generalised seizures involve both cerebral hemispheres, whereas focal seizures originate from one hemisphere, and may then progress to the generalised form. Absence seizures, on the other hand, involve a decreased level of consciousness that lasts for about 10 seconds [23].

Generalized seizures are of six main types, including tonic-clonic, tonic, clonic, myoclonic, absence, and atonic seizures, all involving sudden seizure occurrence and loss of consciousness. Tonic-clonic seizures manifest contraction and extension of the limbs along with arching of the back and contraction of the chest muscles, lasting for 10–30 seconds. This forms the tonic phase. It is then followed by the clonic phase that involves shaking of the limbs in unison. Tonic seizures produce constant contractions of the muscles, with reduced breathing. In clonic seizures, there is shaking of the limbs in unison. Myoclonic seizures involve muscle spasms in either a few regions of the body or all over. Absence seizures are characterised by subtle phenomena such as slight turn of the head or eye blinking. Atonic seizures involve loss of muscle activity for more than one second, typically on both sides of the body. In some patients, seizures are often triggered by specific events, such as flashing lights and sudden noise. This phenomenon is known as reflex seizure. Such patients encounter seizures only in presence of the stimuli [23].

## **2.2 Traumatic brain injury (TBI) – the predominant cause of acquired epilepsy**

### **2.2.1 Classifications of TBI**

TBI is the predominant cause of acquired epilepsy in both civilian and military population [7, 8]. TBI refers to brain damage caused by an external mechanical force, such as a blow to the head, concussive forces, gunshots etc. [25]. Typically, head injury involves two broad categories: Penetrating and closed brain injury [26, 27]. Penetrating injuries are in most cases caused by gunshots and missile wounds. The severity of this kind of injury depends on factors such as mass, shape, direction of travel and velocity of the projected missile, as well as the nature of the human skull at the location of impact. The common properties for this type of injury include: (i) Transmission of kinetic energy through brain as pressure impulses of varying magnitude and duration, and (ii) Direct damage to the vascular and neuronal structures of the brain. Closed brain injury, on the other hand, involves movement of the brain inside skull as an impact of the trauma and propagation of stress waves through the brain from the point of impact, thereby producing tissue strain [26, 27]. Closed brain injury is the most common form of TBI in civilian cases, as it include falls, assaults and accidents [27].

Based on the severity, traumatic brain injuries are classified as mild, moderate or severe. The most common assessment criteria is the 15-point Glasgow coma scale (GCS), that assesses the level of consciousness of a patient based on verbal, motor and eye movements in response to stimuli. TBI with a GCS score of 13 and above is usually classified as mild injury, 9-12 as moderate and a score of 8 or below is considered severe [25]. Loss of consciousness (LOC) and post-traumatic amnesia (PTA) following the injury are also important factors to be considered to determine severity. Mild injuries mostly involve no LOC and skull fracture, or PTA for less than 30 minutes. Moderate injuries involve PTA or LOC extending from 30 minutes-24 hours, or a skull fracture, or a combination of these features, whereas severe injuries include brain contusion, intracranial/intracerebral hematoma, or either LOC or PTA extending over 24 hours. Penetrating injuries are common in military services, and have a higher severity [28-30].

### **2.2.2 Primary and secondary brain damage post-TBI**

Brain damage post-TBI includes primary and secondary injuries. Primary TBI occurs as a result of the inflicted mechanical force, and involves impact on the skull and tissue disruptions at the point of injury. These deformations include damage to axons, neurons, blood vessels and glial cells. The extent of damage can be in a focal, multifocal or diffused pattern, with focal and diffused patterns co-existing in most cases. Secondary brain injury follows the primary impact. It is also initiated at the moment of injury, but requires a longer manifestation time. It encompasses the complex cellular and biochemical alterations initiated in the brain after the primary impact, and develops over a period of hours, days, or weeks [26, 31]. These alterations include changes in the cerebral blood flow, organization of the blood-brain barrier (BBB), cerebral metabolism and ion homeostasis, or direct toxic effects on neuronal and glial cells [27].

### **2.2.3 Mechanisms of epileptogenesis associated with secondary injury**

Secondary injuries associated with TBI trigger epileptogenic processes in the brain, leading to abnormal neuronal reorganisation, such as neurodegeneration, neurogenesis, axonal sprouting and injury, glial cell activation, invasion of peripheral inflammatory cells, vascular damage, angiogenesis and alterations in the structure of cellular components like ligand and receptor-gated ion channels, reviewed in [32]. Acute symptomatic SE is a major epileptogenic factor associated with the after-effects of TBI, and has been reported to be the cause of symptomatic epilepsy in 41% TBI cases [33].

Neurons tend to depolarize in response to the trauma, associated with release of excitatory neurotransmitters such as aspartate and glutamate. This leads to opening of the NMDA receptor associated ion channels and massive influx of  $\text{Ca}^{2+}$  ions. Consequently, down-regulation of glial glutamate transporter proteins GLAST and GLT-1, responsible for clearing glutamate from the extrasynaptic space is observed, indicating that increase in tissue glutamate concentration can contribute to excitatory neuronal activation [34]. The post-traumatic  $\text{Ca}^{2+}$  influx results in cytoskeletal collapse via inactivation of oxidases, generation of free radicals and reactive oxygen species (ROS), mitochondrial dysfunction, cytoskeletal protein degradation and damage to the neuronal cell structure [35]. Upregulation of genes responsible for apoptosis and production of stress proteins, such as the heat shock proteins (HSPs) is also observed. HSPs are responsible for proper folding and intracellular transport of damaged proteins, indicating that traumatic injury is associated with abnormal protein production in the brain. Additionally, upregulation of HSPs in response to TBI serve as potential diagnostic markers [36]. Secondary damage initiates alterations in the immunogenic architecture as well, such as infiltration and accumulation of polymorphonuclear leukocytes in the brain, activation of microglial cells and release of inflammatory cytokines-  $\text{TNF}\alpha$  and interleukins, thereby inducing injured tissue repair, along with neuroinflammatory responses [37].

Biomechanical/biochemical effects of the injury are also reported to alter the composition of neuronal plasma membrane. This leads to changes in ion channel configurations, alterations in  $\text{Na}^+$ ,  $\text{K}^+$  and  $\text{Ca}^{2+}$  currents, thereby enhancing neuronal excitability. The principal inhibitory neurotransmitter that counterbalances effects of the excitatory amino acids,  $\gamma$ -aminobutyric acid (GABA) and its receptor  $\text{GABA}_A$ , are in turn observed to be reduced in the hippocampus along with cell loss in response to

trauma. In experimental TBI and SE models of epilepsy, loss of GABAergic interneurons have been observed, with a significantly higher rate in TBI rat models. However, correlation between the severity of hippocampal interneuron loss and risk for spontaneous seizure development is not yet established [38].

Studies have revealed that genetic susceptibility may also be crucial in increasing the risk of acquiring epilepsy after a head trauma. For instance, patients with a decreased level of serum haptoglobin possess an inherent predisposition towards PTE [39]. This is because haptoglobins are acute phase glycoproteins that reduce oxidative stress by forming stable complexes with haemoglobin and sequestering free iron. Impairment of haptoglobin synthesis would thus increase ROS concentration in the brain and induce seizure susceptibility. Another such example is the association of Apolipoprotein E (APOE) allele APOε4 inheritance with increased likelihood of developing post-traumatic seizures (PTSs) after encountering moderate to severe brain injuries [40]. However, these genetic associations are not established in other observational studies [41]. Also, it is not known if genetic predisposition is responsible for some patients with TBI developing PTE, whereas others with similar extent of injury not developing the phenomenon.

#### **2.2.4 Animal models for TBI**

*Disease or syndrome modification* usually refers to a therapeutic approach that alters the development or progression of a disease. In case of epilepsy, treatment methods aimed at disease or syndrome modification are termed as antiepileptogenic processes. Antiepileptogenic treatments thus aim at: (a) preventing or delaying the development of epilepsy (lower percentage of subjects developing epilepsy or enhancing the latency period), (b) seizure modification (shorter and less frequent seizures), and (c) cure. Such treatments could also modify comorbidities such as improvement of memory and cognitive responses. However, current treatment methods for epilepsy predominantly include AEDs that suppress seizure frequency, but trials with AEDs as antiepileptogenic agents have not quite been successful. Thus, alteration or prevention of epileptogenic processes is still an unmet challenge [32, 42].

Developing animal models that mimic human epileptic forms is thus of high clinical significance. These models would allow large scale molecular profiling studies, and would also provide insights into the mechanisms involved in ictogenic neuronal reorganization and effects of AED treatments on the epileptic brain. However, one major challenge in comparing studies with such models is the inherent variability caused due to differences in the number of animals being used to obtain significant statistical power, the species or strains being used, analysis of different brain structures, use of varied methods to induce epileptogenesis, and selection of different timepoints for analysis. To optimise these inherent variabilities and to improve comparisons among different studies, it is important to define common data elements (CDEs) for each study. CDEs are standardized terms that describe the type of data being collected, but not the data itself [43]. The advantages of defining CDEs are as follows:

- to identify discrete, defined items for data collection
- to promote consistent data collection
- to eliminate unnecessary and redundant data collection

- to promote consistent reporting and analysis
- to reduce the possibility of error related to data translation and transmission
- to facilitate data sharing

Since the underlying mechanisms of epileptogenesis are not well understood, experimental models play an important role in understanding the complex changes associated with epileptogenic phases [27, 44]. Prolonged latency periods and spontaneous late seizures, for instance in cases of PTE, makes in-vivo animal model studies further important. Such models should follow certain criteria such as:

- Replicate the type of injury observed in human patients
- Employ standardised experimental protocols including control (uninjured) animals for control of systemic variables
- Replicate the neuronal circuitry reorganisation as observed in human PTE
- Have a latent period between the insult and generation of unprovoked seizures
- Display spontaneous, recurrent seizures as a final result of the structural and functional neuronal reorganisation occurring during the latent period

Different animal models have been developed to study molecular and cellular alterations involved in epileptogenesis associated with TBI. The weight drop model, for instance, creates seizure susceptibility towards pentylenetetrazol (PTZ), a proconvulsant drug, when administered in high doses. Histological alterations in this model include progressive mossy fiber sprouting and hippocampal neuron loss [45]. Parasagittal FPI has been associated with neuronal loss, reactive gliosis and calcification in the thalamus and temporal neocortex immediately after TBI (acute phase), along with hippocampal cell loss and mossy fiber sprouting at later timepoints [46, 47]. Controlled cortical impact (CCI) is a model of closed head injury that mimics the key behavioural, functional and anatomical features of human PTE and TLE. The closed skull midline impact model is associated with lowering of seizure threshold in mice, with enhanced astrocyte and microglial activation [9].

FPI is the most widely studied model for human closed brain TBI. Lateral FPI has been observed to produce cortical contusions along with intraparenchymal and subdural hematomas in the rat brain, characteristics associated with an increased risk of PTE. At a cellular level, the model induces progressive cortical cell loss, hippocampal sclerosis, cytokine mediated neuroinflammation, reactive gliosis and alterations in ROS levels in the brain [27]. Data suggest that this model of brain injury reproduces the entire spectrum of secondary injury, neuronal circuit reorganization and neuropathophysiological features of epileptogenesis associated with human PTE.

The FPI model involves exposing a part of the skull by trephination through which the injury is produced. The impact is created by a rapid fluid bolus that strikes the intact dura through the exposed area of the skull, with diffusion into the epidural space concentrically from the injection area. The position of the craniectomy affects the location and size of the brain lesion produced. The midline FPI produces contusions directly at the site of impact with compression of the brainstem structures, resulting in coma like behaviour in case of a severe injury [48]. If the pressure impulse is induced adjacent to the sagittal suture, it produces both ipsilateral and contralateral damage. However, shifting the site laterally

associates with more ipsilateral damage, correlating with the increase in distance from the sagittal suture.

### **2.3 Post-traumatic epilepsy (PTE) as a consequence of TBI**

PTE is the most frequent complication associated with TBI. It is defined as a recurrent seizure disorder as a consequence of severe brain insult. In most cases, susceptibility to PTE positively correlates with the severity of injury [49], with a higher mortality rate in case of moderate-to-severe head injuries coupled with SE [50]. TBI is estimated to cause about 5% of all epilepsies and 20% of symptomatic epilepsies [51], and is the predominant cause of acquired epilepsy in youths [25].

Seizures occurring after TBI are categorized as immediate (<24 hours), early (1–7 days), or late seizures (>1 week after TBI). The immediate and early PTSs are often non-specific and result from the severity of the injury itself, whereas late seizures occur as a consequence of the epileptogenic pathology [42, 52]. TBI associated with more than one unprovoked late seizure thus qualify for PTE diagnosis. Early seizures mostly occur as an impact of the injury severity, and are presumed to have a different pathogenesis than the later counterparts, but in some prolonged cases, they can also play a role in epileptogenesis. The factors identifying patients with higher susceptibility to PTE include early post-traumatic seizures and incidents of severe head injury, such as penetrating insults, intracranial/intracerebral hematoma, skull fracture, haemorrhagic contusion and LOC for more than 24 hours [52, 53].

An essential clinical feature of PTE is the latency period. *Latency period* refers to the time between an insult and occurrence of the first unprovoked seizure [32]. Latency to the first late unprovoked seizure depends on the injury severity as well [54]. The risk is maximum in the first year after trauma, and decreases gradually with progression of time. However, the exact duration of this period is unknown, since the risk remains even up to 10-20 years after the injury [49]. *Epileptogenesis*, on the other hand, is the gradual process whereby normal brain is transformed into a state predisposed towards spontaneous, recurrent seizures through initiation and maturation of the epileptogenic focus. It is a slow process involving histological and biochemical changes in the brain tissue over months and years after the insult [27]. The neurobiological alterations occur sequentially, as well as in a complex interaction during this phase. Epileptogenesis is not synonymous to latency period, since the abnormal neuronal reorganisation occurring during the latency period continues to progress even after epilepsy has been diagnosed [55]. Thus, epileptogenesis is re-defined as the development and extension of tissue capable of generating spontaneous seizures, including (a) development of an epileptic condition and (b) progression after the condition is established [32]. Evidences also support the relevance of inflammation in epileptogenesis, particularly in transforming the neuronal architecture from normal to a seizure generating one [14].

Clinical diagnosis of PTE in patients requires occurrence of a head trauma and no history of seizures prior to the injury. Also, the brain insult must be identified as the sole reason for seizures, excluding

other possibilities such as hypoxia, ischemia, alcohol withdrawal and others. The major diagnostic indicator of PTE is an abnormal electroencephalography (EEG) recording, with sleep EEG being more likely to show abnormal ictal spikings than waking EEG. However, sensitivity of this method is low and often patients with PTE do not demonstrate significant abnormal EEG spikings [56]. Followed by EEG, magnetic resonance imaging (MRI) and positron emission tomography (PET) can be used to identify structural damages in the brain and location of the epileptogenic focus. However, not all patients with recurrent seizures demonstrate an underlying pathology, and vice versa, thus reducing the sensitivity of these imaging techniques.

## **2.4 Importance of biomarkers in characterization of TBI and epilepsy**

### **2.4.1 Characteristics of an ideal biomarker**

The term “biomarker” refers to a broad subcategory of medical indications that define the current health condition of a person. According to the National Institutes of health (NIH), a biomarker is a characteristic that is objectively measured and evaluated as an indicator of normal biological processes, pathogenic processes, or pharmacologic responses to a therapeutic intervention or other health care intervention. The biomarker is either produced by a diseased organ, or by the body in response to disease. The biomarker concept has gained immense scientific and diagnostic value, typically along the whole spectrum of the disease process. Prior to diagnosis, they can be used for susceptibility and risk assessment. For diagnosed patients, biomarkers can help in determining the current stage of disease development, and for selection of appropriate therapy. During the treatment phase, monitoring biomarker levels can provide insights related to treatment effects and disease recurrence [57].

### **2.4.2 MicroRNAs as biomarker candidates for diagnosis of TBI and epilepsy**

Along with administration of AEDs for seizure suppression, treatment methods in epilepsy now also focus on biomarker identification for determining at-risk patients of epilepsy suffering from brain insults, for characterization of epileptogenic progression, as well as to determine effects of implemented therapeutic approaches. A plausible approach to characterize biomarkers for epileptogenic progression involves studying global changes in transcriptome to identify metabolic pathways that are altered during epileptogenesis. Apart from gene expression analysis, recent studies also stress on determining changes in miRNA profiles, since they are powerful players in regulating and fine tuning gene expression [5]. It is predicted that miRNA alterations occur much earlier in response to a disease state than conventional protein biomarkers, thus making them crucial for detection in early stages of disease development [17]. Current data related to the role of miRNAs in determining both severity of brain injury and identification of epileptogenic progression is limited, prompting the need for extensive research in this new dimension of post transcriptional regulation.

MicroRNAs (miRNAs) are a small class of non-coding RNAs (~20-24bp length) that regulate developmental processes at the post transcriptional level, through degradation of messenger RNAs (mRNAs) or by translational repression. Most of the miRNAs are transcribed by RNA polymerase II, with a minor fraction lying within the repetitive region of the genome, transcribed by RNA polymerase III. The

primary miRNA transcripts (pri-miRNAs) are then processed in the nucleus and later in the cytosol by the Drosha and Dicer enzymes respectively. Processing of the pri-miRNAs by Drosha yields a miRNA precursor (pre-miRNA) of ~70 nucleotides in length, which undergoes further processing by Dicer to produce a mature double-stranded miRNA [58]. One strand of this mature miRNA duplex, termed as the guide strand, associates with the RNA-induced silencing complex (RISC), and the other strand (passenger strand) is unwound and eventually degraded under most circumstances. The miRNA-RISC complex then interacts with the mRNA targets through partial sequence complementation, typically within the 3' untranslated region of target mRNAs. It is predicted that the extent of the complementary base pairing between a miRNA and its mRNA target determines mRNA degradation or translational repression. However, unlike small interfering RNAs (siRNAs) miRNAs can also enhance mRNA translation and induce positive regulation of gene expression by binding to the target gene promoter [15, 59].

Apart from cellular miRNAs, extracellular circulating miRNAs have also been observed in body fluids, such as serum/plasma, urine and cerebro-spinal fluid (CSF). Interestingly, serum and other body fluids are known to contain ribonucleases, indicating that in some cases, the secreted miRNAs are probably packaged in enclosed vesicles, to protect them against ribonuclease (RNase) digestion. For instance, this might include miRNA packaging in exosomes and microvesicles. The origin and function of these circulating extracellular miRNAs is not completely understood. However, one intriguing idea is that the extracellular miRNAs may be involved in paracrine signalling and cell-cell communication [58].

In humans, it is estimated that miRNAs regulate as much as 60% of mRNAs, and one miRNA can control the expression of multiple genes. The human brain exhibits an exceptionally high miRNA expression level, suggesting significant association between neurological disorders and miRNA dysfunction [5]. Changes in miRNA expression levels have already been evident in pathogenic conditions like ischemia, Alzheimer's disease, and epilepsy [5, 14, 60-62].

Alterations in miRNA expression have been observed in TBI, and are predicted to play a role in TBI mediated PTE. At acute timepoints following severe injury, significant alterations in plasma miRNA profiles have been observed in human patients. Interestingly, the patterns of miRNA expression alteration associated with moderate injury, in comparison with severe cases, have been different [63], indicating variations in miRNA expressions to be dependent on injury severity. Additionally, significant alterations in expression of miRNAs have also been evident in clinically relevant animal models of TBI [64-67].

Along with PTE, the brain expresses significant aberrations in miRNA levels in other forms of epilepsy as well [16]. Moreover, miRNA profiling from different brain regions in epilepsy have demonstrated variations in expression pattern, indicating that changes in miRNA expression are not only time-dependent during epileptogenesis, but also region specific [61]. Variations in miRNAs associated with synaptic plasticity, neuronal development and higher brain functions, along with dicer loss have been considered as important factors for progression in epileptic conditions [14, 68].



However, routine biopsies from an organ is not a practical option, for instance, while studying susceptibility towards development of epilepsy in individuals immediately after brain injury. Also, imaging techniques prove to be of limited success. This underscores the importance of profiling brain enriched biomarkers through other non-invasive techniques. The clearance mechanisms of brain release brain-specific components in systemic circulation. In association with injury induced neuropathological developments, production of these brain-specific components is altered, and such changes are reflected in body fluids like CSF and blood. This leads to the hypothesis that profiling circulating brain-enriched components (e.g. miRNAs) from biofluids may serve to study injury severity and epileptogenic phases.

### **2.4.3 Known miRNA biomarkers in TBI and epilepsy**

Differential expression of miRNAs has been observed in human TLE cases, as well as in animal models with induced epileptic conditions. Particularly, the differentially expressed miRNAs have been associated with inflammation, development, pro-apoptotic and neuronal death associated functions in epilepsy models [15]. Some of the epilepsy specific miRNAs include miR-146a, miR-34a, miR-134, miR-132 and miR-21 [14], all of which have been validated in two or more independent studies. Upregulation of miR-146a has been observed in experimental models and human TLE, suggesting its potential role in TLE pathogenesis [69]. Similarly, upregulation of miR-34a and miR-134 has been observed in SE based epileptic models [70, 71], and targeting these miRNAs with specific antagomirs have produced neuroprotective effects, with reduced seizure severity. MiR-21 plays a major role in various inflammatory signalling pathways, and has become a promising target for inflammation associated disorders [14]. Antagomirs targeted against miR-132 have not demonstrated reduction in seizure severity, but demonstrated neuroprotective effects by reducing neuronal cell death in the CA3 region of the hippocampus post-injury [72].

Post-TBI, significant up-regulation in plasma levels of miR-765 and down-regulation of miR-16 and miR-92a have been observed in severe cases (GCS  $\leq$  8), whereas elevated levels of miR-16 and miR-92a have been observed in moderate cases (GCS > 12) [63]. Up-regulation in miR-21 has also been observed in rats subjected to lateral FPI, and predicted to be associated with improved neurological outcome [73].

MicoRNA-124 is one of the most abundant and highly conserved miRNA in human and rodent brain, forming about 25-48% of all brain-specific miRNAs [74]. Expression of this miRNA is considered crucial during neuronal differentiation and development [75-78]. Particularly, miR-124 suppresses the expression of PTBP1 protein, a global repressor of neuronal cell development, thereby promoting neuronal specific differentiation [79]. Along with other miRNA targets, some studies have revealed upregulation of miR-124 as well, in acute and chronic phases of mesial temporal lobe epilepsy (MTLE), followed by return to normal levels in the latent phase, indicating that expression of miR-124 is altered in seizure associated stages [14]. Significant up-regulation of miR-124 has also been identified at acute timepoints post brain injury, in animal models of stroke [75, 80]. Based on these earlier observations that characterized miR-124 as a potential biomarker candidate for stroke-induced brain damage and epileptogenesis, this study was planned to investigate the temporal patterns of miR-124 expression in rats subjected to lateral FPI.

## 2.5 Challenges in profiling miRNAs from serum/plasma and other biofluids

Circulating miRNAs from serum, plasma and other biofluids serve as potential minimally invasive diagnostic biomarkers. Though limited in number, miRNAs have been observed to be relatively stable in biofluid samples, presumably due to its complex formation with argonaute proteins, or due to packaging in cellular vesicles. They exhibit resistance to nuclease digestion, extended storage, repeated freeze-thaw cycles and variable pH, making them promising biomarker candidates [15]. MiRNA levels in blood have been found to be reproducible and indicative of the current disease state. However, profiling miRNAs from biofluids is relatively complicated based on several factors. Firstly, plasma and serum are cell free samples, meaning that the total RNA content is significantly low for appropriate OD measurements in NanoDrop or quality control in Agilent Bioanalyzer systems. Secondly, when interested in extracellular circulating miRNAs, it is important to avoid haemolysis to prevent cellular RNA contamination. Thirdly, biofluid samples contain high amounts of reverse transcriptase and polymerase enzyme inhibitors. Thus, increasing the starting volume of serum/plasma does not simply lead to increased miRNA yield. Minimising carry-over of the inhibitors to the downstream applications also becomes a major obstacle. Finally, normalization of the miRNA PCR profiles become challenging due to lack of suitable endogenous controls. Larger small RNA species, such as U6 and 5S rRNA are commonly used as reference genes, but they are expressed within cells and at a much higher level than most miRNAs. On the contrary, their concentration in serum, plasma and other cell-free biofluids is significantly low. Also, they are much larger in size than the miRNAs and may exhibit very different behaviour during extraction and reverse transcription [81].

Collection of whole blood forms the first step in plasma/serum preparation. EDTA, citrate and heparin are the common anticoagulants used in preparation of plasma, but to avoid downstream inhibition in cDNA synthesis and PCR steps, EDTA is preferred over citrate and heparin. Since biofluid samples contain only small amounts of RNA, a significant portion tends to get lost during the extraction procedure. The miRNAs are also in most cases bound to argonaute or lipoproteins, or are enclosed in exosomes, microvesicles or extracellular vesicles. Isolation of miRNAs from these complexes add to the methodological challenges of miRNA extraction. Adding carrier RNA during this step is thus a common experimental approach to obtain consistent yields. RNA from bacteriophage MS2 is typically used as it is free from miRNAs. Presence of this carrier makes measurement of miRNAs in the biofluid sample through spectrophotometric methods impossible. Also to monitor the efficiency of RNA isolation, cDNA synthesis and PCR amplification processes, exogenous synthetic RNA spike-ins are commonly added in each step of miRNA profiling [81].

Since measuring miRNA levels in body fluid samples is complicated by extremely low RNA concentrations, determining the suitable amount of input RNA for downstream reverse transcriptase and PCR reactions becomes impossible, making cross platform comparisons challenging. Thus, instead of RNA concentration of the sample, total biofluid input in the RNA isolation step, and subsequent dilutions in cDNA synthesis and PCR reactions are measured to obtain an estimate of the starting concentration.

Another complexity involved in miRNA expression profiling is that although several miRNAs show differential expression in diseased condition, identification of a unique, disease-specific alteration

pattern is quite complicated. Often, variations in extraction methods and downstream analysis steps induce alterations in these expression patterns. Also, when using extracellular, circulating serum/plasma miRNAs as biomarkers, identifying the exact source of these miRNAs become quite challenging. Additionally, the amount of starting material acts as a limiting factor, since smaller volumes of clinical biofluid samples are typically obtained from patients, and increasing the starting volume can in turn enhance effects of the inhibitors [17].

Normalisation of miRNA PCR profiles is another significant step. The purpose of most miRNA profiling studies is to investigate the differences in miRNA expression as a response to different biological conditions, rather than mere technical variability of sample handling and downstream extraction methods. Therefore, normalisation of the miRNA profiles is essential to mask technical variability, and to make the biological differences obvious. This involves selecting the optimal reference gene or a combination of reference genes to normalize the miRNA qRT-PCR results. One plausible approach in studies involving few miRNAs is to choose candidate references through extensive literature review, or select stably expressed endogenous controls from previous experimental studies. Characteristics of a good endogenous control candidate are as follows:

- Invariant expression across all samples included in the study, irrespective of the experimental or disease conditions
- Similar expression level to that of the miRNA of interest in the study
- Similar size as that of the target miRNA

Suitability of a reference gene varies with cell/tissue types being studied. Thus it is important to perform an experimental validation to choose the most suitable endogenous control for a specific study. The candidate references most commonly used for miRNA profiling include hsa-miR-103, hsa-miR-423-3p, hsa-miR-423-5p, hsa-miR-191, hsa-miR-16, hsa-let-7a and others [82].

## **2.6 Droplet Digital PCR in quantification of circulating miRNAs**

### **2.6.1 Advantages of ddPCR over qRT-PCR**

The main aim of digital PCR techniques is to carry out absolute nucleic acid quantification based on partitioning the target molecule into individual replicate reactions at limiting dilution [83]. In particular, the ddPCR technology is developed to provide high-precision and absolute quantification of the target sequences, with wide-range applications in research and diagnostic fields. The ddPCR protocol has been successfully used with both probe based TaqMan assays and EvaGreen dye based assays, but not yet with SYBR Green systems [84, 85]. It is an end-point measurement method based on partitioning the reaction mixture into thousands of nanoliter sized oil emulsion micro droplets. This massive partitioning enables reliable quantification of small fold differences in target concentration across samples. Also the quantification process is made simpler, since instead of relative quantification based on standard curves and endogenous controls (as performed in qRT-PCR), ddPCR measures absolute concentration of the target in a sample by estimating target copies per  $\mu\text{L}$  of the input sample. Thus it

avoids the requirement of external calibrators, factors of critical importance while profiling circulating miRNAs from biofluids with qRT-PCR. In addition, the technology has been proved to be more tolerant to RT and PCR inhibitors than qRT-PCR.

In miRNA profiling studies, the ddPCR technology has consistently shown lower day-to-day variation in results across replicates and greater precision than real time PCR, but with comparable sensitivity [83]. In statistics, precision or positive predictive value is defined as the proportion of true positives against all positive results obtained. Sensitivity, or true positive rate, defines the proportion of true positives that are correctly identified. Mathematical definitions for precision and sensitivity are as follows:

$$\textit{Precision} = \frac{\textit{number of true positives}}{\textit{number of true positives} + \textit{false positives}} \quad (1)$$

$$\textit{Sensitivity} = \frac{\textit{number of true positives}}{\textit{number of true positives} + \textit{false negatives}} \quad (2)$$

Since biofluid samples contain very low amounts of RNA, as well as higher concentration of inhibitors, ddPCR technology is believed to provide more sensitive results than qRT-PCR reactions, in quantification of rare circulating miRNAs from limited amount of starting material.

### 2.6.2 Principle of ddPCR

Prior to droplet generation, the reaction mixture is prepared in a manner similar to qRT-PCR. For TaqMan systems, hydrolysis probes labelled with FAM and HEX (or VIC) reporter fluorophores are used, whereas intercalating dyes are used in EvaGreen systems. The reaction mixture consists of ddPCR supermix for probes (for TaqMan systems) or ddPCR EvaGreen supermix, template DNA or cDNA, and template specific PCR primers. Droplet generation oil for probes or for EvaGreen chemistry are used accordingly. The droplet generator combines water-oil emulsion droplet technology with microfluidics for droplet generation. It partitions the reaction mixture into ~20,000 emulsion droplets of nanoliter size. Each droplet acts as a PCR reaction system with either 0, 1 or more copies of the target sequence. Droplets with uniform size and volume are produced, enabling unbiased quantification. PCR amplification within each droplet is carried out in a thermal cycler, followed by quantification of fluorescent positive or negative droplets in the QuantaSoft software. Droplets are assigned as positive or negative based on their fluorescence amplitudes with respect to an automatically determined threshold. Manual alteration of the threshold is also possible in the software for defining positive and negative amplitudes. Positive droplets contain at least one copy of the target DNA molecule, whereas negative droplets possess none. Since the sample is randomly partitioned into discrete droplets, a Poisson distribution based on the fraction of positive partitions is applied to determine target concentration [86]. The formula used for Poisson modelling is [87]:

$$\textit{Copies per droplet} = -\ln(1-p), \textit{ where } p = \textit{fraction of positive droplets} \quad (3)$$

### 2.6.3 TaqMan® and EvaGreen chemistries in PCR reactions

Both real time and ddPCR techniques are able to quantify target amplification using TaqMan and EvaGreen based chemistries. TaqMan method is based on measuring the fluorescence intensity of hydrolysis probes to estimate target amplification in a PCR reaction. The TaqMan probe consists of a

fluorophore covalently attached to the 5'-end of the oligonucleotide probe and a quencher at the 3'-end. In the bound state, the quencher molecule remains in proximity to the fluorophore, and quenches the fluorescence emitted by the fluorophore. During PCR reaction, the probe anneals to the single stranded target DNA downstream of the primer binding site, within the amplification region. As the *Taq* polymerase extends the primer and synthesizes the nascent strand, it degrades the probe annealed to the template. Degradation of the probe releases the fluorophore from the quencher, thus emitting the fluorescence signal. In real time PCR, the intensity of the fluorescence signal is directly proportional to the amount of DNA template present in the sample. In droplet digital technology, each droplet that emits this signal is considered to possess at least one copy of the target, and are included in copy number calculations.

EvaGreen, on the other hand, is a DNA binding dye that intercalates with double stranded DNA (dsDNA). In its native free state, the dye displays a relatively low fluorescence. When bound to dsDNA, the fluorescence intensity increases by about 1000 fold. Thus, the fluorescence intensity is directly proportional to the concentration of double-stranded DNA in sample. In PCR reactions, as the concentration of the target in the sample increases exponentially, the number of binding sites for EvaGreen dye increases, and it can be measured by the proportional increase in fluorescence intensity. Designing PCR reactions with DNA binding dyes are usually simpler than probe based methods, and relatively inexpensive and flexible than the latter. However, one inherent disadvantage is the non-specific binding of the dye to any double stranded amplicon. This can be avoided to some extent by performing the melt curve analysis after qRT-PCR run. Since the melting temperature for each amplicon is different due to differences in length and sequence composition, this analysis can be used to detect off-target amplifications. SYBR Green follows similar DNA binding chemistries, but EvaGreen is usually preferred over SYBR Green since it is less inhibitory to PCR and less toxic.

## **2.7 Cresyl violet staining for analysis of brain cytoarchitecture in epilepsy**

Cresyl violet staining is a common method implemented for identification of neuronal structures in the brain and spinal cord. This method uses a basic aniline dye that stains ribosomal RNA of endoplasmic reticulum. Since both neurons and glial cells possess the endoplasmic reticulum, they uptake the stain. In case of brain injury, this staining method is frequently performed to characterize histological changes in response to the injury, such as neuronal cell loss and development of brain lesions. For instance, reduction in hippocampal areas and cell loss in CA1 and CA3 regions, in epilepsy cases, have been detected with this staining method [88]. In this study, cresyl violet staining was implemented to characterize brain lesion size post-TBI.

### **3 AIMS OF THE STUDY**

#### **3.1 Objective**

The main objective of this study was to set up the ddPCR technique for profiling expression of a brain enriched miRNA, miR-124, from plasma obtained from tail vein of rats subjected to lateral FPI. MicroRNA profiling was performed at baseline (prior to injury), acute and chronic timepoints, to study the temporal pattern of miR-124 expression, and to identify if the levels of miR-124 in plasma can act as a biomarker of TBI at acute and/or chronic timepoints. Levels of miR-124 in plasma in relation with the brain lesion size developed as an impact of injury was also inspected. Additionally, sensitivity of both qRT-PCR and ddPCR techniques in quantifying miR-124 from plasma was compared.

Along with plasma profiling, analysis of miR-124 was also performed on brain tissue samples (ipsilateral cortex) of a separate cohort of animals subjected to the same model of TBI, only at 3 months post-injury (figures 1 and 2).

#### **3.2 Hypotheses tested**

Up-regulation of miR-124 has already been observed at acute timepoints in animal models with middle cerebral artery occlusion [75, 80]. Some studies also identify it as an early biomarker of haemorrhagic stroke in humans, possibly indicating cell death and disruption of the BBB at stroke onset to be responsible for release of miR-124 in systemic circulation [89]. In our previous study of miR-124 expression profiling in blood, up-regulation has also been observed, in rats subjected to lateral FPI, at 2 days post-injury [18]. Based on these previous observations, it was hypothesized that plasma levels of brain enriched miR-124 may also serve as a potential diagnostic marker of TBI.

Along with this, from already published study reports, it was presumed that ddPCR would prove to be more sensitive than qRT-PCR in profiling low abundance miRNAs from plasma samples [83]. Both these hypotheses were tested in this work.

#### **3.3 Specific questions addressed**

The specific questions addressed in the study were as follows:

1. To check if the plasma level of brain-enriched miR-124 can be used as a diagnosis marker for TBI in acute and/or chronic timepoints after injury.
2. If droplet digital PCR (ddPCR) can provide higher sensitivity and precision than quantitative reverse-transcription PCR (qRT-PCR) in assessing plasma level of miR-124 at different timepoints.
3. To check if the plasma level of miR-124 in an acute timepoint after TBI can predict histological changes found in a chronic timepoint after TBI.

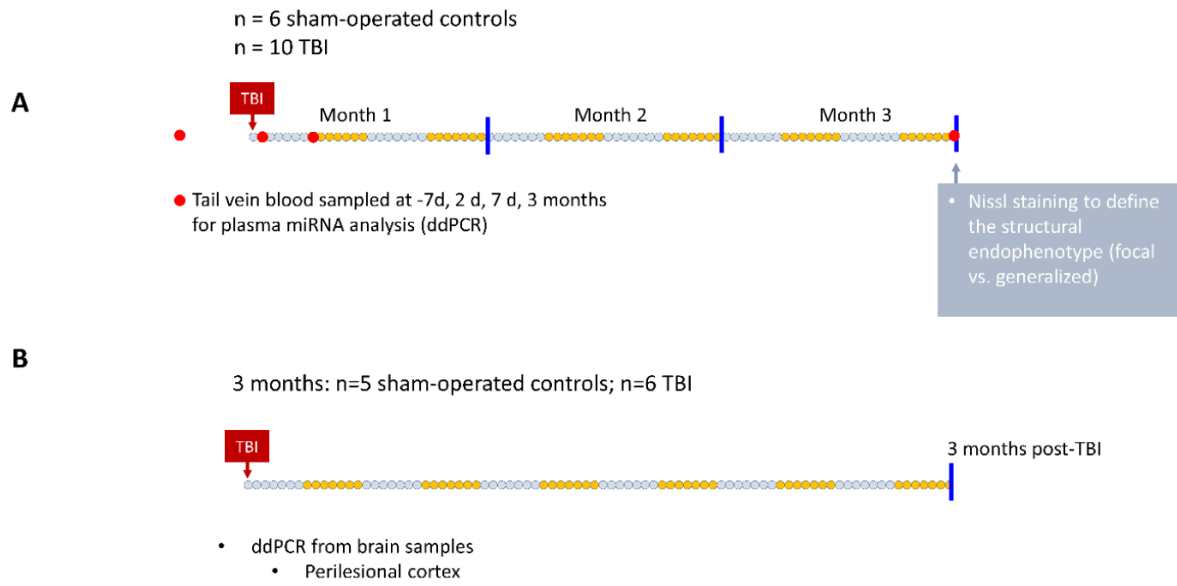
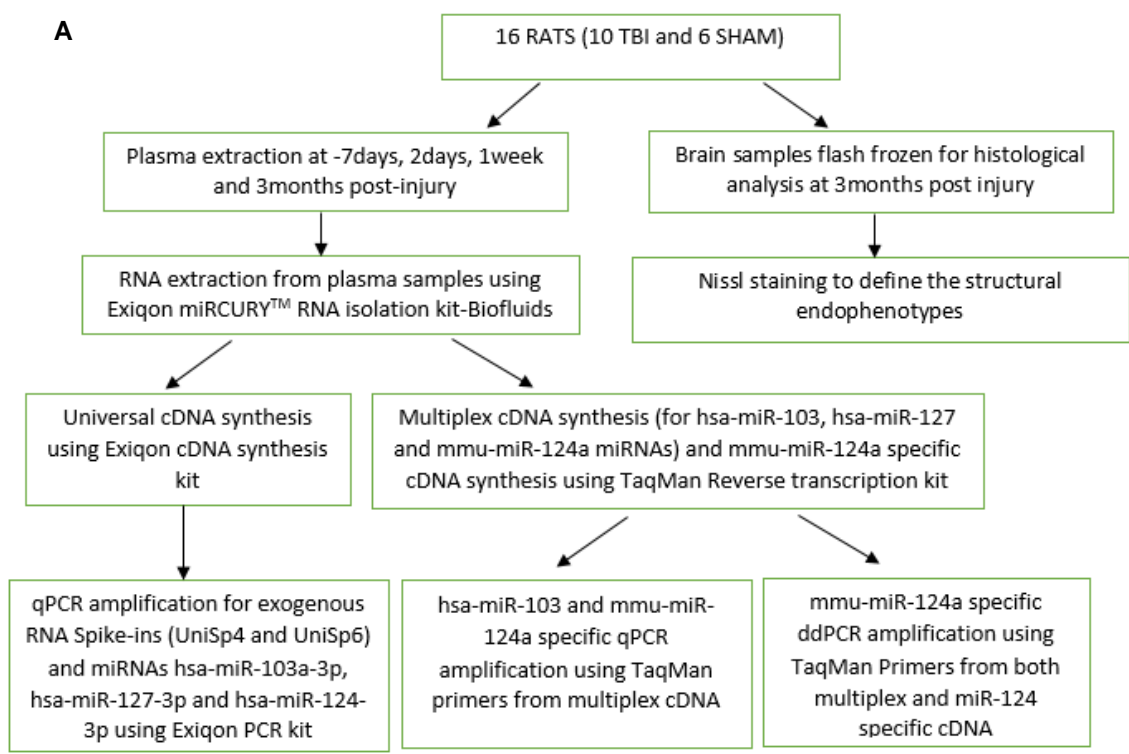


**Figure 1: Study design for miR-124 profiling from (A) cohort A: tail vein plasma samples, (B) cohort B: brain tissue (ipsilateral cortex) samples**



**B**

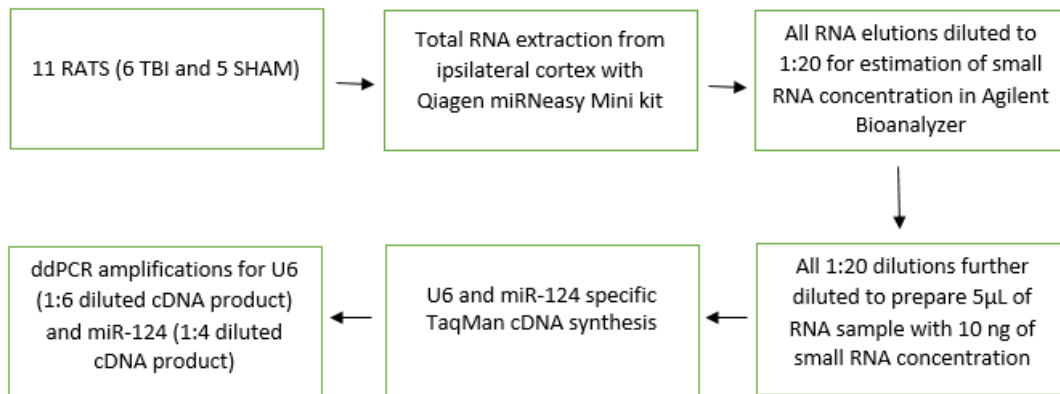


**Figure 2: Implemented methodology for (A) miR-124 profiling from plasma and Nissl Staining in cohort A, (B) miR-124 profiling from ipsilateral cortex in cohort B**



## **4 MATERIALS AND METHODS**

### **4.1 Animals**

Adult male Sprague-Dawley rats (Harlan Netherlands B.V., Horst, The Netherlands) were used in this study. All rats were individually housed in a controlled environment (temperature  $22\pm 1^{\circ}\text{C}$ , humidity 50-60%, lights on from 07:00 to 19:00 h). Pellet food and water were provided *ad libitum*. All animal procedures were conducted in accordance with the guidelines of the European Community Council Directives 86/609/EEC and Committee for the Welfare of Laboratory animals.

### **4.2 Procedure for induction of lateral FPI**

Induction of TBI was performed according to the lateral FPI protocol [9, 53]. Animals were placed in a Kopf stereotactic frame (David Kopf Instruments, Tujunga, CA, USA). First, the skull was exposed with a midline incision followed by extraction of the periosteum. The left temporal muscle was detached from the lateral ridge and then a circular craniectomy ( $\varnothing$  5 mm) was performed over the left parietal lobe midway between lambda and bregma keeping the dura mater intact. The edges of the craniectomy were sealed with a modified Luer-Lock cap that was filled with saline while the calvaria was covered with dental acrylate (Selectaplast CN, Dentsply DeTrey GmbH, Dreieich, Germany). Lateral FPI was induced 90 minutes after the administration of anesthesia by connecting the rat to the fluid-percussion device (AmScien Instruments, Richmond, VA, USA), via a female Luer-Lock fitting. For control animals, anesthesia and all surgical procedures were performed, except for the induction of lateral FPI.

### **4.3 Sample preparation for microRNA analysis**

#### **4.3.1 Extraction of plasma for miR-124 profiling**

The study was performed on a cohort of 16 rats (cohort A: 6 control and 10 TBI), with an average body weight of 375 g (360-385 g). For inducing the lateral FPI, rats were anesthetized with an intraperitoneal (i.p) injection, containing a solution of sodium pentobarbital (58mg/kg), magnesium sulphate (127.2 mg/kg), propylene glycol (42.8%) and absolute ethanol (11.6%). A severe impact of about  $3.15 \pm 0.02$  atm (3.05 – 3.25 atm) pressure was induced. There was no incidence of mortality as a result of the impact (figure 3(A)). For each animal, blood collection and plasma miRNA profiling was performed at four different follow-up time-points: baseline (1 week prior to injury), 2 days, 1 week and 3 months post-injury. For blood sampling, rats were anesthetized with 4% isoflurane and 500 $\mu\text{L}$  of tail vein blood was collected in K2-EDTA tubes (Product code: 368841, BD Vacutainer<sup>®</sup>, Belliver Industrial estate, Plymouth UK). The samples were immediately processed by centrifuging at 1500 x g for 10 minutes at  $4^{\circ}\text{C}$ . Plasma was extracted and stored in aliquots of 50 $\mu\text{L}$  at  $-70^{\circ}\text{C}$  until further use. At 3 months post-injury, the rats were deeply anesthetized with 4% isoflurane and decapitated with guillotine. Brains were quickly extracted and flash frozen in  $-70^{\circ}\text{C}$  isopentane, followed by subsequent storage at  $-70^{\circ}\text{C}$  until further use.

#### 4.3.2 Extraction of brain tissue for miR-124 profiling

This study was performed only at a 3 months post-injury timepoint. A separate cohort of 11 rats were used for this purpose (cohort B: 5 control and 6 TBI). The initial set consisted of 30 healthy adult rats with an average body weight of 326 g (300-354 g), out of which 18 were subjected to the lateral FPI (figure 3(B)). The rats were anesthetized with an intraperitoneal (i.p) injection, containing a solution of sodium pentobarbital (58mg/kg), chloral hydrate (60mg/kg), magnesium sulphate (127.2 mg/kg), propylene glycol (42.8%) and absolute ethanol (11.6%). A severe impact of about  $3.23 \pm 0.01$  atm (3.13 – 3.35 atm) pressure was induced to cause the brain injury. 13 out of the 18 TBI rats survived the 3 months follow-up time period, and 6 out of these were included in the final study. On the other hand, 11 out of the 12 control rats survived the follow-up period and 5 of them were included in the final analysis. At 3 months post-injury, the animals were deeply anesthetized with CO<sub>2</sub> and decapitated with guillotine. Brains were quickly extracted and cortex, thalamus and hippocampus were separated and flash frozen in liquid nitrogen, and subsequently stored at -70°C until further use.

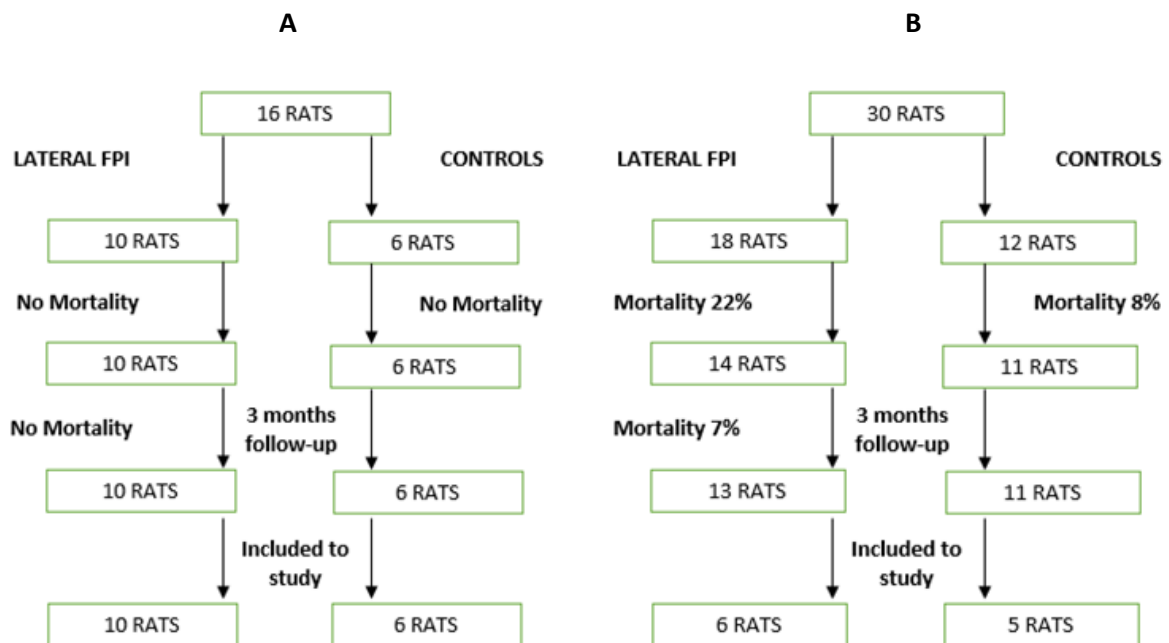


**Figure 3: Animal cohorts used for (A) miR-124 profiling from tail vein plasma at -7 days, 2 days, 1 week and 3 months post-injury, (B) ipsilateral cortex at 3 months post-injury (Abbreviations: FPI-fluid percussion injury)**

## **4.4 Total RNA extraction from plasma and brain tissue**

### **4.4.1 RNA extraction protocol for plasma samples**

Total RNA extraction from plasma samples was performed using the Exiqon miRCURY™ RNA isolation kit – biofluids (Product code: 300112, Exiqon, Vedbæk, Denmark) [90]. According to the protocol, 50µL of rodent tail vein plasma was used as the starting sample, topped up with nuclease free water (Product code: AM9937, Ambion, Life Technologies, Carlsbad, CA, USA) to a final volume of 200µL. Also to reduce the effect of inhibitors/nucleases, the 50µL plasma volume was centrifuged at 3000 x g for 5 minutes, to pellet any debris or insoluble cellular components.

Membranized particles in the sample were lysed by adding 60µL of the lysis solution BF per sample, followed by vortexing and incubation for 3 minutes at room temperature. The lysis buffer is provided with guanidine thiocyanate that inactivates RNases and prevents RNA degradation. To minimize technical variation among replicates and to enhance isolation of low abundance miRNAs, 1µg of MS2 carrier RNA (Product code: 10165948001, Roche Diagnostics GmbH, Mannheim, Germany) was added per 60µL of the lysis buffer. Also, to monitor the efficiency of RNA extraction step, 1µL of Exiqon RNA Spike-in template mixture (Product code: 203203, Exiqon, Vedbæk, Denmark) was added per 60 µL of the lysis buffer. The Spike-in template is designed as a mix of three spike-ins, UniSp2, UniSp4 and UniSp5, such that UniSp2 is present at a concentration 100-fold higher than UniSp4, and UniSp4 at a concentration 100-fold higher than UniSp5. Thus, UniSp2 amplifies at the level of very abundant miRNAs, UniSp4 amplifies at approximately 6.6 cycles later than UniSp2, and UniSp5 amplifies at approximately 6.6 cycles later than UniSp4, corresponding to successful extraction of weakly expressed miRNAs.

Proteins were precipitated by adding 20µL of Protein Precipitation solution BF to each sample. The samples were vortexed and incubated at room temperature for 1 minute, followed by centrifugation at 11,000 x g for 3 minutes. The supernatant was isolated and added with 270µL of isopropanol (Product code: 33539, Sigma-Aldrich, Seelze, Germany) to adjust the binding conditions on the column. The entire volume of supernatant was then loaded on a microRNA Mini Spin Column, incubated at room temperature for 2 minutes, followed by centrifugation at 11,000 x g for 30 seconds. This facilitates binding of the RNA to the spin column based on specific ionic concentrations, allowing removal of residual proteins. The column was then washed with 700µL of Wash Solution 2 BF at 11,000 x g for 30 seconds, followed by drying with 250µL of Wash solution 2 BF at 11,000 x g for 2 minutes. An on-column DNA digestion was performed by incubating the column for 15 minutes with 50µL of rDNase. This avoids DNA contamination in the samples. Finally, the column was washed with 100µL of Wash solution 1 BF at 11,000 x g for 30 seconds, with two steps of wash and dry with Wash solution buffer 2 BF as performed prior to rDNase addition. RNA samples were then eluted in 25µL of nuclease free water (provided with the Exiqon RNA isolation kit), particularly to obtain a concentrated eluate of small RNAs, while larger RNAs were retained on the column. For long-term storage, the purified RNA samples were kept at -70°C. All centrifugations were performed at room temperature and the optional Proteinase K treatment was omitted.

#### **4.4.2 RNA extraction protocol for brain tissue samples (ipsilateral cortex)**

Total RNA extraction for ipsilateral cortex samples was performed using the Qiagen miRNeasy Mini kit (Product code: 217004, Qiagen GmbH, Hilden Germany) [91]. The tissue samples were placed in 1000µL of Qiazol lysis reagent, and homogenised in the TissueLyser (TissueLyser II, Qiagen, CA, USA) for 3 minutes at 30Hz. The homogenate was then allowed to stand at room temperature for 10 minutes to subside the foam and to promote dissociation of the nucleoprotein complexes. 140µL of chloroform (Product code: 10293850, Fisher Scientific UK, Loughborough, Leics, UK) was then added to the homogenate and mixed vigorously for 15 seconds, followed by incubation at room temperature for 2-3 minutes. The homogenate was then centrifuged at 12,000 x g for 15 minutes at 4°C. This allowed separation of the sample into three phases: the upper, aqueous phase containing RNAs, a white interphase and a lower, red organic phase. The aqueous phase was transferred to a new tube and mixed thoroughly by pipetting with 1.5 volumes of 100% ethanol (Altia Oyj, Rajämäki, Finland). The entire volume was then transferred to an RNeasy Mini spin column and centrifuged at 16,000 x g for 15 seconds. Once the entire sample volume had passed through the column, three washing steps were performed. First wash was performed with 700µL of Buffer RWT at 16,000 x g for 15 seconds. This was followed by two washes, each with 500µL of buffer RPE, at 16,000 x g for 15 seconds and 2 minutes respectively. All these centrifugations were performed at room temperature. Total RNA was then eluted from the spin column in two elution steps of 50µL of nuclease free water (provided with the Qiagen miRNeasy kit). Elution was performed at 16,000 x g for 1 minute. Finally, total RNA eluate was obtained in 100µL of nuclease free water.

Total RNA concentration was measured in both NanoDrop 1000 spectrophotometer (Thermo Fisher Scientific, Wilmington, DE, USA) and in Agilent Bioanalyzer 2100 (Agilent Technologies, Santa Clara, CA, USA) with the Agilent RNA 6000 Nano kit (Product code: 5067-1511, Agilent Technologies, Thermo Fisher Scientific Baltics UAB, Vilnius, Lithuania). All RNA elutions were diluted to 1:20, prior to estimation of small RNA concentration using the Agilent Small RNA kit (Product code: 5067-1548, Agilent Technologies, Thermo Fisher Scientific Baltics UAB, Vilnius, Lithuania).

#### **4.5 cDNA synthesis with Exiqon miRCURY LNA™ Kit**

For this study, the Exiqon miRCURY LNA™ Universal RT microRNA PCR kit (Universal cDNA synthesis kit II, 8-64 rxns, Product code: 203301, Exiqon, Vedbæk, Denmark) was implemented for monitoring RNA extraction and RT reaction efficiencies [92]. This quality control was performed only for elutions from plasma samples, since the extracted RNA volumes were too low to be detected reliably by NanoDrop or Agilent Bioanalyzer. Since RNA volumes from tissue samples could be reliably measured, quality control was omitted for those samples. For the plasma RNA elutions, slight modification of the Exiqon cDNA synthesis protocol, as stated in the instruction manual was performed. The 10µL universal cDNA synthesis reaction mixture was thus set up as follows (table 1):

**Table 1: Reverse transcription reaction setup with Exiqon Universal cDNA synthesis kit**

Reagent	Volume ( $\mu\text{L}$ )
5x Reaction Buffer	2
Nuclease-free water	4
Enzyme Mix	1
Synthetic UniSp6 RNA spike-in template	1
Template total RNA (undiluted)	2
<b>Total volume</b>	<b>10</b>

The exogenous RNA spike-in template UniSp6 (provided with the cDNA synthesis kit) was added during cDNA synthesis to monitor RT reaction efficiency. The lyophilised UniSp6 template was resuspended in 80 $\mu\text{L}$  of nuclease free water prior to use. Since it is presumed that the abundance of miR-124 in cell-free plasma samples would be considerably low, undiluted template RNA samples were used for cDNA synthesis. The reaction mixture was vortexed well and cDNA synthesis was performed in a 96-well thermal cycler (BIO-RAD T100™ thermal cycler, CA, USA). The thermal cycling conditions for cDNA synthesis were as follows: Incubation for 60 minutes at 42°C, heat-inactivation of the reverse transcriptase for 5 minutes at 95°C, followed by immediate cooling to 4°C and storage at -20°C for later usage.

#### 4.6 qRT-PCR amplification with Exiqon kit for quality control

To monitor efficiencies of the RNA extraction and cDNA synthesis reactions, PCR amplification of UniSp4 and UniSp6 templates were performed respectively, using the miRCURY LNA™ Universal RT microRNA PCR system designed for biofluids (ExiLENT SYBR® Green master mix, Product code: 203403, Exiqon, Vedbæk, Denmark) [92]. The UniSp4 template was chosen for amplification from the template spike-in mix (UniSp2, UniSp4 and UniSp5 mix), as its amplification corresponded with consistent threshold cycles ( $C_t$ ) across all samples from all tested time-points, indicating successful RNA extraction. The UniSp6 primer was already available ready-to-use with the PCR kit, whereas lyophilised UniSp4 primer (Product code: 203953, Exiqon, Vedbæk, Denmark) was resuspended in 220 $\mu\text{L}$  of nuclease free water. In this step, the cDNA samples were diluted to 40x in nuclease free water according to the protocol (195 $\mu\text{L}$  nuclease free water to each 5  $\mu\text{L}$  cDNA sample). ROX is a passive reference dye that allows normalization of signals from individual PCR wells, enabling comparison of amplification signals across an entire PCR plate. Since the Exiqon PCR Master Mix (ExiLENT SYBR® Green master mix) does not contain this dye, 0.2 $\mu\text{L}$  of ROX (Product code: 12223-012, Invitrogen, Life Technologies, Carlsbad, CA, USA) per PCR replicate was added to each of the diluted cDNA samples prior to PCR amplification. PCR amplification for spike-ins was performed in triplicates. The 10 $\mu\text{L}$  PCR reaction mixture was designed according to the protocol guidelines (Protocol A: Table 3) [92], and qRT-PCR amplification followed by melting curve analysis was then performed in a StepOnePlus™ Real-Time PCR system (Applied Biosystems), as indicated in the protocol (Protocol A: Table 4) [92]. Results were analysed with StepOne Software v2.1 (Applied Biosystems, Foster City, CA, USA).

Since dye based assays like the Exiqon system are cost-effective and easier to design than probe-based TaqMan assays, real-time amplification efficiencies of possible endogenous controls miR-103 (hsa-miR-103a-3p, Product code: 204063, Exiqon, Vedbæk, Denmark) and miR-127 (hsa-miR-127-3p, Product code: 204048, Exiqon, Vedbæk, Denmark), and the target miRNA miR-124 (hsa-miR-124-3p, Product code: 206026, Exiqon, Vedbæk, Denmark) were also checked in pilot studies with the Exiqon kit, in order to compare with the TaqMan system. Similar to UniSp4, the lyophilised hsa-miR-103a-3p, hsa-miR-127-3p and hsa-miR-124-3p primers were resuspended in 220µL of nuclease free water prior to use. Amplification in plasma for these miRNAs were tested at 40x, as well as for 20x and undiluted template cDNA conditions. No template controls (NTCs) were included in every PCR plate.

#### **4.7 MicroRNA specific cDNA synthesis with TaqMan® small RNA assay**

Next, the TaqMan small RNA assay (TaqMan® MicroRNA Reverse Transcription Kit, Product code: 4366596, Applied Biosystems, Foster City, CA, USA) was used to perform miRNA specific reverse transcription (RT) of the RNA samples extracted from brain tissue and plasma, followed by quantitative PCR amplification of the target miRNAs with probe based TaqMan qRT-PCR chemistry. The cDNA synthesis reaction master mix was designed according to the protocol guidelines [93]. The 15µL RT reaction was then prepared by adding 7µL of the master mix, with 3µL of 5x miR-124 RT primer (Product code: RT 001182, Applied Biosystems, Foster City, CA, USA) and 5µL of the undiluted template RNA. In order to test if microRNAs miR-103 and miR-127 can act as possible endogenous controls, a second multiplexed cDNA synthesis reaction was also set up as follows: 7µL of the master mix, with 1µL each of 5x miR-124 (Product code: RT 001182, Applied Biosystems, Foster City, CA, USA), miR-103 (Product code: RT 000439, Applied Biosystems, Foster City, CA, USA) and miR-127 RT primers (Product code: RT 000452, Applied Biosystems, Foster City, CA, USA), and 5µL of the undiluted template RNA.

For tissue samples, the small RNA concentration for each diluted RNA elution (1:20 dilution) was estimated in the Agilent Bioanalyzer, and from these 1:20 dilutions, 5 µL of RNA template with 10 ng of small RNA concentration was prepared. Since small nuclear RNA U6 is a known endogenous control, multiplexed cDNA synthesis reaction for the cortex samples was set up as follows: 7µL of the master mix, with 1.5µL each of 5x snRNA U6 (Product code: RT 001973, Applied Biosystems, Foster City, CA, USA) and miR-124 RT primers, and 5µL of the diluted template RNA (small RNA concentration 10 ng). The reaction components were mixed well and loaded on the thermal cycler (BIO-RAD T100™ thermal cycler, CA, USA) with the reverse transcription conditions stated in the protocol [93].

#### **4.8 MicroRNA specific qRT-PCR reaction with TaqMan® chemistry**

MicroRNA specific qRT-PCR was setup to estimate the concentrations of miR-103 and miR-124 in purified plasma RNA samples. For cortex samples, qRT-PCR amplification step was omitted and quantification was only performed using ddPCR. In qRT-PCR, each sample was run in duplicate with suitable NTCs. The reaction setup was designed as indicated in the protocol [93]. The components of the qRT-PCR setup included: miR-124 (Product code: TM 001182) and miR-103 (Product code: TM 000439) specific 20X PCR primers (Applied Biosystems, Foster City, CA, USA), undiluted cDNA

template obtained from the TaqMan RT reactions and TaqMan Universal PCR Master Mix (2X) with UNG (Product code: 4440038, Applied Biosystems, Foster City, CA, USA).

Thermal cycling for qRT-PCR was also performed according to the guidelines, in the StepOnePlus™ Real-Time PCR system (Applied Biosystems). Results were analysed with StepOne Software v2.1 (Applied Biosystems, Foster City, CA, USA) [93].

Due to the absence of established endogenous controls for quantifying miRNA expression in circulating biofluids, the expression levels for individual miRNAs were obtained by normalising the  $C_t$  values (from TaqMan qRT-PCR) with the exogenous spike-in UniSp4 expression data obtained from the Exiqon qRT-PCR amplification system. Normalisation was performed using the  $2^{-\Delta\Delta C_t}$  method. For miR-103, normalization of qRT-PCR expression was performed as follows:

$$\text{Fold change in miR-103 expression} = 2^{[(\text{Mean } C_t \text{ for UniSp4}) - (\text{Mean } C_t \text{ for miR-103})]} \quad (4)$$

In a similar way, normalisation of miR-124 to UniSp4 expression was performed:

$$\text{Fold change in miR-124 expression} = 2^{[(\text{Mean } C_t \text{ for UniSp4}) - (\text{Mean } C_t \text{ for miR-124})]} \quad (5)$$

#### 4.9 Absolute quantification of target miRNA concentration with ddPCR

The reaction mixtures for ddPCR based quantification of miR-124, in brain tissue and plasma samples, were prepared according to the Droplet Digital™ PCR protocol. Reverse transcription of the target miRNA template was performed with the TaqMan reverse transcription kit (TaqMan® MicroRNA Reverse Transcription Kit, Product code: 4366596, Applied Biosystems, Foster City, CA, USA), according to the instructions mentioned in section 4.7. Amplification was then carried out by adding 1.33µL of the cDNA template (undiluted cDNA template for plasma samples, and diluted cDNA template for cortex samples) to a 20µL reaction mixture, containing 10µL BioRad 2x ddPCR supermix for probes (Product code: 186-3010, BIO-RAD, CA USA), 1µL 20x miR-124 PCR primer (Product code: TM 001182, Applied Biosystems, Foster City, CA, USA) and 7.67µL nuclease-free water [84]. The 20µL reaction mixtures were loaded in disposable droplet generator cartridges (Product code: 186-4008, DG8™ Cartridges for QX100™/QX200™ Droplet Generator, BIO-RAD, Germany) along with 70µL of droplet generation oil for probes (Product code: 186-3005, Droplet generation oil for probes, BIO-RAD, CA, USA). The cartridges were then covered with gaskets (Product code: 186-3009, Droplet Generator DG8™ Gaskets, BIO-RAD, CA, USA) and placed in the droplet generator (Product code: 186-3001, BIO-RAD QX100™ Droplet Generator, Solna, Sweden) for creation of oil-emulsion droplets. Once droplets were generated, they were transferred to 96-well PCR plates (Twin. tec PCR plate 96, semi-skirted, colorless, Product code: E951020303, Hamburg, Germany) sealed (Product code: 181-4040, Pierceable foil heat seal, BIO-RAD, UK), thermal cycled (96-well PTC-200 thermal cycler, MJ Research) and quantified at end-point in the droplet reader (Product code: 186-3001, BIO-RAD QX100™ Droplet Reader, Solna, Sweden) using the QuantaSoft software (v1.7, Product code: 186-4011, BIO-RAD, CA, USA). In ddPCR, target concentrations are reported in terms of copy number / µL of the input reaction mixture, as well as copy number / 20µL well (for the total target concentration in one ddPCR well). In this study, for each

sample, reaction was performed in duplicates, and miR-124 expression was calculated as the sum of target copies / 20µL well for the two replicates, as indicated below:

$$\text{Concentration of miR-124} = \text{Copy no. /20}\mu\text{L well for replicate 1} + \text{Copy no. /20}\mu\text{L well for replicate 2} \quad (6)$$

To identify positive droplets, the threshold amplitude was set at 6000 for all ddPCR runs in the QuantaSoft software. This was performed to ensure maximum possibility of considering only true positive amplifications and neglecting false positive droplets with lower amplitudes.

For cortex samples, ddPCR based amplification of snRNA U6 (Product code: TM 001973, Applied Biosystems, Foster City, CA, USA) as an endogenous control was also performed. To obtain detectable limits of target concentration in ddPCR, the cortex cDNA samples were diluted to 1:6 for U6 and 1:4 for miR-124 quantification, and 1.33µL of these dilutions were taken for ddPCR amplification. Expression of miR-124 was studied with and without normalisation to U6 expression. For each sample, normalisation to endogenous reference was performed as follows:

$$\text{Concentration of miR-124} = \text{Copy no. /20}\mu\text{L well for replicate 1} + \text{Copy no. /20}\mu\text{L well for replicate 2} \quad (6)$$

$$\text{Concentration of U6} = \text{Copy no. /20}\mu\text{L well for replicate 1} + \text{Copy no. /20}\mu\text{L well for replicate 2} \quad (7)$$

$$\text{Normalised miR-124 expression} = \text{Concentration of miR-124} / \text{Concentration of U6} \quad (8)$$

The thermal cycling conditions for TaqMan based ddPCR were as follows [84]: 95°C for 10 minutes, 40 cycles of 95°C for 15 seconds and 60°C for 1 minute, and a final inactivation step at 98°C for 10 minutes. NTCs were included in every PCR plate.

#### 4.10 Cost analysis for one PCR reaction (2 technical replicates) in TaqMan® qRT-PCR and ddPCR

The cost of performing a single PCR reaction, with two technical replicates, for qRT-PCR and ddPCR settings is listed below (tables 2 and 3):

**Table 2: Reagents and consumables for TaqMan qRT-PCR (single sample with two replicates)**

Reagents and Consumables	Volume/Number required	Cost/sample(2 replicates)
TaqMan® Universal PCR Master Mix (2X) with UNG	20.00µL	1.668€
20x miR-124 PCR primer	2.00µL	2.62€
Nuclease-free water	15.34µL	0.04€
Reaction plate for qRT-PCR*	1	0.12€
Adhesive PCR plate sealer**	1	0.087€
<b>Total cost</b>		<b>4.535€<sup>#</sup></b>

\*MicroAmp® fast optical 96-well reaction plate with barcode (0.1 mL), Product code: 4346906, Applied Biosystems, Ca, USA

\*\* MicroAmp® optical adhesive film kit, Product code: 4313663, Applied Biosystems, Foster City, CA, USA



**Table 3: Reagents and consumables for TaqMan ddPCR (single sample with two replicates)**

Reagents and Consumables	Volume/Number required	Cost/sample(2 replicates)
BioRad 2x ddPCR supermix for probes	20.00µL	1.7€
20x miR-124 PCR primer	2.00µL	2.62€
Nuclease-free water	15.34µL	0.04€
Droplet generation oil for probes	140.00µL	0.44€
Droplet generator cartridges	1	2€
Gasket	1	0.57€
Reaction plate for ddPCR	1	0.097€
Pierceable foil heat seal	1	0.017€
<b>Total cost</b>		<b>7.484 €<sup>#</sup></b>

# Cost of performing PCR amplification for a single sample (with two technical replicates) is comparable for qRT-PCR and ddPCR, with ddPCR being slightly costly due to addition consumables required for droplet generation

#### 4.11 Cresyl violet staining for characterization of lesion size

Brain lesions developed as an impact of the inflicted trauma was studied with cresyl violet staining. At 3 months post-TBI, 10-µm-thick coronal sections were cut from brains of the cohort A animals, with a cryostat (Leica CM3050 S, Leica Microsystems Nussloch GmbH, Germany). The sections were then transferred to Superfrost glass slides (Menzel-Gläser Superfrost® Plus Microscope slides, Thermo Scientific, Gerhard Menzel GmbH, Braunschweig, Germany) and allowed to dry at room temperature for 5 minutes, followed by storage at -70°C until further use. The sections were stained with cresyl violet (Merck, Darmstadt, Germany). First, sections were placed in 96% ethanol for 30 seconds, then 70% ethanol for 30 seconds, 50% ethanol for 30 seconds, followed by staining with 1% cresyl violet in 100% ethanol for 40 seconds. Next, the sections were placed in 50% ethanol for 30 seconds, 70% ethanol for 30 seconds, 96% ethanol for 30 seconds and 100% ethanol for 30 seconds. Finally, the sections were washed twice in xylene for 5 minutes each. The slides were immediately coverslipped using DePeX® (Product code: 361254D, BDH Chemical, Poole, UK) as the mounting medium, and left to dry for overnight. For each rat, digital RGB colour images were captured using Leica DMRB microscope equipped with a Nikon DXM1200F camera operated by a Nikon ACT-1 2.7 software. A scale bar taken with the same magnification as the digital images was used.

#### 4.12 Statistical analysis

For qRT-PCR, the normalized expression values ( $2^{-\Delta\Delta C_t}$ ) of the miRNAs were considered as test variables. For ddPCR, absolute concentrations of miR-124 for each sample (sum of target copies / 20µL well for the two ddPCR replicates, with application of the threshold) were considered. Independent-samples Mann-Whitney U test was performed to compare miRNA expression levels between control and TBI samples at a particular time-point. The related-samples Friedman's two-way ANOVA test was then performed to check for differences in expression across all TBI samples over the four timepoints. If the Friedman's test was found to be significant, variation in expression between pairwise TBI samples

was tested using the related-samples Wilcoxon signed rank test. Similarly, the Friedman's two-way ANOVA tests and Wilcoxon signed rank tests were also performed for control samples. Receiver operator characteristic (ROC) curve analyses were also performed to determine the potential of miR-124 to act as a reliable biomarker for head injury. All analyses were performed in IBM SPSS Statistics 21 software (SPSS Inc., Chicago, IL, USA) and GraphPad Prism (version 5.03, GraphPad software). All data were represented as mean  $\pm$  standard error of the mean. Statistical significance was considered at  $p < 0.05$ .

## **5 RESULTS**

### **5.1 Mortality**

The study was based on two separate animal cohorts (figure 3). Profiling of miR-124 from plasma was performed with cohort A. Even though a severe injury was inflicted, no mortality was observed in this group of animals, at 24 hours post-TBI, as well as at chronic timepoints. For analysis of miR-124 expression in brain tissue, animals from cohort B were used. For this group, 22% mortality was observed in case of injury (4 out of 18 rats), and 8% in case of controls (sham operated animals, 1 out of 12), at 24 hours post-TBI, indicating moderate severity of the TBI. During the 3 months follow-up period, mortality of 7% was observed in case of the injured group (1 out of 14 rats). None of the remaining control animals died during this period.

### **5.2 Optimisation of the ddPCR protocol**

To our knowledge, this study was the first to implement ddPCR technique for miR-124 quantification in plasma. Thus, accuracy of the ddPCR protocol in conjunction with TaqMan chemistry, for quantification of miR-124 expression, was tested using synthetic miR-124 (Integrated DNA Technologies, Coralville, IA, USA) and the ipsilateral cortex samples available from animal cohort B. Also, a thermal gradient was set up to determine the suitable annealing temperature for the ddPCR amplifications.

#### **5.2.1 Dilution series from synthetic miR-124 and tissue samples**

Dilution series were performed for both synthetic miR-124 and brain tissue samples. For synthetic miR-124, 12 points of 1:5 serial dilutions were prepared, out of which miR-124 concentrations for dilution points 6-12 could be accurately estimated in ddPCR (earlier dilutions possessed too high target concentration; beyond the detection limit of ddPCR). A linear curve was obtained for the tested dilution points, indicating specificity of the primers and high accuracy of ddPCR in estimating target concentrations. In case of brain tissue, a similar estimation was performed on a 1:5 dilution series from RNA elution of a single ipsilateral cortex sample. Six points of 1:5 dilutions were prepared from the undiluted cDNA template. Target concentration for the undiluted RT product was beyond the limit of detection, but a linear curve was obtained for the remaining 1:5 dilution points tested, indicating that miR-124 quantification with ddPCR was close to 100% accuracy in this case too (figure 4).

However, since plasma samples demonstrated very low target copy numbers even when undiluted RT products were used for amplification, dilution series based estimations could not be designed for these samples, to check for the efficiency of ddPCR based quantification in case of low target abundance.

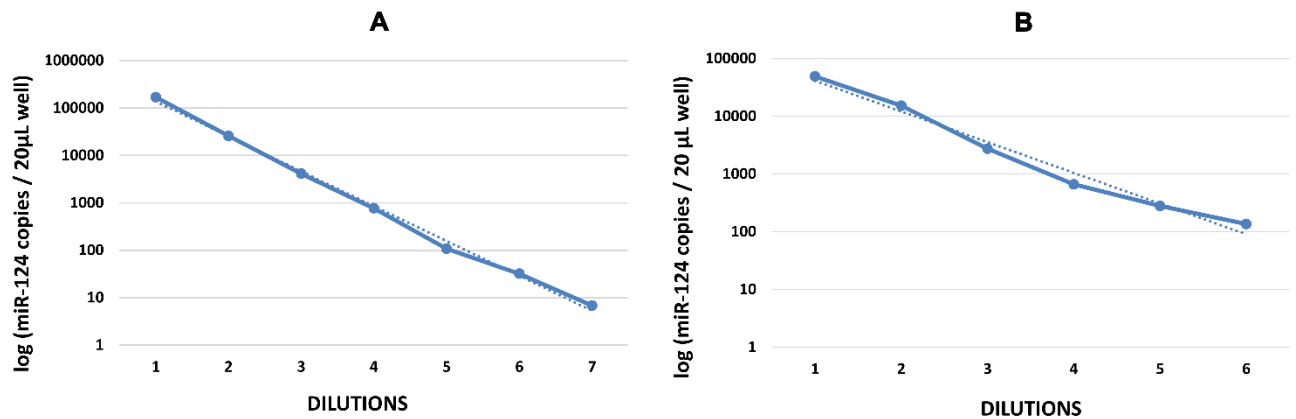


**Figure 4: Target concentration / 20µL ddPCR well for the 1:5 dilution series of (A) synthetic miR-124, (B) ipsilateral cortex (exponential ddPCR based amplifications of miR-124 plotted to the logarithmic scale).** Optimization of the ddPCR protocol was performed to check for the sensitivity of this technique in quantifying miR-124 expression levels. Linear curves were obtained when dilution series from synthetic miR-124 and ipsilateral cortex samples were analysed. This indicated that the ddPCR methodology, in conjunction with TaqMan primer-probes were suitable for quantification of this miRNA. However, dilution series based curves from plasma samples could not be established, since very few copy numbers were obtained when ddPCR was tested with undiluted RT products. (Dilutions: number of dilution points tested, miR-124 concentration: miR-124 copies/20µL well (exponential amplification in ddPCR plotted to the logarithmic scale with base 10)).

### 5.2.2 Optimisation of the annealing temperature using thermal gradients

Since miRNAs are only ~22bp long with a variable GC content, a wide range of annealing temperatures ( $T_m$ ) have been observed for different miRNA species. The TaqMan qRT-PCR protocol specified  $T_m=60^\circ\text{C}$  to be suitable for miRNA quantification [93, 94]. Thus, a thermal gradient test was set up to check if  $T_m=60^\circ\text{C}$  was optimal for ddPCR based amplifications as well. Reaction specificities in tissue samples were first tested. A temperature gradient of 52-63°C was set and run for a single tissue sample (The first dilution from the 1:5 serial dilution prepared earlier for tissue based estimations; section 5.2.1). Annealing temperatures for individual ddPCR wells were as follows: A01= 63°C (NTC), B01= 62.2°C, C01= 60.8°C, D01= 58.7°C, E01= 56.2°C, F01= 54.1°C, G01= 52.8°C, H01=52°C (figure 5).

In ddPCR, the optimal annealing temperature is the one that results in largest fluorescence amplitude difference between positive and negative droplet clusters. In this test, proper separation between clusters was observed for  $T_m=58.7^\circ\text{C}$  (~60°C) and  $T_m= 56.2^\circ\text{C}$ , with  $T_m= 56.2^\circ\text{C}$  being the best. At higher temperatures (60.8 – 62.2°C), as well as for lower  $T_m$  (54.1 - 52°C), poor separation between clusters was observed (figure 5(A)).

Also, from this test, fluorescence amplitude of 6000 was considered suitable to avoid inclusion of non-specific amplifications. Thus, the amplitude threshold for all ddPCR runs was manually set to 6000 prior to estimation of target concentration.

Similar annealing temperature gradients were then run for few plasma samples (with undiluted RT products). However, in this case, no proper separation between positive and negative droplets was observed at any temperature. Too high temperatures led to very few positive droplets, whereas at too low temperatures, increase in positive droplets at a lower threshold level was observed, indicating non-

specific amplifications. For  $T_m=58.7^\circ\text{C}$  and  $T_m= 56.2^\circ\text{C}$ , no difference in positive droplet number was observed above the amplitude threshold of 6000, whereas increased positive droplets were observed at lower threshold level (at ~1500-2000) for  $T_m= 56.2^\circ\text{C}$  (figure 5(B)). Thus, based on these results,  $T_m=60^\circ\text{C}$  was considered optimal for all ddPCR amplifications.

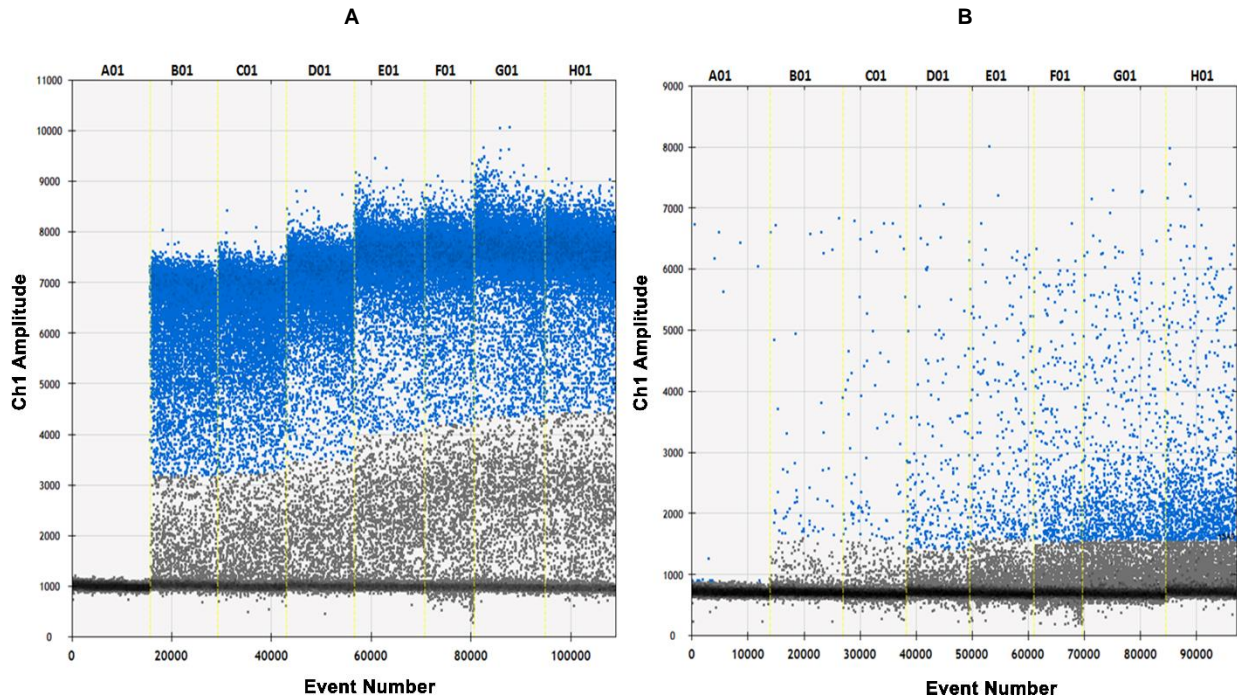


**Figure 5: Annealing temperature gradient for ddPCR based miR-124 expression in (A) Ipsilateral cortex, (B) Plasma (blue-positive droplets, black-negative droplets).** Impact of the thermal gradient for annealing temperature was not evident from plasma ddPCR data. Lowering the annealing temperature resulted in an increase of positive droplets at lower thresholds, possibly indicating enhanced non-specific amplifications. Hence,  $T_m=60^\circ\text{C}$  was maintained for all ddPCR amplifications, similar to the qRT-PCR protocol. Annealing temperatures for individual ddPCR wells were as follows: A01=  $63^\circ\text{C}$  (NTC), B01=  $62.2^\circ\text{C}$ , C01=  $60.8^\circ\text{C}$ , D01=  $58.7^\circ\text{C}$ , E01=  $56.2^\circ\text{C}$ , F01=  $54.1^\circ\text{C}$ , G01=  $52.8^\circ\text{C}$ , H01=  $52^\circ\text{C}$ . (Ch1 Amplitude: fluorescence amplitudes for positive and negative droplets, Event number: number of droplets generated, NTC: no template control).

### 5.3 Quantification of miRNAs based on real-time qRT-PCR amplification

Prior to ddPCR based estimation of miR-124, amplification efficiencies for exogenous spike-in RNAs (for quality control) were tested with Exiqon qRT-PCR system. Along with this, expression profiles for miRNAs miR-103, miR-124 and miR-127 were tested in qRT-PCR, with Exiqon (EvaGreen) and TaqMan chemistries.

#### 5.3.1 Quality control for plasma samples with exogenous RNA spike-ins

Amplification of the exogenous RNA spike-in UniSp4 was tested for all RNA elutions from plasma samples, to monitor RNA extraction efficiency. For each sample, three PCR replicates were run and the mean threshold cycle ( $C_t$ ) was considered for analysis. Mean  $C_t$  values for UniSp4 ranged from 26.9 – 29.8 across all samples at the four different time-points, with good agreement among the technical replicates (standard deviation between  $C_t$  values of technical replicates  $\leq 0.1$ ), indicating successful RNA extraction for all. Few samples demonstrated higher variability among replicates (standard

deviation of  $C_t$  values ranging from 0.2-0.4), indicating possible variations due to pipetting (figure 6 (A) and (B)).

UniSp6 amplification was also tested for monitoring efficiency of the reverse transcription reaction. Three PCR replicates were run and mean threshold cycle ( $C_t$ ) ranged from 17.08 – 18.08 across all samples at the four different time-points, with good agreement among the technical replicates for each sample (standard deviation between  $C_t$  values of technical replicates  $\leq 0.3$ ) (figure 6 (C) and (D)). Amplification of both these spike-ins were performed with the Exiqon qRT-PCR kit.

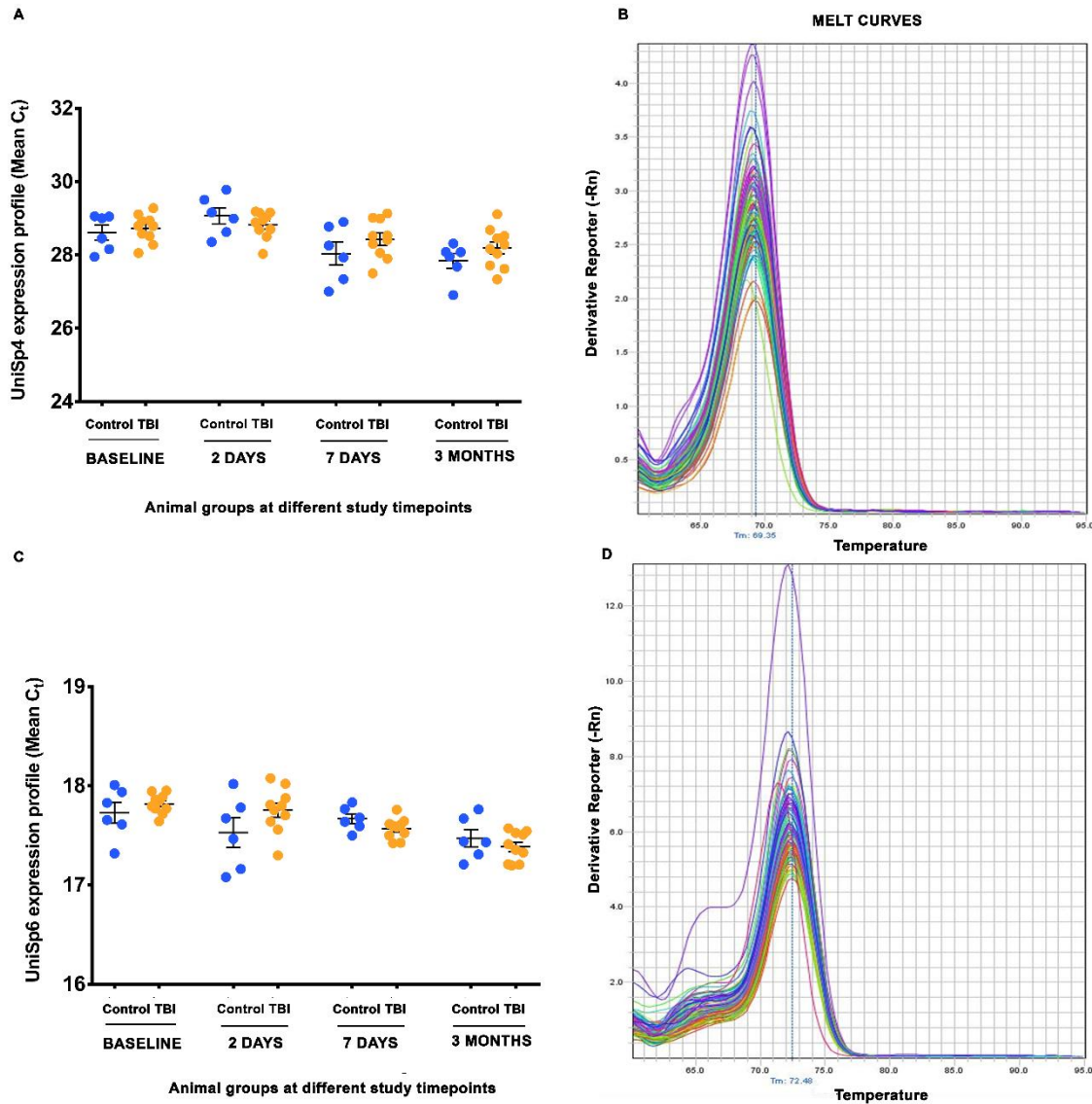


**Figure 6: (A) UniSp4 amplification represented as the mean  $C_t$  for the three qRT-PCR replicates, (B) UniSp4 melt curve analysis, (C) UniSp6 amplification represented as the mean  $C_t$  for the three qRT-PCR replicates, (D) UniSp6 melt curve analysis.** All samples (Baseline, 2days, 1 week and 3 months post-TBI) demonstrated uniform expression levels for the spike-in UniSp4 (Mean  $C_t$  values ranging from 26.9 – 29.8), indicating successful RNA extraction for all. A single peak was obtained in the melt curve analysis, indicating specificity of the qRT-PCR amplification ( $T_m$ : 69.35°C)). Also, for all samples (Baseline, 2days, 1 week and 3 months post-TBI), uniform expression levels for the spike-in UniSp6 (Mean  $C_t$  values ranging from 17.08 – 18.08) was obtained, indicating successful reverse transcription reactions. A single peak was obtained in the melt curve analysis, indicating specificity of the qRT-PCR amplification ( $T_m$ : 72.48°C), (Abbreviations used:  $C_t$ -threshold cycle, TBI-traumatic brain injury).

qRT-PCR amplifications with the Exiqon system were then tested for miR-103, miR-127 and miR-124 at 40x, 20x and undiluted template cDNA conditions, for pilot study samples. Successful amplification of miR-103 was observed in all cases, whereas miR-127 and miR-124 amplifications failed for all. Thus, only quality control studies were performed with the Exiqon system and target miRNA quantifications were solely based on TaqMan chemistries.

### **5.3.2 Amplification of miR-103 in plasma as a possible endogenous control**

Consistent amplifications for miR-103 were obtained from all plasma samples of pilot study, with the Exiqon system. Thus, to check if this miRNA can act as a possible endogenous control, its amplification efficiency was tested in qRT-PCR from the multiplexed cDNA templates, now using the TaqMan chemistry. No variation in miR-103 expression was observed at a particular time-point, between control and injured animals. However, differential expression was observed for the controls at the four studied timepoints ( $p < 0.01$ ), as well as for the TBI samples across the four timepoints ( $p < 0.01$ ). From this, it could be deduced that expression of miR-103 remains similar across biological conditions (control vs. TBI) at a particular timepoint, whereas, within a single animal, difference in miR-103 expression can be observed at different time-points, irrespective of the biological condition. Particularly, up-regulation in miR-103 expression was observed for both control and TBI groups at 1 week post-injury. On performing the pair-wise tests, difference in expression was observed between the following control groups: baseline control and 1 week control ( $p < 0.05$ ), baseline control and 3 months control ( $p < 0.05$ ), 2 days control and 1 week control ( $p < 0.05$ ), 2 days control and 3 months control ( $p < 0.05$ ) and 1 week control vs. 3 months control ( $p < 0.05$ ). Similarly for injured animals, difference in expression was observed between the following TBI groups: baseline TBI vs. 1 week post-TBI ( $p < 0.05$ ), baseline TBI vs. 3 months post-TBI ( $p < 0.05$ ), 2 days post-TBI and 1 week post-TBI ( $p < 0.01$ ), and 1 week post-TBI vs. 3 months post-TBI ( $p < 0.01$ ). This variability in expression over time for both uninjured and injured cases indicated that the plasma enriched miR-103 is not a suitable endogenous control candidate for qRT-PCR data normalization (figure 7).

Amplification efficiencies of miR-127 as a possible endogenous control was not tested with TaqMan systems, since pilot studies already indicated no amplification of this miRNA in plasma samples (with the Exiqon kit).

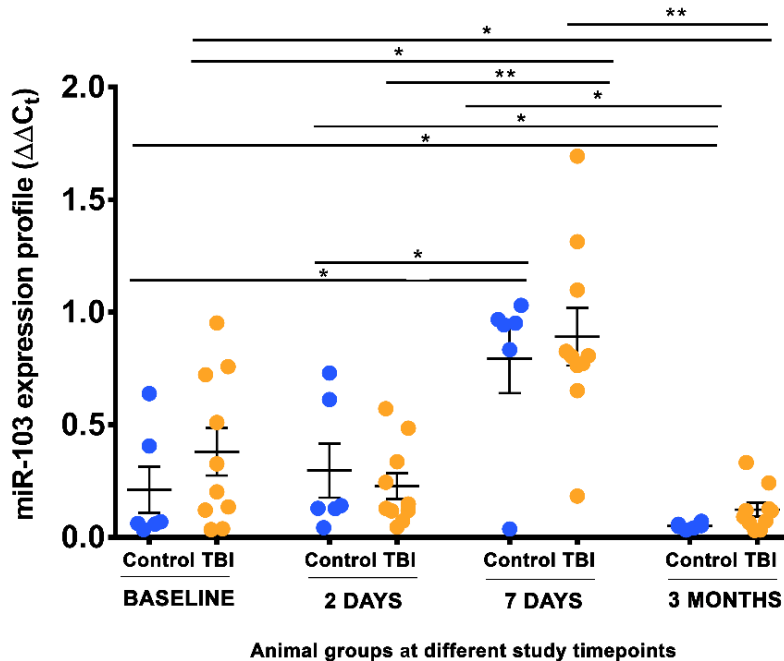


**Figure 7: Analysis of miR-103 expression in plasma samples using TaqMan qRT-PCR chemistry.** Expression levels of miR-103 showed considerable variation in controls, as well as in injured animals, across the four tested timepoints. From this data, it was concluded that miR-103 cannot be used as a potential endogenous control to normalize miRNA expression data from circulating biofluids like plasma (Abbreviations used:  $C_T$ -threshold cycle, TBI-traumatic brain injury, \* $p < 0.05$ , \*\* $p < 0.01$ ,  $\Delta\Delta C_T$ - miR-103 expression normalised to UniSp4).

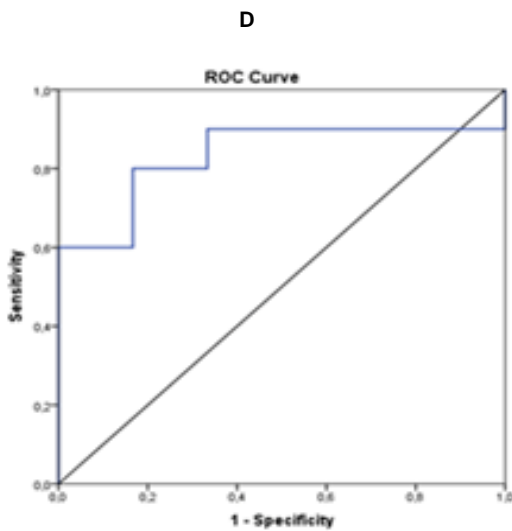
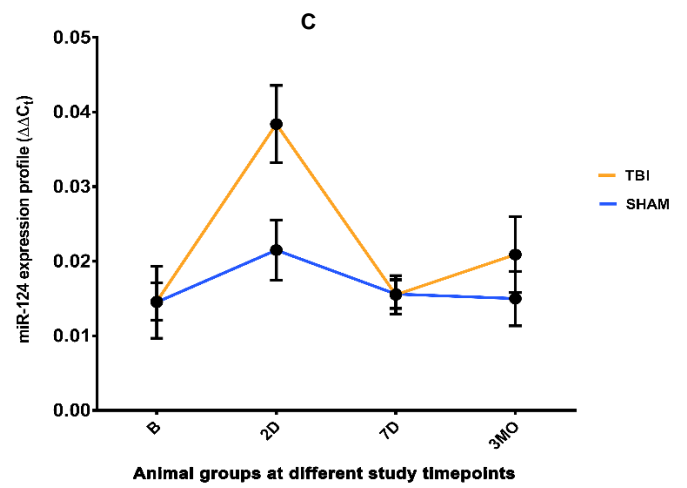
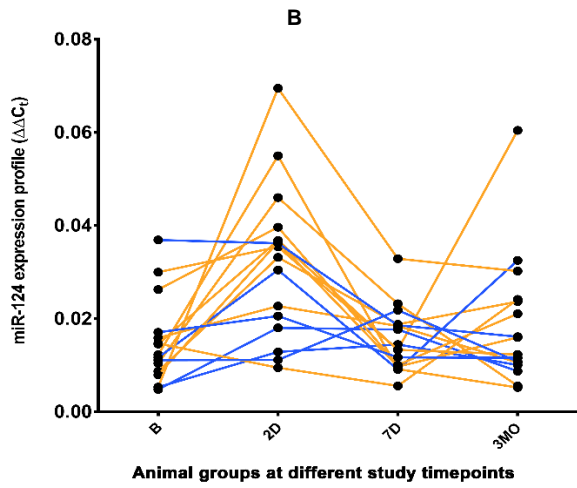
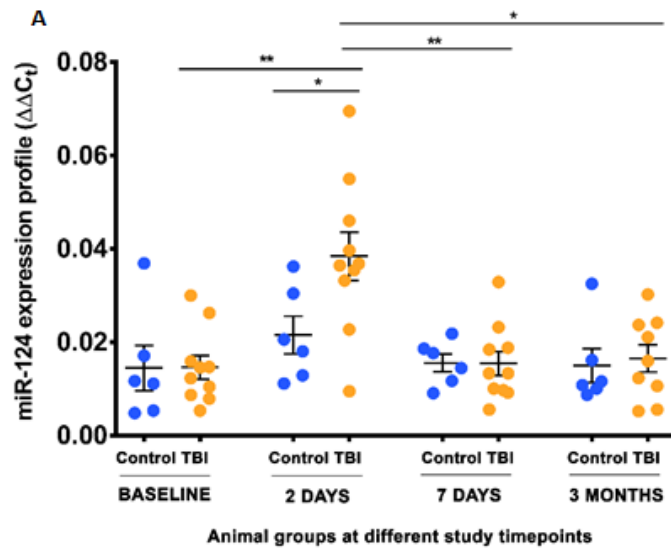
### 5.3.3 Expression analysis of miR-124 in plasma across different time-points

Real-time qRT-PCR amplification for miR-124 was also performed from the multiplexed cDNA templates, for all samples across the four time-points, using the TaqMan qRT-PCR chemistry. Since miR-103 failed as an endogenous control candidate, miR-124 expression data was also normalised to the exogenous spike-in UniSp4.

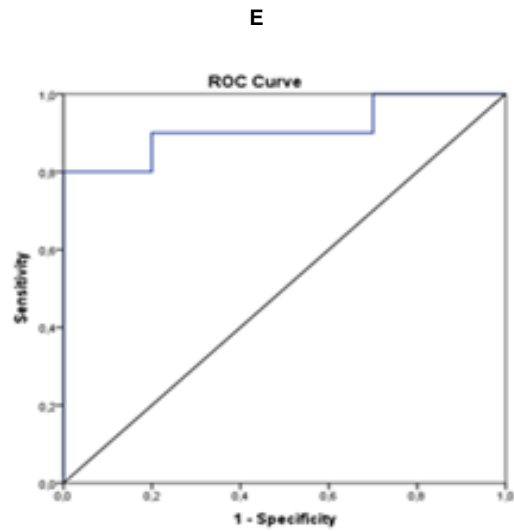
Expression of miR-124 remained similar across control samples at all timepoints. Also, at baseline, 1 week and 3 months post trauma, no difference in miR-124 expression was observed between the control and injured cases. However, difference in expression was observed between control and TBI samples at 2 days post-injury timepoint ( $p < 0.05$ ). Also, up-regulation of miR-124 expression was observed across all TBI samples. Up-regulation was observed at 2 days post-injury, compared to the same samples at baseline ( $p < 0.01$ ), 1 week post-injury ( $p < 0.01$ ), and 3 months post-injury ( $p < 0.05$ , excluding one outlier from the 3 months post-injury group). Receiver operator characteristic (ROC) analyses were good since all tests demonstrated an  $AUC > 0.81$  with  $p < 0.05$ .

Expression analysis in individual animals across the four timepoints revealed that miR-124 was up-regulated in plasma samples of the injured animals only at an acute timepoint (2 days post-injury), and gradually returning back to normal levels (similar to baseline expression) at a chronic timepoint (3 months post-injury), for most of the injured cases. Overall expression remained unchanged in the control animals at all times. However, a slight up-regulation in miR-124 expression was also observed in this case at 2 days post-TBI, but this variation was not significant (figure 8).





**AUC=0.833; p<0.05**



**AUC=0.910; p<0.01**

**Figure 8: (A) Analysis of miR-124 expression in plasma samples using TaqMan qRT-PCR chemistry, (B) Individual animal variability in miR-124 expression across the four timepoints of study, (C) Average miR-124 expressions for control and TBI animals across the four timepoints, ROC analysis for (D) 2 days control vs. 2 days post-TBI and (E) Baseline TBI vs. 2 days post-TBI (qRT-PCR dataset).** Up-regulation of miR-124 expression was observed in injured animals, only at an acute timepoint (2 days post-TBI), with levels gradually returning to baseline at chronic timepoints. However, individual animal variability exists, and thus, few injured animals exhibited no elevation in miR-124 levels at 2days post-TBI, whereas some retained the elevated expression even at chronic timepoints. For controls (sham operated animals), miR-124 levels remained similar across all timepoints, with a slight, non-significant up-regulation at 2days post-TBI (Abbreviations used: ROC-receiver operator characteristics, AUC-area under curve, C<sub>t</sub>-threshold cycle, TBI-traumatic brain injury, B-baseline, 2D-2days, 7D-7days, 3MO-3months,  $\Delta\Delta C_t$ - miR-124 expression normalised to UniSp4, \*p<0.05, \*\*p<0.01,). ROC analyses indicated the possibility of using miR-124 as a diagnostic marker for TBI at acute timepoints.

### 5.3.4 Pattern of miR-124 expression in relation with lesion size

Though the entire procedure and impact of induced injury for the lateral FPI model was kept as similar as possible for all animals, difference in lesion size at the ipsilateral cortex was observed when brains were flash frozen for histological analysis at 3 months post trauma. Based on size, the brain lesions could be classified as big cavities, or mid-size cavities and smaller lesions (figure 9 (A-D)). To check if miR-124 expression in plasma at an acute timepoint post-injury can predict the brain lesion size observed at a chronic timepoint, expression of miR-124 at 2 days post-injury was compared among controls (uninjured), injured animals characterized with big cavity, and injured animals with smaller lesions (animals with mid-size and smaller lesions were grouped together for analysis in the smaller lesion group).

Statistical analysis revealed up-regulation of miR-124 expression in plasma at 2 days post-injury, for the rats characterized with big sized cavities, compared to controls (p<0.05). Also, expression of miR-124 was higher in these animals compared to the ones with mid-size and smaller cavities (p<0.05). However, no difference was observed between controls and smaller lesion groups. ROC analysis for miR-124 levels in rats with larger cavities, compared to controls, was perfect with an AUC of 1.0 and p<0.05. In comparison to the rats with middle and small sized cavities, an AUC of 0.917 with p<0.05 was obtained (figure 10). Thus, larger lesion size was associated with higher expression of miR-124 at an acute timepoint after injury induction.

To confirm the lesion size and the extent of cell loss at the site of impact, cresyl violet staining was performed for 10- $\mu$ m-thick coronal brain sections, for both controls and TBI rats at 3 months post-injury. Rats with larger cavities demonstrated huge lesion size, with a greater extent of cell loss at the site of injury, as compared to the ones with smaller and mid-size cavities. Controls demonstrated no cell loss or lesion formation in any brain area (figure 9 (E-G)).

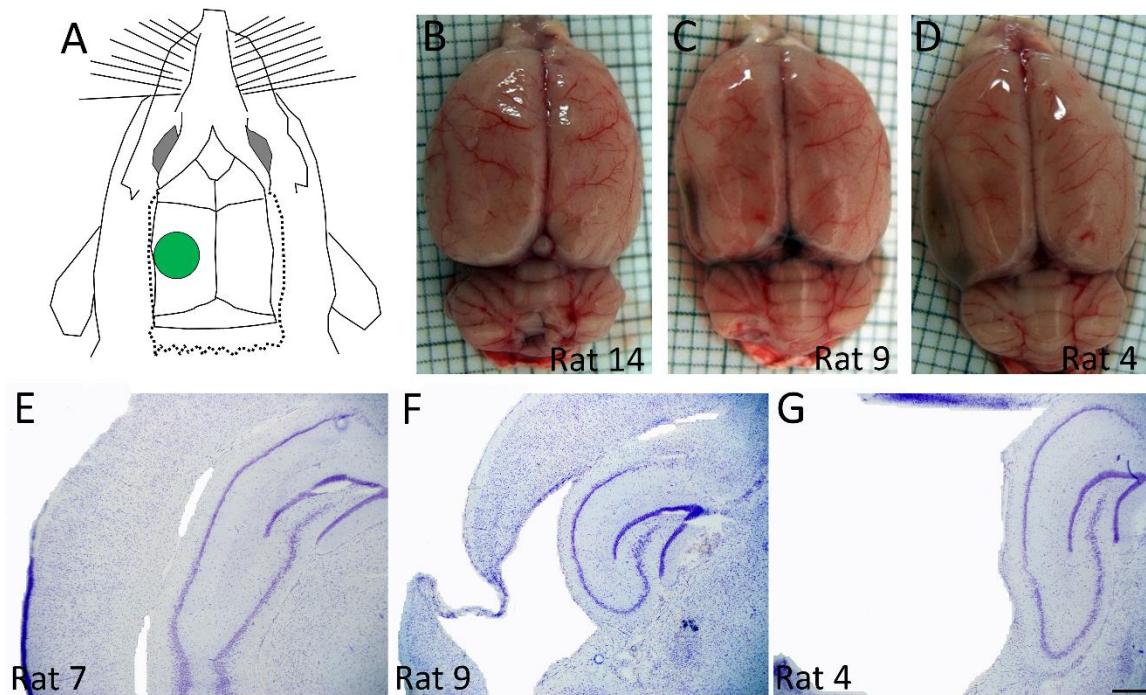


**Figure 9: (A) Site of impact for the lateral FPI, (B) Whole brain image for control rat 14 with no lesion due to absence of injury, (C) Whole brain image for TBI rat 9 with mid-size cavity, (D) Whole brain image for TBI rat 4 with big cavity, (E) Cresyl violet staining for control rat 7 reveals absence of lesion at the ipsilateral cortex, (F) Middle sized cavity observed at the ipsilateral cortex for TBI rat 9, with cell loss at the area of impact, (G) Large cavity with a higher extent of cell loss observed at the lesion area for TBI rat 4.** To characterize the lesion types, cresyl violet staining was performed for 10- $\mu$ m-thick coronal brain sections. Sham operated controls exhibited no cell loss or lesion formation, whereas cell loss at the site of impact was clearly visible for all injured animals. Also, increased lesion size and greater extent of neuron loss was observed in rats characterized with larger cavities, in comparison to the one with smaller and middle-sized lesions (Abbreviations used: FPI: fluid percussion injury, TBI-traumatic brain injury).

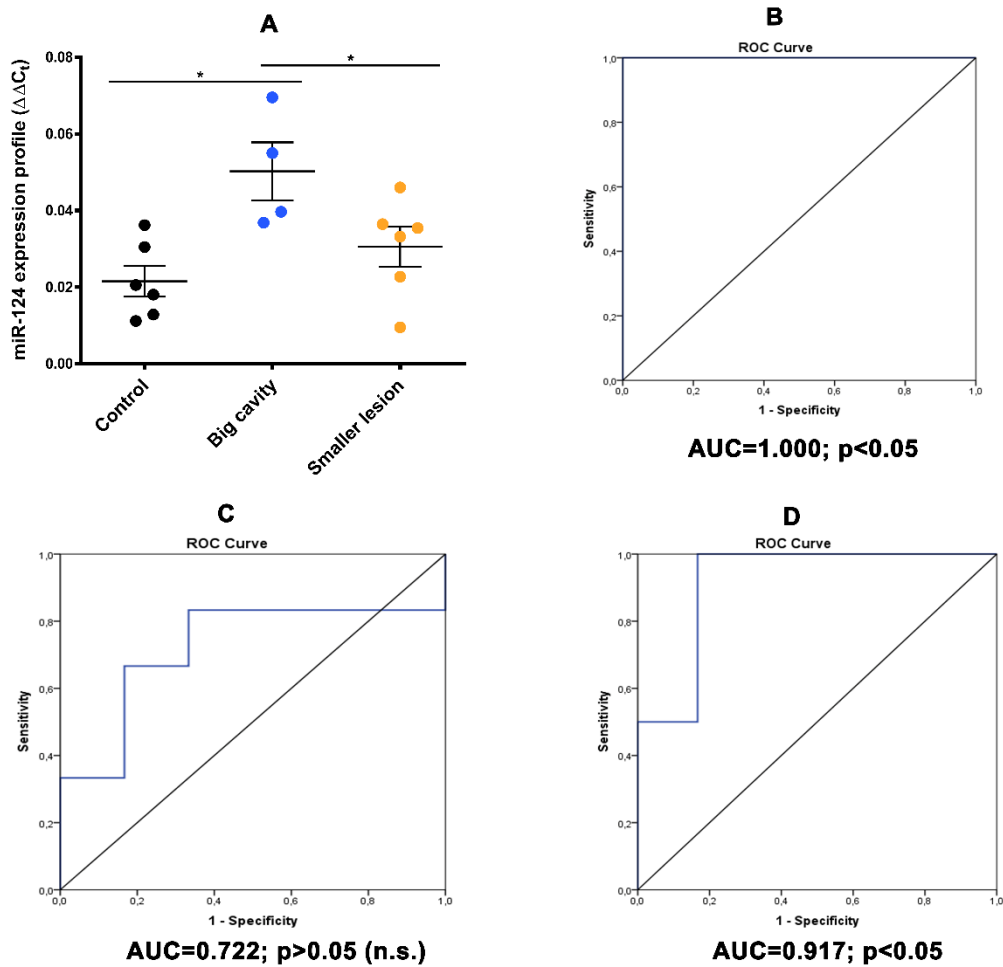


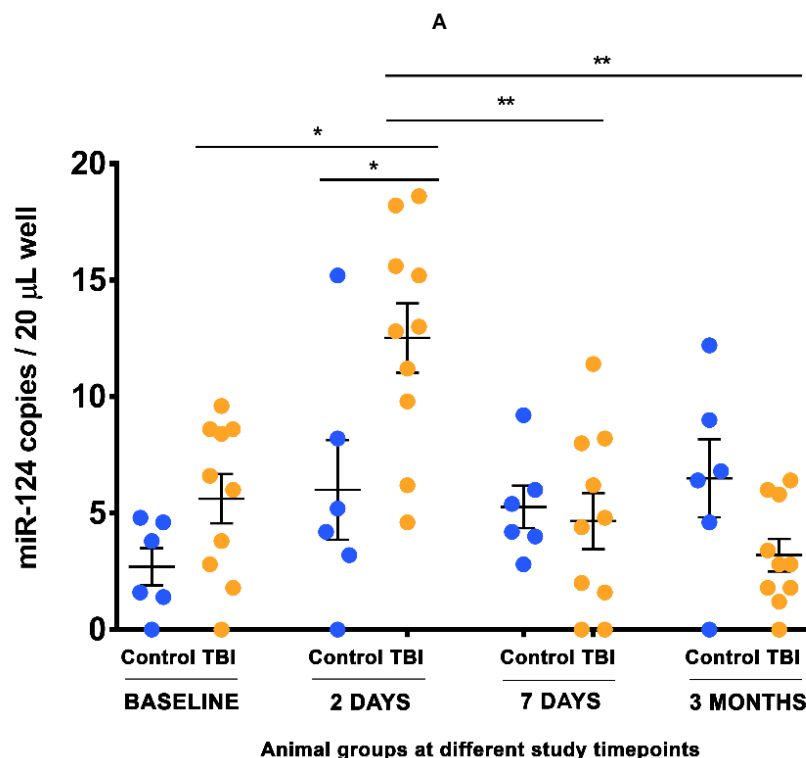
**Figure 10: (A) Up-regulation in miR-124 expression observed in plasma of rats characterized with larger brain lesions at 2 days post-injury (qRT-PCR data), ROC analysis for (B) control vs. big lesion group (C) control vs. smaller lesion group, (D) big lesion vs. smaller lesion group (qRT-PCR data).** Among the injured animals, pattern of miR-124 expression at 2 days post-TBI was found to correlate with the brain lesion type developed in response to the inflicted trauma. Rats characterized with larger lesions demonstrated elevated miR-124 levels in plasma at acute timepoints post injury. On the other hand, rats with middle-sized and smaller cavities had miR-124 expression levels almost similar to controls, indicating that larger brain lesions possibly lead to increased extravasation of miR-124 from brain to the peripheral blood. ROC analyses revealed good accuracy of the miR-124 levels in relation with larger lesion size (Abbreviations used: ROC-receiver operator characteristics, AUC- area under curve,  $C_t$ - threshold cycle, n.s- not significant,  $\Delta\Delta C_t$ - miR-124 expression normalised to UniSp4, \* $p<0.05$ , \*\* $p<0.01$ ).

## 5.4 Quantification of miR-124 with ddPCR from multiplexed RT products using TaqMan® chemistry

### 5.4.1 Expression analysis of miR-124 in plasma across all timepoints

Since no endogenous controls could be identified from qRT-PCR analyses of plasma, expression profiles in ddPCR were only tested for the target miR-124. In this case, miR-124 levels for the four study timepoints was tested with multiplexed cDNA using ddPCR. The expression pattern observed in qRT-PCR could be successfully replicated. Levels of miR-124 remained similar across control samples at all timepoints. Also, at baseline, 1 week and 3 months post trauma, no difference in miR-124 expression was observed between the control and injured cases. Difference in expression was observed between control and TBI samples only at 2 days post-injury ( $p < 0.05$ ). For TBI samples, up-regulation of miR-124 expression was observed across all the studied timepoints ( $p < 0.01$ ). Thus, the pairwise tests were performed for all TBI cases. Significance was observed at 2 days post-injury, compared to the same samples at baseline ( $p < 0.05$ ), 1 week post-injury ( $p < 0.01$ ), and 3 months post-injury ( $p < 0.01$ ). ROC analyses revealed an  $AUC > 0.84$  for all cases ( $p < 0.05$ ).

Expression pattern in injured animals across the four timepoints also resembled the qRT-PCR dataset. Up-regulation of miR-124 was only observed in the injured animals at an acute timepoint (2 days post-injury), which gradually returned back to normal levels (similar to baseline expression) at chronic timepoints (1 week and 3 months post-injury). Expression remained unchanged for most control animals at all times. However, up-regulation at 2days timepoint was observed in few controls, possibly due to pipetting errors during ddPCR reaction preparation, since technical replicates for these cases showed higher variation (figure 11).



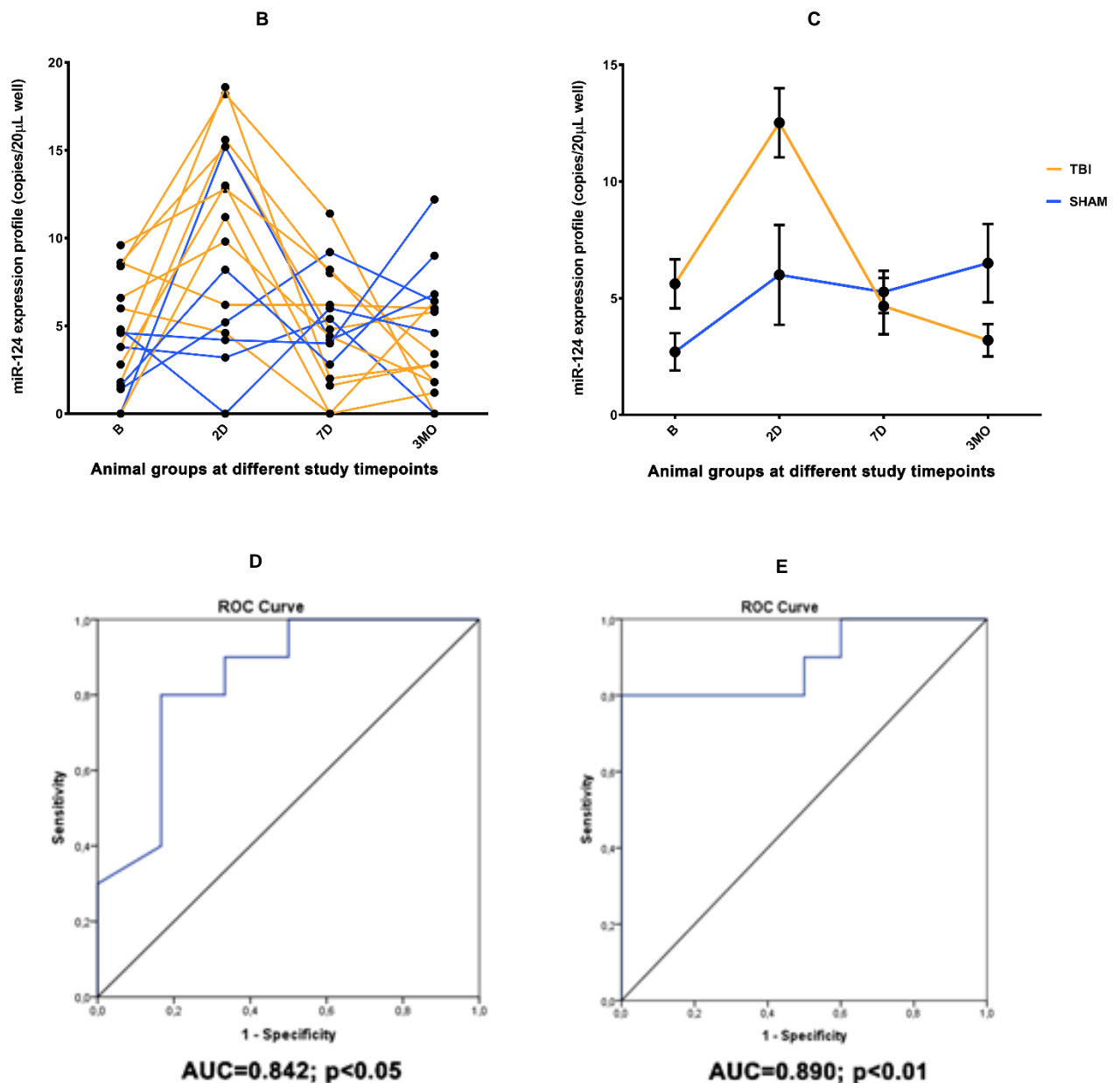


**Figure 11: (A) Expression profile for miR-124 across all timepoints in plasma (multiplexed ddPCR), (B) Individual animal variability in miR-124 expression across the four timepoints of study, (C) Average miR-124 expressions for control and TBI animals across the four timepoints, ROC analysis for (D) 2 days control vs. 2 days post-TBI, (E) Baseline TBI vs. 2 days post-TBI.** Using the multiplexed cDNA templates, similar pattern of miR-124 expression was observed in ddPCR, as earlier in qRT-PCR. Elevation in miR-124 expression in injured animals was observed at 2 days post-TBI timepoint, with levels returning to baseline at chronic timepoints. For control animals, slight up-regulation pattern in miR-124 expression at 2 days post-TBI (non-significant) was observed. Additionally, this up-regulation pattern in few control (sham operated) animals, was observed even at 3 months post-TBI timepoint. Nevertheless, none of the variations among controls were significant (Abbreviations used: ROC-receiver operator characteristics, AUC- area under curve, TBI-traumatic brain injury, B-baseline, 2D-2days, 7D-7days, 3MO-3months , miR-124 expression profile- miR-124 concentrations represented as the sum of target copies / 20 $\mu$ L well for the two ddPCR replicates; threshold adjusted to 6000, \* $p<0.05$ , \*\* $p<0.01$ ). ROC analyses revealed the possibility of considering miR-124 as a TBI biomarker.

#### 5.4.2 Droplet PCR based estimation of miR-124 expression in relation with lesion size

Similar to the previous qRT-PCR analysis, comparison of miR-124 expression in plasma at 2 days post-TBI in relation with the lesion size observed at 3 months, was studied using ddPCR method from the multiplexed cDNA. However, for this test, the results obtained from qRT-PCR could not be replicated. No difference in expression was observed in any of the cases (figure 12). It was observed that only one control animal exhibited very high miR-124 copy number (15,2 copies in total in the two replicates). However, since this datapoint was not marked as an outlier in SPSS analysis, it was not excluded from analysis.

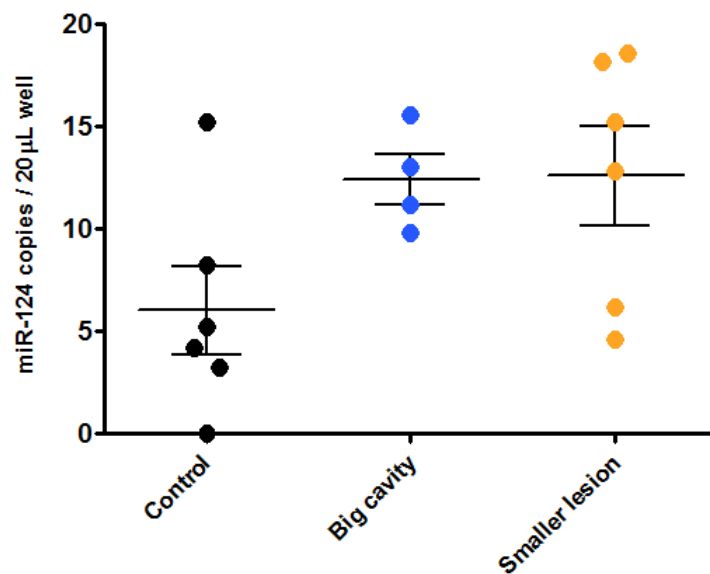


**Figure 12: No up-regulation in miR-124 expression observed in relation to lesion size with the ddPCR multiplex data.** Unlike the qRT-PCR data, no relation between miR-124 expression levels and lesion size was observed when the same multiplexed cDNA samples were amplified with ddPCR protocol. Since the miR-124 concentrations reported in this case were significantly low (~0-20 copies), it is presumed that the pattern of miR-124 expression with respect to lesion size might have been obscured due to this low rate of target amplification.

#### 5.5 Quantification of miR-124 with ddPCR from miR-124 specific RT products using TaqMan® chemistry

Droplet PCR run with multiplexed cDNA templates could successfully demonstrate up-regulation in miR-124 expression in trauma samples at 2 days post-injury. However, the main drawback of this run was that very few target copies could be obtained for each sample, and with considerably low fluorescence amplitudes. Particularly, for few samples, application of the manual threshold of 6000 resulted in no positive amplifications at all. However, when tested without the manual threshold setup (with automatically assigned thresholds from QuantaSoft), the up-regulation pattern of miR-124 at 2 days post-TBI could no more be observed. To check if the multiplex setup of cDNA synthesis reaction with multiple PCR primers was responsible for this low target amplification, ddPCR runs were repeated with only miR-124 specific RT reaction products. Reactions were again performed in duplicates and miR-

miR-124 expression was calculated as the sum of target copies / 20 $\mu$ L well for the two replicates. For this case, ddPCR runs for samples from different timepoints were run on different days to account for the impact of day-to-day variability on miR-124 expression levels.

#### **5.5.1 Expression analysis of miR-124 in plasma across all timepoints**

Expression profile of miR-124 across all the four study timepoints was now tested in the miR-124 specific RT samples using ddPCR. Higher copy numbers were in fact observed with these RT products, compared to multiplex samples. The expression pattern observed in qRT-PCR for the acute timepoint (2 days post-injury) could be successfully replicated. However, unlike the previous results, decrease in miR-124 concentration in the trauma samples at chronic timepoints (1 week and 3 months post-injury) could not be observed. Thus, for these samples, up-regulation of miR-124 occurred in response to trauma at 2 days post-TBI, and the levels remained consistent till 1 week and 3 months post-TBI timepoints.

Levels of miR-124 remained similar across control samples at all timepoints. Also, no difference in miR-124 expression was observed between the control and injured animals at baseline, 1 week and 3 months post trauma. Difference in expression was observed between control and TBI samples only at 2 days post-injury ( $p < 0.05$ ). For TBI samples, up-regulation of miR-124 expression was observed across all the studied timepoints ( $p < 0.05$ ). Thus, the pairwise tests were performed for all TBI cases. Significance was observed only at 2 days post-injury, compared to baseline ( $p < 0.05$ ). ROC analyses revealed only fair accuracy with AUC in the range of 0.7-0.8.

Individual animal variability pattern for this dataset also did not match the previous observations, possibly because the ddPCR runs were performed over different days. Up-regulation in miR-124 expression in injured animals, compared to controls, could still be observed at the acute timepoint (2 days post-injury). However, concentrations of miR-124 in TBI cases remained the same over 1 week and 3 months post-injury timepoints, as compared to the 2 days state. For few TBI samples, in fact, very high copy numbers were obtained at 3 months post-TBI. These results underscored the importance of running all ddPCR amplifications in the same day to minimize day-day variability in results (figure 13).



A

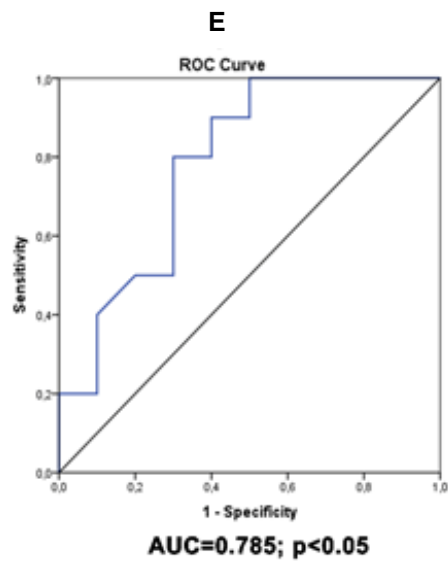
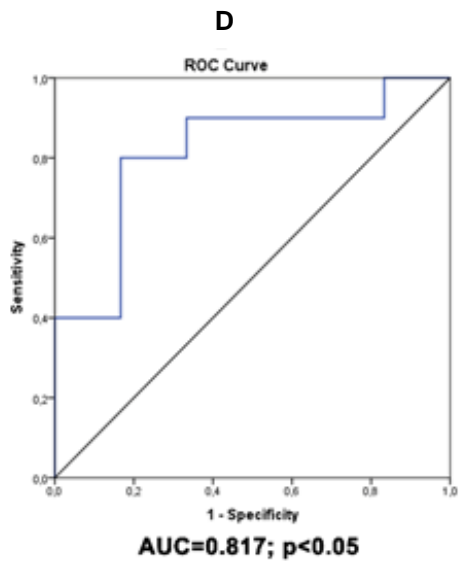
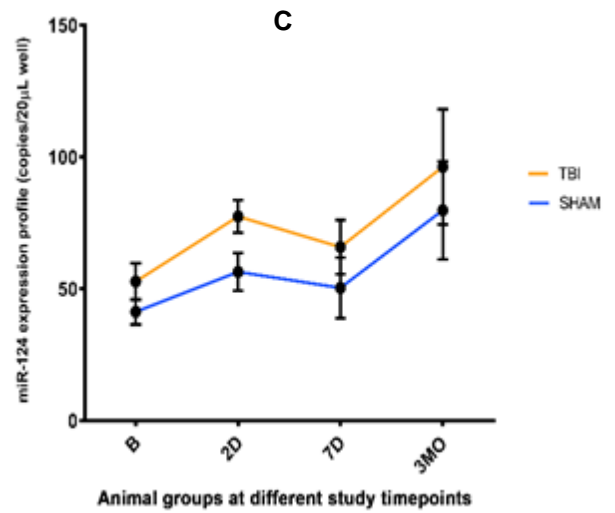
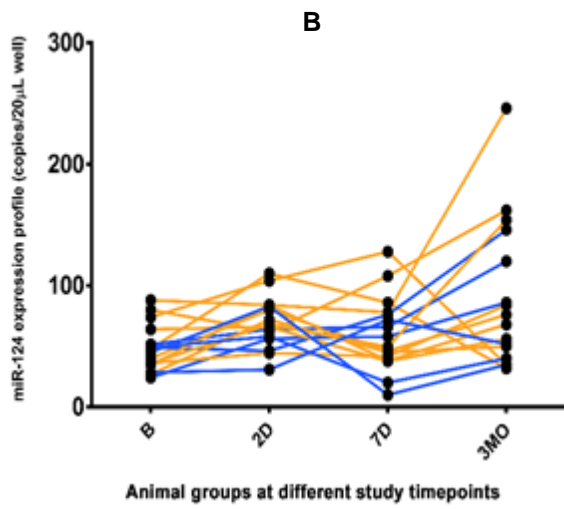
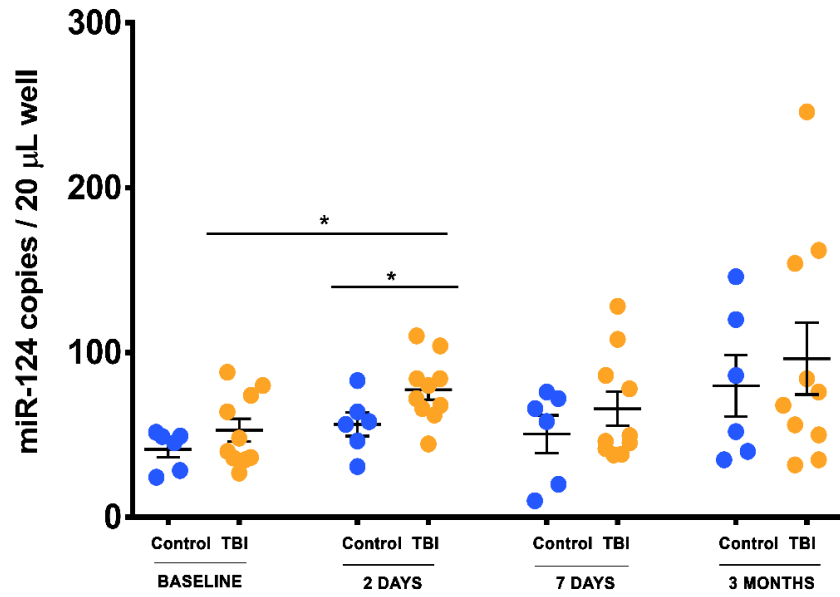


**Figure 13: (A) Expression profile for miR-124 across all timepoints in plasma samples with ddPCR (miR-124 specific ddPCR), (B) Individual animal variability in miR-124 expression across the four timepoints of study, (C) Average miR-124 expressions for control and TBI animals across the four timepoints, ROC analysis for (D) 2 days control vs. 2 days post-TBI and (E) Baseline TBI vs. 2 days post-TBI.** Using the miR-124 specific cDNA templates, upregulation in miR-124 expression in injured animals was observed at 2 days post-TBI timepoint, compared to 2 days controls and baseline TBI samples. However, in this case, the elevated miR-124 levels were not observed to be returning to baseline at chronic timepoints. Up-regulated levels of miR-124 in TBI cases were retained over the 1 week and 3 months post-injury timepoints. For few TBI samples, in fact, very high copy numbers were obtained at 3 months timepoint. Another surprising observation was that the controls also followed similar expression pattern as the TBI cases, although there was no significant difference in expression among them. Day-to-day variability in ddPCR sensitivity and impact of manual variation in reaction preparation over days were considered as the factors responsible for this unexpected (Abbreviations used: ROC-receiver operator characteristics, AUC- area under curve, TBI-traumatic brain injury, n.s- not significant, B-baseline, 2D-2days, 7D-7days, 3MO-3months, miR-124 expression profile- miR-124 concentrations represented as the sum of target copies / 20 $\mu$ L well for the two ddPCR replicates; threshold adjusted to 6000, \* $p < 0.05$ , \*\* $p < 0.01$ ). In this case, ROC analyses revealed fair accuracy with AUC in the range of 0.7-0.8.

### **5.5.2 Droplet PCR based estimation of miR-124 expression in relation with lesion size**

Comparison of miR-124 expression in plasma at 2 days post-TBI in relation with the lesion size observed at 3 months, was also studied using the ddPCR for miR-124 specific RT products. The expression pattern obtained in this case was different from both qRT-PCR and multiplexed ddPCR results. Up-regulation in miR-124 expression was observed in rats characterized with big sized cavities, compared to controls ( $p < 0.05$ ). Corresponding ROC analysis revealed high accuracy of miR-124 in differentiating rats with larger lesions from the controls (AUC=0.917 and  $p < 0.05$ ). This resembled the qRT-PCR pattern observed earlier. However, no difference in miR-124 expression was observed between the big cavity and smaller lesion groups. Also, no difference was observed between controls and rats with smaller lesions (figure 14).

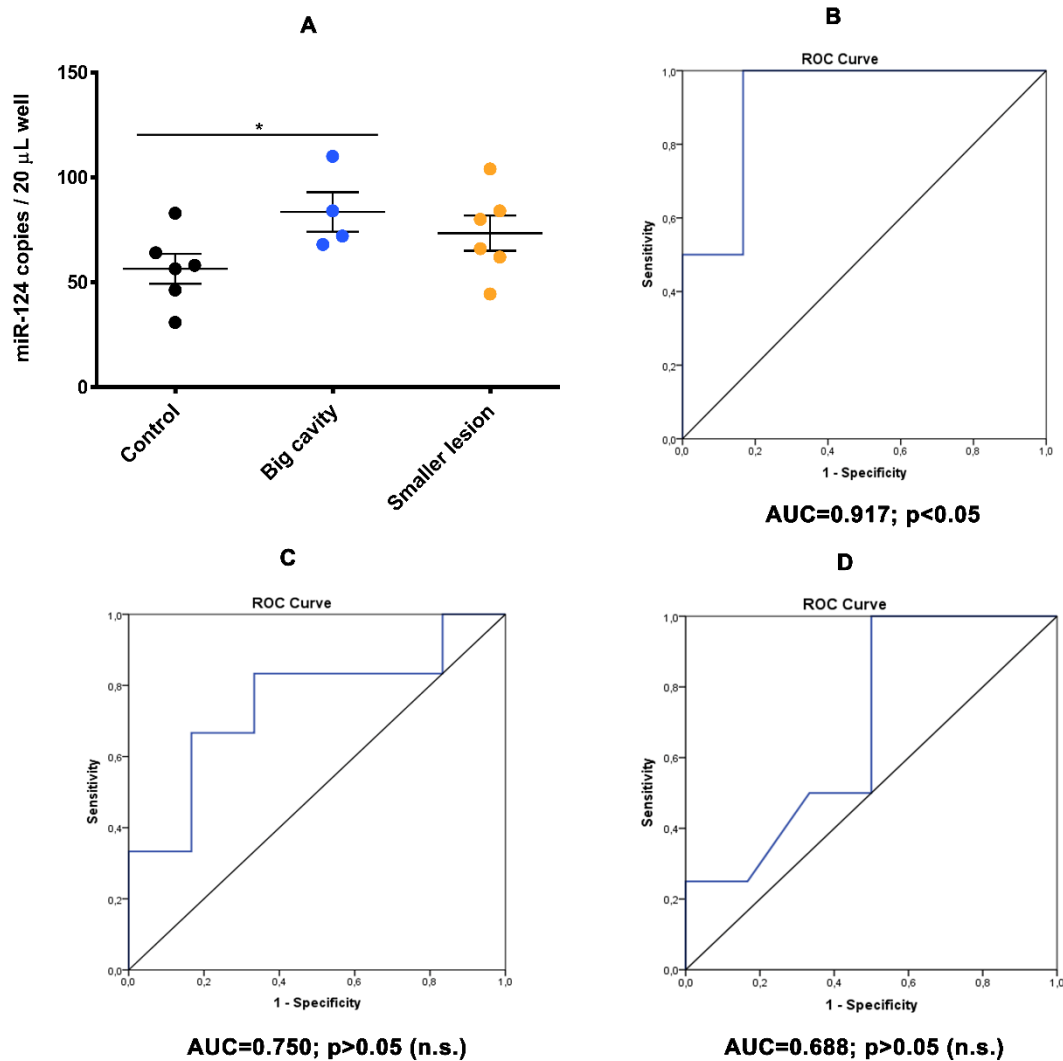


**Figure 14: (A) Up-regulation in miR-124 expression was observed in the ddPCR method only for rats with larger brain lesions compared to controls (miR-124 specific dataset), ROC analysis for (B) control vs. big lesion group (C) control vs. smaller lesion group, (D) big lesion vs. smaller lesion group using the ddPCR quantification method for miR-124 specific dataset.** Similar to the qRT-PCR data, up-regulation in miR-124 levels in rats with larger cavities was obtained compared to controls. However, in this case, no difference was observed between the rats with larger cavities and the ones with middle sized and smaller lesions. Thus relation of miR-124 with respect to lesion size was not consistent when the same samples were tested with qRT-PCR and ddPCR protocols (Abbreviations used: ROC-receiver operator characteristics, AUC- area under curve, n.s-not significant, \* $p<0.05$ , \*\* $p<0.01$ ).

## 5.6 Correlation between qRT-PCR and ddPCR expression patterns

Bivariate correlation analysis between the qRT-PCR and ddPCR datasets was first performed at 2 days post-TBI timepoint. For the multiplexed dataset, there was a correlation trend, but did not achieve significance (Spearman Correlation coefficient ( $\rho$ ) = 0.447 and  $p>0.05$ ). For the miR-124 specific dataset, correlation was observed (Spearman Correlation coefficient ( $\rho$ ) = 0.74 and  $p<0.01$ ) (figure 15 (A) and (B)). However, when analysis between the whole qRT-PCR and ddPCR datasets was performed, correlation was observed for both qRT-PCR vs. multiplexed ddPCR and qRT-PCR vs. miR-

124 specific datasets. This was possibly as a result of inclusion of more data points in the analysis. For the multiplexed dataset, Spearman Correlation coefficient ( $\rho$ ) of 0.387 and  $p < 0.01$  was obtained. For the miR-124 specific dataset, Spearman Correlation coefficient ( $\rho$ ) was 0.343 and  $p < 0.01$  (figure 15 (C) and (D)).

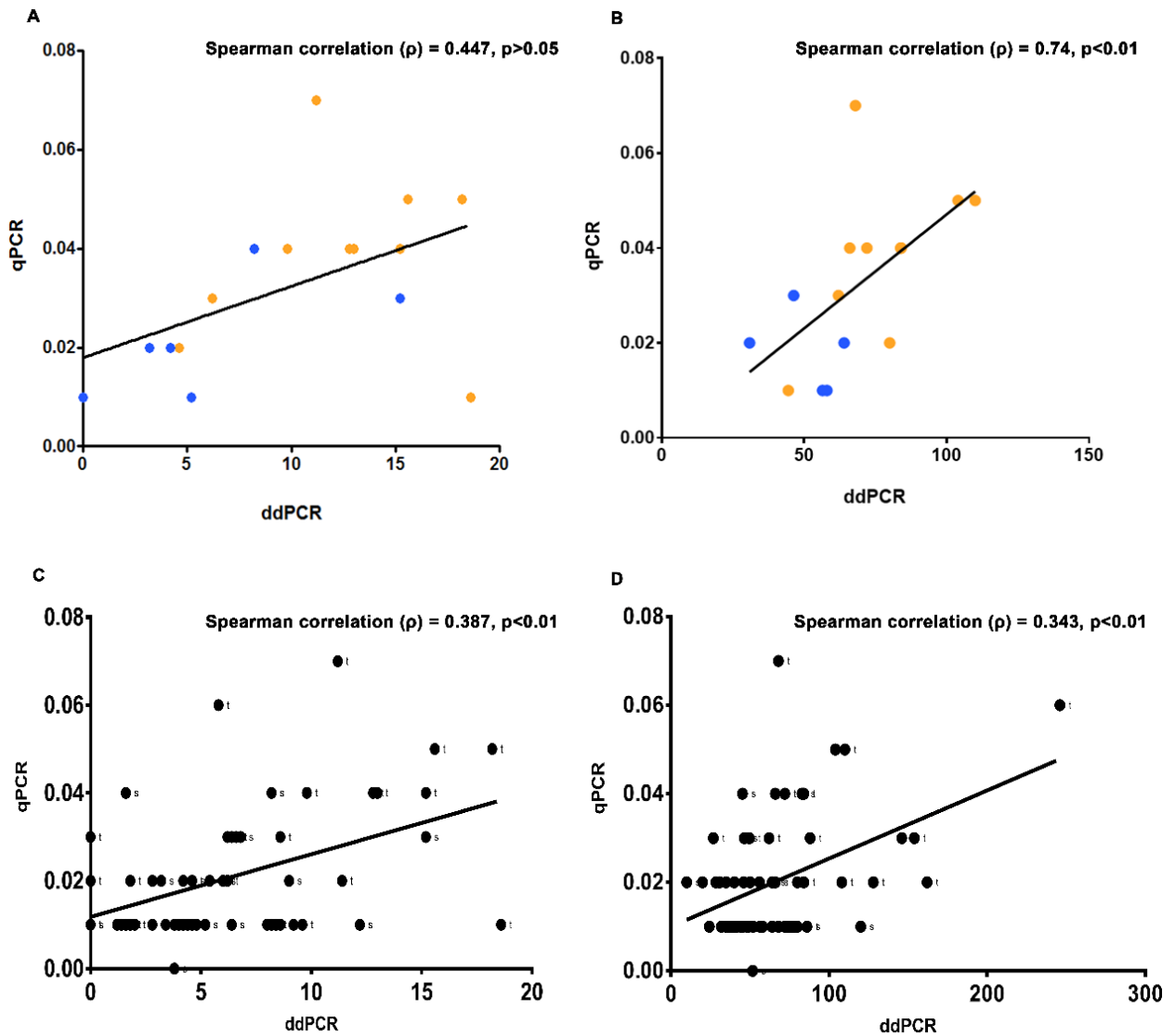


**Figure 15: Correlation between qRT-PCR and ddPCR amplifications at 2 days post-TBI for (A) multiplexed cDNA, (B) miR-124 specific cDNA. Correlation between qRT-PCR and ddPCR amplifications across all timepoints for (C) multiplexed cDNA, (D) miR-124 specific cDNA.** Correlation between qRT-PCR and ddPCR expression patterns were obtained for the miR-124 specific dataset at 2 days post-TBI, as well as when all timepoints were considered. On the other hand, correlation between qRT-PCR and multiplexed ddPCR was slightly below significance ( $p = 0.082$ ) for 2 days post-TBI, but the overall correlation across all timepoints revealed significance (Abbreviations used: s-sham. t-TBI).

## 5.7 Expression analysis of miR-124 in brain tissue samples (ipsilateral cortex)

To assess changes in miR-124 expression in the perilesional cortex, multiplexed TaqMan RT products (U6 and miR-124 specific) were used. Expression of miR-124 was studied with and without normalisation to U6 expression. Slight upregulation was observed in the trauma samples whereas all controls represented uniform expression (without normalisation). However, this up-regulation was not statistically significant. When normalised to U6, both controls and TBI samples demonstrated similar expression pattern, and no up-regulation was observed in this case (figure 16).

Thus, for both normalised and non-normalised conditions, ddPCR demonstrated no difference in miR-124 expression between controls and TBI, indicating the robustness of this technique in miRNA quantification from tissue samples in absence of endogenous controls. Also, this result was in concordance with our previous miRNA sequencing results that demonstrated no change in miR-124 expression in the ipsilateral cortex at 3 month post-TBI (unpublished data).

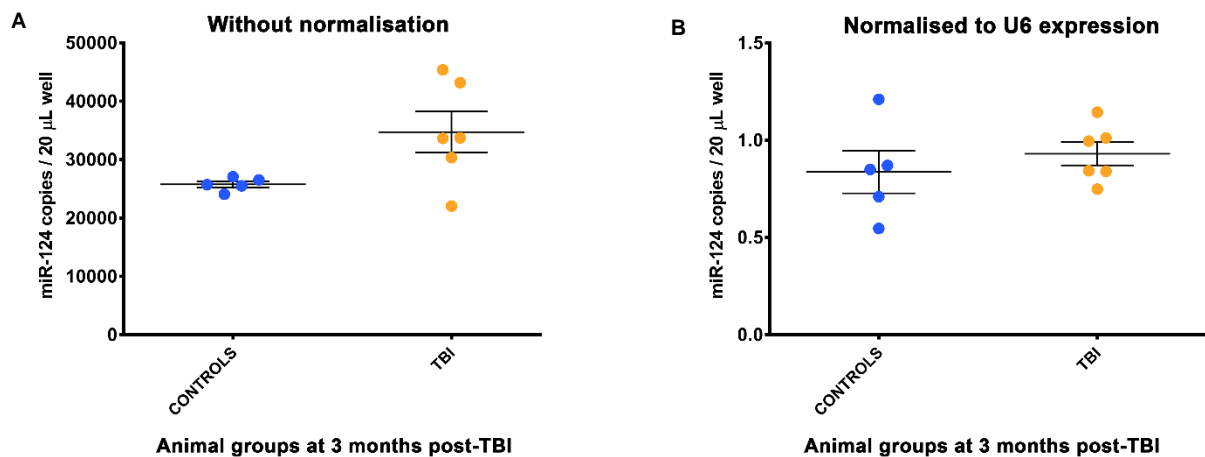


**Figure 16: Comparison of miR-124 expression between controls and TBI samples from ipsilateral cortex at 3 months post-injury, (A) without normalisation to U6, (B) data normalised to U6 expression.** Expression levels of miR-124 in the ipsilateral cortex at 3 months post injury was studied with ddPCR. No difference in expression was observed between the controls and injured animals. Expression patterns remained same when miR-124 concentrations were normalised to the known endogenous control snRNA U6, as well as when studied without normalization. This indicated the accuracy of ddPCR technique in unbiased target quantification without requiring normalisation. Expression patterns also successfully replicated the miRNA sequencing data obtained previously for these samples (Abbreviations used: TBI-traumatic brain injury).

## **6 DISCUSSION**

MicroRNA biomarkers are believed to play a significant role in predicting susceptibility towards post-traumatic epilepsy, since alterations in miRNA expression levels have already been identified in ischemia, Alzheimer's disease, and several other neurological disorders [5, 14, 60-62, 80]. Several studies aiming at prevention of epileptogenesis thus involve investigation of biomarkers at acute and/or chronic timepoints, which can reveal susceptibility of an individual towards developing epilepsy in future. Blood based biomarkers are gaining attention, since cytosolic components released from the damaged brain tissue (neurons and glial cells) are believed to reach peripheral blood through leakage in the BBB, and also in part by the recently discovered glymphatic system of the CNS [95-97]. Plasma concentrations of these brain specific macromolecules thus form markers of injury severity and extent of brain damage. Also, blood samples can be easily obtained from patients with minimal surgical intervention, thus making clinical diagnosis easier.

In concordance with this hypothesis, recent studies with blood samples from Sprague-Dawley rats subjected to lateral FPI have indicated up-regulation of brain-enriched miRNAs at an acute timepoint (2 days post-TBI) [18]. Thus, the aim of this thesis study was to profile the expression of a brain-enriched miRNA, miR-124 from plasma samples of a similar animal cohort subjected to lateral FPI, over both acute and chronic timepoints. Furthermore, expression levels of miR-124 in the ipsilateral cortex at chronic time post-injury, and association of plasma miR-124 levels with size of brain lesion developed as a result of the inflicted trauma were investigated.

The major findings were as follows:

1. Up-regulation in plasma miR-124 expression was observed in case of animals receiving the brain injury, at 2 days post-TBI, with both qRT-PCR and ddPCR techniques. In the ipsilateral cortex, similar miR-124 expression levels were observed for the sham operated controls and injured animals, at 3 months post-TBI.
2. Both real-time qRT-PCR and ddPCR demonstrated comparable sensitivity in profiling miR-124 levels from plasma. However, absence of a known endogenous reference for qRT-PCR based plasma miRNA quantification was a major limitation. On the other hand, ddPCR demonstrated very low rate of target amplification when multiplexed cDNA products were used. Also, when reactions were performed in different days, significant day-to-day variability in expression patterns was observed.
3. Relation between miR-124 levels at acute timepoints, in relation with lesion size developed at chronic periods, was established with qRT-PCR. Rats with small and middle sized cavities at 3 months post-injury demonstrated almost similar miR-124 levels in plasma as controls, whereas rats with larger cavities demonstrated significantly elevated levels of plasma miR-124 at 2 days post-TBI. However, results from ddPCR were not totally consistent with this observation.

The significance of this study lies in the increasing demand for identification of non-invasive biomarkers to predict susceptibility towards post-traumatic epilepsy. Obtaining brain tissue samples from individuals who have immediately suffered from a head trauma, but without signs of epilepsy or any cognitive

impairment as of yet, can be challenging, as well as unethical in some situations. Also, imaging techniques have limited accuracy in predicting susceptibility towards epileptogenesis post-trauma. In such cases, there is a need to profile blood-based biomarkers, to predict susceptibility towards such conditions. Also, animal model based studies provide significant clues in the pre-clinical stage. For instance, this study not only revealed changes in expression patterns of miR-124 in plasma, but also indicated a probable association between the miR-124 levels and the size of the brain lesion developed. Such associations, if proved consistently with multiple datasets, would allow prediction of lesion size in humans as well based on the miR-124 expression level, to a certain extent, without surgical interventions.

## **6.1 Methodological considerations**

### **6.1.1 RNA isolation from plasma**

Cell-free biofluids such as plasma possess significantly low RNA concentrations, with miRNAs forming only a small fraction of the total RNA volume. Thus, successful extraction of these miRNA targets pose a challenge. Several commercially available kits have been designed for this purpose. Two methods are principally used: chemical extraction and immobilization on glass or silica. Chemical methods use high concentration chaotropic salts in conjunction with acid phenol or phenol-chloroform based extraction to inactivate RNases and purify RNA. The mirVana™ PARIS™ kit is a high performance RNA isolation kit that uses the acid phenol-chloroform method for RNA extraction, followed by immobilization to a glass-fiber filter for elution. The Exiqon miRCURY™ RNA isolation kit – biofluids, on the other hand, is particularly suitable for RNA extractions from serum, plasma, CSF and other biofluids. This kit is able to purify RNAs smaller than 1000 nucleotides (including mRNAs, tRNAs, miRNAs and siRNAs) based on spin column chromatography, using a proprietary resin as the separation matrix. This protocol is able to extract small RNAs without the use of phenol-chloroform based extraction methods. Both kits were tested in pilot studies and comparable performance was observed. However, based on ease of use, absence of phenol carryover and lower costs, the Exiqon method was chosen for total RNA extraction in this study. Also, the amount of starting material is critical for RNA isolation from body fluids, since they contain high amounts of cDNA and PCR inhibitors that affect downstream reactions [81]. Thus, following the manufacturer's protocol, RNA isolation was performed from a starting volume of 50µL of rat plasma, to obtain detectable levels of the target miRNA with minimum reaction inhibition [90].

### **6.1.2 Trade-off between Exiqon and TaqMan® chemistries**

The TaqMan small RNA assays are pre-designed primer-probe based assays that aim at targeted quantification, screening and validation of mature microRNA sequences [93]. Due to target specificity of both primers and probes, only miRNA specific reverse transcription and qRT-PCR reactions can be performed with TaqMan chemistry. However, a combination of multiple primers can be used to develop a multiplexed reverse transcription reaction that allows simultaneous amplification of multiple targets from the same cDNA products in downstream qRT-PCR.

On the other hand, the Exiqon miRCURY LNA™ Universal RT microRNA PCR system is a microRNA specific, locked nucleic acid (LNA™) system that enables specific and accurate quantification of miRNAs

using intercalating dye based real-time PCR amplification (SYBR Green for qRT-PCR and EvaGreen for ddPCR reaction methods) [92]. Unlike the miRNA specific TaqMan system, this method involves universal reverse transcription (RT) of all miRNAs followed by PCR amplification with LNA<sup>TM</sup> enhanced primers. The universal RT reaction saves required sample volume and other reagents, along with lower technical variation and reaction time. However, due to the inherent tendency of intercalating dyes to bind with non-specific amplicons, the reaction specificity of this system is lower as compared to TaqMan. This was also verified in this study, since the Exiqon system consistently failed for miR-124 amplification from plasma samples, whereas successful detection was observed with TaqMan chemistry.

However, the Exiqon kit provided exogenous spike-ins to monitor both RNA isolation and RT reaction efficiencies, and this feature was not available with TaqMan system. Since extracted RNA volumes from plasma samples were below the detection limit of NanoDrop and Agilent Bioanalyzer, monitoring the spike-in RNA expressions was the only available option.

### **6.1.3 Absence of suitable endogenous control for plasma miRNA quantification**

For cell-free plasma samples, suitable endogenous control miRNAs are not known yet. Thus, the plasma enriched miR-103 was tested as a potential candidate. However, significant differences in expression was observed at different timepoints, in both control and injured animals. The exogenous spike-in expression data from Exiqon kit was then utilized. Normalization of miRNA expression from TaqMan was performed to these exogenous spike-ins.

### **6.1.4 Limitations in optimizing the ddPCR protocol**

Annealing temperature ( $T_m$ ) is the most critical parameter for reaction specificity in PCR, since setting it too low may lead to non-specific amplifications and setting it too high might reduce the yield of the desired PCR product [86]. Thus, a thermal gradient was set up to check for the suitable annealing temperature for miR-124 quantification with ddPCR. For tissue samples, proper separation of positive and negative clusters were obtained at  $T_m \sim 60^\circ\text{C}$ . However, for plasma, no proper separation of clusters was observed at any temperature. Lowering the  $T_m$  only resulted in increase of positive droplets at lower fluorescence amplitudes, a possible indication of non-specific amplification. Thus,  $T_m = 60^\circ\text{C}$  could not be identified to be suitable for the ddPCR method with certainty.

Overall, the Exiqon RNA isolation kit-biofluids was successful in total RNA extraction from plasma. Both Exiqon (dye-based) and TaqMan (probe-based) qRT-PCR systems were implemented for miR-124 profiling. For qRT-PCR, the attempt to identify a potential endogenous control for normalization of plasma miRNA expression failed. Attempts to optimise the ddPCR protocol for unbiased miRNA quantification was performed, but some unmet challenges remained.

## **6.2 Potential of plasma miR-124 to act as a TBI biomarker**

Since miR-103 failed as an endogenous control candidate, miR-124 expression was also normalized to the exogenous spike-in expression. However, no negative impact in results was observed due to this normalization, since identical expression patterns were also obtained in ddPCR, where absolute miR-124 quantification was performed without requiring normalization controls. Previous studies in animal



models of stroke have demonstrated up-regulation of miR-124 at acute-timepoints post-occlusion, with levels beginning to increase at ~6 hours after surgery, and peaking at ~24-48 hours [75, 80]. In this case, levels of miR-124 were assessed both at acute and chronic timepoints post injury. Similar to the stroke models, in all the three tested datasets (qRT-PCR with multiplexed cDNA templates, ddPCR with multiplexed cDNA templates and ddPCR with miR-124 specific templates), up-regulation of miR-124 in injured animals at an acute timepoint (2 days post-TBI) was validated. Also, this was in agreement with the previous study of miR-124 expression profiling post-TBI, in whole blood [18].

A major consideration in profiling plasma levels of miRNA expression for predicting TBI, is that the trauma affects not only the brain, but also peripheral organs. Thus the possibility of the target miRNA expression level to reflect such bodily injuries as well, cannot be ruled out [63]. However, several studies indicate the high specificity of miR-124 in brain specific areas (CNS, cerebral cortex, spinal cord) [74, 98], thereby prompting the assumption that most of the altered miR-124 expression patterns observed in the plasma reflect only severity of brain injury due to TBI.

The other consideration is the rate of clearance of brain-specific components post injury. Recent studies have indicated impairment of several clearance mechanisms of the brain post-TBI, leading to reduction in brain clearance [95, 96, 99]. Thus, even if brain-specific components profiled from body fluids reveal significant alterations in expression pattern in response to injury, they may not reflect the actual extent of injury severity, because of the impaired clearance. In future studies aiming at profiling brain-specific components from body fluids, this aspect has to be considered.

Another interesting observation is that in in-vitro models of Alzheimer's disease, miR-124 levels are observed to be inversely proportional with A $\beta$  accumulation, thus indicating that alterations of this miRNA in response to TBI may also pose some relation with Alzheimer's-like pathology [100].

Thus, to sum up, the study was in support of the hypothesis that miR-124 levels in blood and/or plasma may possibly act as biomarkers for brain injury. Any involvement of peripheral tissue in this expression is unlikely, but warrants further investigation. Also, studying miR-124 expression and associated co-morbidities in relation with both TBI and dementia-like disorders, with focus on impacts of impaired clearance systems, would significantly enhance our knowledge of the common underlying pathologies.

### **6.3 Sensitivity of ddPCR in assessing plasma levels of miR-124**

Droplet PCR could successfully replicate the up-regulation pattern of miR-124 in injured animals at 2 days post-TBI. However, variability was observed between the multiplexed and miR-124 specific datasets. For the multiplexed products, very few target copies could be obtained, with significantly low fluorescence amplitudes. For few samples, application of the manual threshold of 6000 resulted in no positive amplifications at all, and when tested without the manual threshold setup, the predicted pattern of miR-124 up-regulation at 2 days post-TBI could no more be observed. This indicated the importance of manual adjustment of the threshold, especially for low target abundance samples, to exclude non-specific amplifications and to detect significant changes in expression patterns.

On the other hand, for miR-124 specific cDNA samples, higher copy numbers were obtained, with higher fluorescence amplitudes as well. This indicated that variability in ddPCR results can also be observed when upstream reaction methods are different, possibly in this case due to different mechanisms of cDNA synthesis reaction (multiplex vs. miR-124 specific).

Differences were also observed between the two ddPCR datasets at chronic timepoints post-injury. The multiplexed dataset replicated the qRT-PCR observation pattern, whereas for the miR-124 specific case, up-regulated levels of miR-124 were observed at 1 week and 3 months post-injury timepoints as well. This was possibly due to the day-day variability in reaction preparation, since ddPCR runs for the miR-124 specific samples from different timepoints were performed on different days. Importance of performing all ddPCR runs for a single analysis at once, to minimize technical variations, was thus elucidated.

For ddPCR, few NTCs also exhibited positive amplifications, possibly due to contamination while reaction preparation and the high sensitivity of this technique. However, similar results have been reported in other studies as well [101, 102], where chances of cross-contamination were minimized as far as possible. The extent to which positive amplification of NTCs affect the ddPCR results is not known yet, and needs to be investigated further. In qRT-PCR, none of the NTCs showed any amplification.

Thus from both qRT-PCR and ddPCR runs, it was deduced that in absence of endogenous controls, ddPCR can be a reliable tool for target quantification. However, particularly for low target abundance samples, the ddPCR technique is highly variable, with results being altered due to variations in upstream experimental steps (variations in RNA extraction and cDNA synthesis protocols), as well as due to technical variations in manual reaction preparation, when performed over days. Also, defining suitable thresholds for excluding off-target amplifications was found to be important. The study also indicates that for rare miRNAs, validation of expression patterns with qRT-PCR prior to ddPCR analysis may add to the reliability of results. It states that Droplet PCR results can be trusted, but suitable optimization methods and minimization of manual variability in reaction preparation should be considered.

#### **6.4 Relation between plasma levels of miR-124 at acute timepoints post-injury with histological changes observable at chronic timepoints**

Cresyl violet staining for the coronal brain sections revealed association of elevated miR-124 plasma levels at 2 days post-TBI, with development of larger brain lesions and greater extent of cell loss at the impact site. This relation was validated with qRT-PCR. Rats characterized with larger cavities, in fact, demonstrated higher levels of miR-124 in plasma at 2 days post-TBI. One possible explanation for this could be that larger brain lesions are indicative of greater extent of BBB damage post-injury, allowing increased infiltration of miR-124 from the injured brain to blood.

However, the ddPCR results failed to identify this relation. The ddPCR patterns from multiplexed and miR-124 datasets differed between themselves as well. From the multiplexed dataset, no significant difference in expression pattern was observed among controls, rats with bigger cavities, and rats with smaller lesions. The miR-124 specific dataset, on the other hand, could reveal significant up-regulation

of miR-124 in rats with bigger cavities compared to controls, but no difference between these and the ones with smaller lesion was observed.

Thus, relation between lesion type and miR-124 levels in plasma at an acute timepoint post-injury was not totally consistent in this study, and needs to be investigated further in future.

## **7 CONCLUSION AND FUTURE WORK**

The main objective of this time-course profiling study was to identify if miR-124 can act as a diagnostic biomarker for TBI at acute and/or chronic timepoints. The real-time quantitative PCR and ddPCR methods were implemented for miRNA quantification, and the sensitivity of these techniques in detecting the miRNA from low abundance plasma samples was compared. Also, special emphasis was placed on determining the relation between miR-124 expression levels at acute timepoints post-injury, with the size of brain lesion developed at chronic timepoints. The main findings can be summarized as follows:

1. Up-regulation in plasma miR-124 expression was observed in case of animals receiving the brain injury, at 2 days post-TBI, with both qRT-PCR and ddPCR techniques. This underscored the potential of miR-124 as a biomarker for TBI at acute timepoints. The findings were consistent with previous studies performed with whole blood, wherein up-regulation in miR-124 at 2 days post-TBI was also evident in case of trauma samples. Additionally, in concordance with our previous miRNA sequencing data, similar miR-124 levels were observed for controls and injured animals, in the ipsilateral cortex, at 3 months post-TBI.
2. Both real-time qRT-PCR and ddPCR demonstrated comparable sensitivity in profiling miR-124 levels from plasma. However, absence of a known endogenous reference for qRT-PCR based plasma miRNA quantification was a major limitation. Expression levels were thus normalized to the exogenous spike-ins added to monitor reaction efficiency. No negative impact was observed as a result of this normalization, since ddPCR based absolute quantifications reflected similar expression patterns. On the other hand, ddPCR demonstrated very low rate of target amplification when multiplexed cDNA products were used, although the up-regulation pattern was still evident. Also, when reactions were performed in different days, significant day-to-day variability in expression patterns was observed.
3. Relation between miR-124 levels at acute timepoints, in relation with lesion size developed at chronic periods, was established with qRT-PCR. Rats with small and middle sized cavities at 3 months post-injury demonstrated almost similar miR-124 levels in plasma as controls, whereas rats with larger cavities demonstrated significantly elevated levels of plasma miR-124 at 2 days post-TBI. However, results from ddPCR were not totally consistent with this observation.

Altogether, results from this study were in agreement with the previous observation of the possibility of studying miR-124 as a TBI biomarker. A probable relation between larger brain lesions and elevated levels of miR-124 in plasma was also demonstrated. Both ddPCR and real-time qRT-PCR methods were successful in detecting the alterations in miRNA levels at different timepoints post-injury, but several optimizations of these techniques are still required for performing unbiased quantifications.

As far as we know, this study was the first to implement the ddPCR methodology for miR-124 quantification from plasma in relation with TBI, and to monitor alterations in the expression levels of this miRNA over both acute and chronic timepoints. Also, for the first time, the relation between cortical lesion size and plasma miR-124 levels was investigated. Thus, future work involves in-situ hybridization for this target miRNA in 2 days, 1 week and 3 months post-TBI brain samples, to detect the region-specific miR-124 localization and expression. Also, there is a possibility of replicating this study with a

larger cohort of animals with MRI imaging data available, to characterize the altered plasma miR-124 expression with extent of brain damage with more specificity (plasma miR-124 levels at 2 days post-TBI with MRI brain images at 2 months post-TBI). Finally, since detecting endogenous references for qRT-PCR based miRNA quantification from biofluids is still a challenge, potential candidate miRNAs such as miR-191-5p, miR-423-3p and miR-423-5p will be investigated.

## 8 REFERENCES

1. Fisher, R.S., et al., *Epileptic seizures and epilepsy: definitions proposed by the International League Against Epilepsy (ILAE) and the International Bureau for Epilepsy (IBE)*. *Epilepsia*, 2005. **46**(4): p. 470-2.
2. Akhtar, M.S., et al., *Burn injury in epileptic patients: an experience in a tertiary institute*. *Ann Burns Fire Disasters*, 2014. **27**(3): p. 126-9.
3. De Boer, H.M., M. Mula, and J.W. Sander, *The global burden and stigma of epilepsy*. *Epilepsy & Behavior*, 2008. **12**(4): p. 540-546.
4. Espinosa-Jovel, C.A. and F.E. Sobrino-Mejia, *[Drug resistant epilepsy. Clinical and neurobiological concepts]*. *Rev Neurol*, 2015. **61**(4): p. 159-66.
5. Bot, A.M., K.J. Debski, and K. Lukasiuk, *Alterations in miRNA levels in the dentate gyrus in epileptic rats*. *PLoS One*, 2013. **8**(10): p. e76051.
6. Baker, G.A., *The psychosocial burden of epilepsy*. *Epilepsia*, 2002. **43**(s6): p. 26-30.
7. Rao, V.R. and K.L. Parko, *Clinical approach to posttraumatic epilepsy*. *Semin Neurol*, 2015. **35**(1): p. 57-63.
8. Annegers, J.F. and S.P. Coan, *The risks of epilepsy after traumatic brain injury*. *Seizure*, 2000. **9**(7): p. 453-7.
9. Huusko, N., *GABAergic network alterations in rat models of acquired epilepsy, Dissertation in Health Sciences submitted at the Department of Neurobiology, University of Eastern Finland, Kuopio, 2014. ISBN: 978-952-61-1412-5*.
10. Walia, K.S., et al., *Side effects of antiepileptics--a review*. *Pain Pract*, 2004. **4**(3): p. 194-203.
11. Sisodiya, S., *Etiology and management of refractory epilepsies*. *Nat Clin Pract Neurol*, 2007. **3**(6): p. 320-30.
12. Lukasiuk, K. and A.J. Becker, *Molecular biomarkers of epileptogenesis*. *Neurotherapeutics*, 2014. **11**(2): p. 319-23.
13. Wang, J., et al., *Genome-wide circulating microRNA expression profiling indicates biomarkers for epilepsy*. *Sci Rep*, 2015. **5**: p. 9522.
14. Peng, J., et al., *Expression patterns of miR-124, miR-134, miR-132, and miR-21 in an immature rat model and children with mesial temporal lobe epilepsy*. *J Mol Neurosci*, 2013. **50**(2): p. 291-7.
15. Li, M.M., et al., *MicroRNAs dysregulation in epilepsy*. *Brain Res*, 2014. **1584**: p. 94-104.
16. Jimenez-Mateos, E.M. and D.C. Henshall, *Epilepsy and microRNA*. *Neuroscience*, 2013. **238**: p. 218-29.
17. Moldovan, L., et al., *Methodological challenges in utilizing miRNAs as circulating biomarkers*. *J Cell Mol Med*, 2014. **18**(3): p. 371-90.
18. Pyykönen, N., *MicroRNA in post-traumatic epileptogenesis, Master's thesis submitted at the Faculty of Biochemistry and Molecular Medicine, University of Oulu, Published 1 June 2015*.
19. Magiorkinis, E., K. Sidiropoulou, and A. Diamantis, *Hallmarks in the history of epilepsy: epilepsy in antiquity*. *Epilepsy Behav*, 2010. **17**(1): p. 103-8.
20. Fisher, R.S., et al., *ILAE official report: a practical clinical definition of epilepsy*. *Epilepsia*, 2014. **55**(4): p. 475-82.
21. Scharfman, H.E., *Chapter 17 - Epilepsy*, in *Neurobiology of Brain Disorders*, M.J.Z.P.R.T. Coyle, Editor. 2015, Academic Press: San Diego. p. 236-261.

22. England, M.J., et al., *A Summary of the Institute of Medicine Report: Epilepsy Across the Spectrum: Promoting Health and Understanding*. *Epilepsy & behavior: E&B*, 2012. **25**(2): p. 266.
23. Berg, A.T., et al., *Revised terminology and concepts for organization of seizures and epilepsies: report of the ILAE Commission on Classification and Terminology, 2005-2009*. *Epilepsia*, 2010. **51**(4): p. 676-85.
24. Shorvon, S.D., *The etiologic classification of epilepsy*. *Epilepsia*, 2011. **52**(6): p. 1052-1057.
25. Maas, A.I., N. Stocchetti, and R. Bullock, *Moderate and severe traumatic brain injury in adults*. *Lancet Neurol*, 2008. **7**(8): p. 728-41.
26. Risdall, J.E. and D.K. Menon, *Traumatic brain injury*. *Philos Trans R Soc Lond B Biol Sci*, 2011. **366**(1562): p. 241-50.
27. Kharatishvili, I., *Development and Characterization of a Rat Model of Human Post-traumatic Epilepsy in Department of Neurobiology*. 2009, University of Eastern Finland: Kuopio.
28. Saatman, K.E., et al., *Classification of traumatic brain injury for targeted therapies*. *J Neurotrauma*, 2008. **25**(7): p. 719-38.
29. Annegers, J.F., et al., *Seizures after head trauma: a population study*. *Neurology*, 1980. **30**(7 Pt 1): p. 683-9.
30. Lowenstein, D.H., *Epilepsy after head injury: an overview*. *Epilepsia*, 2009. **50 Suppl 2**: p. 4-9.
31. Cernak, I., *Animal models of head trauma*. *NeuroRx*, 2005. **2**(3): p. 410-22.
32. Pitkanen, A., *Therapeutic approaches to epileptogenesis--hope on the horizon*. *Epilepsia*, 2010. **51 Suppl 3**: p. 2-17.
33. Hesdorffer, D.C., et al., *Risk of unprovoked seizure after acute symptomatic seizure: effect of status epilepticus*. *Ann Neurol*, 1998. **44**(6): p. 908-12.
34. Ueda, Y., et al., *Collapse of extracellular glutamate regulation during epileptogenesis: down-regulation and functional failure of glutamate transporter function in rats with chronic seizures induced by kainic acid*. *J Neurochem*, 2001. **76**(3): p. 892-900.
35. Park, E., J.D. Bell, and A.J. Baker, *Traumatic brain injury: can the consequences be stopped?* *Cmaj*, 2008. **178**(9): p. 1163-70.
36. da Rocha, A.B., et al., *Serum Hsp70 as an early predictor of fatal outcome after severe traumatic brain injury in males*. *J Neurotrauma*, 2005. **22**(9): p. 966-77.
37. Ross, S.A., et al., *The presence of tumour necrosis factor in CSF and plasma after severe head injury*. *Br J Neurosurg*, 1994. **8**(4): p. 419-25.
38. Huusko, N., et al., *Loss of hippocampal interneurons and epileptogenesis: a comparison of two animal models of acquired epilepsy*. *Brain Struct Funct*, 2015. **220**(1): p. 153-91.
39. Panter, S.S., et al., *Hypohaptoglobinemia associated with familial epilepsy*. *J Exp Med*, 1985. **161**(4): p. 748-54.
40. Diaz-Arrastia, R., et al., *Increased risk of late posttraumatic seizures associated with inheritance of APOE epsilon4 allele*. *Arch Neurol*, 2003. **60**(6): p. 818-22.
41. Anderson, G.D., et al., *Haptoglobin phenotype and apolipoprotein E polymorphism: relationship to posttraumatic seizures and neuropsychological functioning after traumatic brain injury*. *Epilepsy Behav*, 2009. **16**(3): p. 501-6.
42. Pitkanen, A., T. Bolkvadze, and R. Immonen, *Anti-epileptogenesis in rodent post-traumatic epilepsy models*. *Neurosci Lett*, 2011. **497**(3): p. 163-71.
43. Grinnon, S.T., et al., *National Institute of Neurological Disorders and Stroke Common Data Element Project - approach and methods*. *Clin Trials*, 2012. **9**(3): p. 322-9.

44. White, H.S., *Animal models of epileptogenesis*. Neurology, 2002. **59**(9 Suppl 5): p. S7-s14.
45. Golarai, G., et al., *Physiological and structural evidence for hippocampal involvement in persistent seizure susceptibility after traumatic brain injury*. J Neurosci, 2001. **21**(21): p. 8523-37.
46. D'Ambrosio, R., et al., *Progression from frontal-parietal to mesial-temporal epilepsy after fluid percussion injury in the rat*. Brain, 2005. **128**(Pt 1): p. 174-88.
47. D'Ambrosio, R., et al., *Post-traumatic epilepsy following fluid percussion injury in the rat*. Brain, 2004. **127**(Pt 2): p. 304-14.
48. Dixon, C.E., J.W. Lighthall, and T.E. Anderson, *Physiologic, histopathologic, and cineradiographic characterization of a new fluid-percussion model of experimental brain injury in the rat*. J Neurotrauma, 1988. **5**(2): p. 91-104.
49. Annegers, J.F., et al., *A population-based study of seizures after traumatic brain injuries*. N Engl J Med, 1998. **338**(1): p. 20-4.
50. Vespa, P.M., et al., *Increased incidence and impact of nonconvulsive and convulsive seizures after traumatic brain injury as detected by continuous electroencephalographic monitoring*. J Neurosurg, 1999. **91**(5): p. 750-60.
51. Garga, N. and D.H. Lowenstein, *Posttraumatic epilepsy: a major problem in desperate need of major advances*. Epilepsy Curr, 2006. **6**(1): p. 1-5.
52. Frey, L.C., *Epidemiology of posttraumatic epilepsy: a critical review*. Epilepsia, 2003. **44 Suppl 10**: p. 11-7.
53. Kharatishvili, I., et al., *A model of posttraumatic epilepsy induced by lateral fluid-percussion brain injury in rats*. Neuroscience, 2006. **140**(2): p. 685-97.
54. Englander, J., et al., *Analyzing risk factors for late posttraumatic seizures: a prospective, multicenter investigation*. Arch Phys Med Rehabil, 2003. **84**(3): p. 365-73.
55. Pitkanen, A. and T.P. Sutula, *Is epilepsy a progressive disorder? Prospects for new therapeutic approaches in temporal-lobe epilepsy*. Lancet Neurol, 2002. **1**(3): p. 173-81.
56. Desai, B., S. Whitman, and D.A. Bouffard, *The role of the EEG in epilepsy of long duration*. Epilepsia, 1988. **29**(5): p. 601-6.
57. Kumar, M. and S.K. Sarin, *Biomarkers of diseases in medicine*. Curr Trends Sci, 2009. **70**: p. 403-417.
58. Etheridge, A., et al., *Extracellular microRNA: a new source of biomarkers*. Mutat Res, 2011. **717**(1-2): p. 85-90.
59. Vasudevan, S., Y. Tong, and J.A. Steitz, *Switching from repression to activation: microRNAs can up-regulate translation*. Science, 2007. **318**(5858): p. 1931-4.
60. Tan, L., et al., *Circulating miR-125b as a biomarker of Alzheimer's disease*. J Neurol Sci, 2014. **336**(1-2): p. 52-6.
61. Gorter, J.A., et al., *Hippocampal subregion-specific microRNA expression during epileptogenesis in experimental temporal lobe epilepsy*. Neurobiol Dis, 2014. **62**: p. 508-20.
62. Dharap, A., et al., *Transient focal ischemia induces extensive temporal changes in rat cerebral microRNAome*. J Cereb Blood Flow Metab, 2009. **29**(4): p. 675-87.
63. Redell, J.B., et al., *Human traumatic brain injury alters plasma microRNA levels*. J Neurotrauma, 2010. **27**(12): p. 2147-56.
64. Sharma, A., et al., *Identification of serum microRNA signatures for diagnosis of mild traumatic brain injury in a closed head injury model*. PLoS One, 2014. **9**(11): p. e112019.



65. Redell, J.B., Y. Liu, and P.K. Dash, *Traumatic brain injury alters expression of hippocampal microRNAs: potential regulators of multiple pathophysiological processes*. J Neurosci Res, 2009. **87**(6): p. 1435-48.
66. Liu, L., et al., *Traumatic brain injury dysregulates microRNAs to modulate cell signaling in rat hippocampus*. PLoS One, 2014. **9**(8): p. e103948.
67. Sun, T.Y., et al., *Expression profiling of microRNAs in hippocampus of rats following traumatic brain injury*. J Huazhong Univ Sci Technol Med Sci, 2014. **34**(4): p. 548-53.
68. McKiernan, R.C., et al., *Reduced mature microRNA levels in association with dicer loss in human temporal lobe epilepsy with hippocampal sclerosis*. PLoS One, 2012. **7**(5): p. e35921.
69. Aronica, E., et al., *Expression pattern of miR-146a, an inflammation-associated microRNA, in experimental and human temporal lobe epilepsy*. Eur J Neurosci, 2010. **31**(6): p. 1100-7.
70. Hu, K., et al., *Expression profile of microRNAs in rat hippocampus following lithium-pilocarpine-induced status epilepticus*. Neurosci Lett, 2011. **488**(3): p. 252-7.
71. Jimenez-Mateos, E.M., et al., *Silencing microRNA-134 produces neuroprotective and prolonged seizure-suppressive effects*. Nat Med, 2012. **18**(7): p. 1087-94.
72. Jimenez-Mateos, E.M., et al., *miRNA Expression profile after status epilepticus and hippocampal neuroprotection by targeting miR-132*. Am J Pathol, 2011. **179**(5): p. 2519-32.
73. Ge, X.T., et al., *miR-21 improves the neurological outcome after traumatic brain injury in rats*. Sci Rep, 2014. **4**: p. 6718.
74. Lagos-Quintana, M., et al., *Identification of tissue-specific microRNAs from mouse*. Curr Biol, 2002. **12**(9): p. 735-9.
75. Weng, H., et al., *Plasma miR-124 as a biomarker for cerebral infarction*. Biomed Res, 2011. **32**(2): p. 135-41.
76. Visvanathan, J., et al., *The microRNA miR-124 antagonizes the anti-neural REST/SCP1 pathway during embryonic CNS development*. Genes Dev, 2007. **21**(7): p. 744-9.
77. Cheng, L.C., et al., *miR-124 regulates adult neurogenesis in the subventricular zone stem cell niche*. Nat Neurosci, 2009. **12**(4): p. 399-408.
78. Akerblom, M., et al., *MicroRNA-124 is a subventricular zone neuronal fate determinant*. J Neurosci, 2012. **32**(26): p. 8879-89.
79. Makeyev, E.V., et al., *The MicroRNA miR-124 promotes neuronal differentiation by triggering brain-specific alternative pre-mRNA splicing*. Mol Cell, 2007. **27**(3): p. 435-48.
80. Laterza, O.F., et al., *Plasma MicroRNAs as sensitive and specific biomarkers of tissue injury*. Clin Chem, 2009. **55**(11): p. 1977-83.
81. Zlokovic, B.V. and B. Frangione, *Transport-clearance hypothesis for Alzheimer's disease and potential therapeutic implications*. 2000.
82. Pascale, C.L., et al., *Amyloid-beta transporter expression at the blood-CSF barrier is age-dependent*. Fluids Barriers CNS, 2011. **8**: p. 21.
83. Hindson, C.M., et al., *Absolute quantification by droplet digital PCR versus analog real-time PCR*. Nat Methods, 2013. **10**(10): p. 1003-5.
84. Miotto, E., et al., *Quantification of circulating miRNAs by droplet digital PCR: comparison of EvaGreen- and TaqMan-based chemistries*. Cancer Epidemiol Biomarkers Prev, 2014. **23**(12): p. 2638-42.
85. Yang, S.T., et al., *Accumulation of amyloid in cognitive impairment after mild traumatic brain injury*. J Neurol Sci, 2015. **349**(1-2): p. 99-104.

86. *Bio-Rad, Droplet Digital PCR Applications Guide, accessed 14 April 2015. Available from: [http://www.bio-rad.com/webroot/web/pdf/lsr/literature/Bulletin\\_6407.pdf](http://www.bio-rad.com/webroot/web/pdf/lsr/literature/Bulletin_6407.pdf).*
87. Mazaika, E. and J. Homsy, *Digital Droplet PCR: CNV Analysis and Other Applications. Curr Protoc Hum Genet, 2014. 82: p. 7.24.1-7.24.13.*
88. Swartz, B.E., et al., *Hippocampal cell loss in posttraumatic human epilepsy. Epilepsia, 2006. 47(8): p. 1373-82.*
89. Leung, L.Y., et al., *Comparison of miR-124-3p and miR-16 for early diagnosis of hemorrhagic and ischemic stroke. Clin Chim Acta, 2014. 433: p. 139-44.*
90. *Exiqon, miRCURY™ RNA Isolation Kit -Biofluids, Instruction manual v1.5, accessed 16 March 2015. Available from: <http://www.exiqon.com/ls/documents/scientific/rna-isolation-biofluids-manual.pdf>.*
91. *Qiagen, miRNeasy Mini Handbook, accessed 23 March 2015. Available from: [http://jgi.doe.gov/wp-content/uploads/2014/02/Qiagen\\_miRNeasy\\_Mini\\_Handbook.pdf](http://jgi.doe.gov/wp-content/uploads/2014/02/Qiagen_miRNeasy_Mini_Handbook.pdf).*
92. *Exiqon, miRCURY LNA™ Universal RT microRNA PCR Expression Analysis, Instruction manual v6.0, accessed 2 March 2015. Available from: <http://www.exiqon.com/ls/Documents/Scientific/Universal-RT-microRNA-PCR-manual-serum.pdf>.*
93. *Applied Biosystems, TaqMan® Small RNA Assays Protocol, accessed 2 March 2015. Available from: [http://tools.thermofisher.com/content/sfs/manuals/cms\\_042167.pdf](http://tools.thermofisher.com/content/sfs/manuals/cms_042167.pdf).*
94. Zampetaki, A. and M. Mayr, *Analytical challenges and technical limitations in assessing circulating miRNAs. Thromb Haemost, 2012. 108(4): p. 592-8.*
95. Plog, B.A., et al., *Biomarkers of traumatic injury are transported from brain to blood via the glymphatic system. 2015. 35(2): p. 518-26.*
96. Iliff, J.J., et al., *Impairment of glymphatic pathway function promotes tau pathology after traumatic brain injury. 2014. 34(49): p. 16180-93.*
97. Tarasoff-Conway, J.M., et al., *Clearance systems in the brain-implications for Alzheimer disease. Nat Rev Neurol, 2015. 11(8): p. 457-70.*
98. Mishima, T., et al., *RT-PCR-based analysis of microRNA (miR-1 and -124) expression in mouse CNS. Brain Res, 2007. 1131(1): p. 37-43.*
99. Aspelund, A., et al., *A dural lymphatic vascular system that drains brain interstitial fluid and macromolecules. J Exp Med, 2015. 212(7): p. 991-9.*
100. Fang, M., et al., *The miR-124 regulates the expression of BACE1/beta-secretase correlated with cell death in Alzheimer's disease. Toxicol Lett, 2012. 209(1): p. 94-105.*
101. Strain, M.C., et al., *Highly precise measurement of HIV DNA by droplet digital PCR. PLoS One, 2013. 8(4): p. e55943.*
102. Kiselina, M., et al., *Comparison of droplet digital PCR and seminested real-time PCR for quantification of cell-associated HIV-1 RNA. PLoS One, 2014. 9(1): p. e85999.*